

The Pennsylvania State University  
The Graduate School

MODELING EXTERNAL FORCING ON MICROPARASITE  
DYNAMICS: A TOOL FOR UNDERSTANDING OBSERVED  
ECOLOGICAL PATTERNS AND FORECASTING DYNAMICS

A Dissertation in  
Ecology  
by  
Angela Dawn Luis

© 2010 Angela Dawn Luis

Submitted in Partial Fulfillment  
of the Requirements  
for the Degree of

Doctor of Philosophy

August 2010

The dissertation of Angela Dawn Luis was reviewed and approved\* by the following:

Ottar N. Bjørnstad  
Professor of Entomology and Biology  
Dissertation Advisor, Co-Chair of Committee

Peter J. Hudson  
Willaman Professor of Biology  
Co-chair of Committee

Bryan T. Grenfell  
Alumni Professor of the Biological Sciences

John Fricks  
Assistant Professor in Statistics

Richard J. Douglass  
Professor and Department Head of Biology, Montana Tech of the University  
of Montana  
Special Member

David Eissenstat  
Chair, Intercollege Graduate Degree Program in Ecology

\*Signatures are on file in the Graduate School.

## Abstract

In this thesis I explore the dynamics of infectious diseases in rodents. Using Sin Nombre hantavirus (SNV) in deer mice as a model system and a combination of mark-recapture analysis and mathematical models, I explore how infectious diseases can affect individuals, populations and communities, and analyze population, community, and ecosystem level patterns in disease dynamics. I also explore the effect of infectious disease on evolutionary histories, specifically, how bacterial infection may have shaped mammalian hibernation patterns. I use a combination of statistical analysis of longterm data and mathematical models to understand observed ecological patterns and improve our ability to forecast dynamics.

Microparasites can have a number of effects on individuals, populations, and communities. I explore the effect of SNV on the deer mouse host and what effect this may have on the host population dynamics and persistence of the disease in the population. I find that SNV decreases survival of antibody positive male deer mice by 15.4%. This can affect both the host population dynamics, by leading to regulation of the host population, as well as the population-level patterns seen in SNV infection, by increasing the critical host density and making the chain of transmission more likely to be broken.

Since the host population dynamics can be affected by many intrinsic and extrinsic factors, such as environmental forcing, disturbance, availability of resources, competition, and other food web interactions, these can all have strong influences on the persistence and spread of a pathogen in the host population. I quantitatively evaluate the proposed bottom-up trophic cascade hypothesis to explain the original SNV outbreak, using 15 years of data from Montana. I show that mouse population dynamics in Montana are strongly correlated to precipitation and temperature with a 0 to 5 month lag. These changing environmental conditions alter the carrying capacity of the environment, which can lead to delayed density dependence in prevalence of the virus (with a lag of up to 16 months or more) in

the mouse population and intermittent crossing of the critical host density necessary for hantavirus endemicity. My work helps shed some light on the notoriously difficult to understand dynamics of the virus, such as seemingly inverse density dependence in prevalence and sporadic disappearance of the virus from local populations. Since there is no effective treatment or vaccine for HPS, the most effective strategy is to take preventative measures. This quantitative understanding of the lags between environmental conditions and prevalence of the virus may allow us advance warning (up to 20 months or more) of increased risk to humans.

# Table of Contents

<b>List of Figures</b>	<b>viii</b>
<b>List of Tables</b>	<b>xi</b>
<b>Acknowledgments</b>	<b>xiii</b>
<b>Chapter 1</b>	
<b>Introduction, Overview and Synthesis</b>	<b>1</b>
1.1 Microparasite effects on individuals . . . . .	2
1.2 Microparasites and populations . . . . .	4
1.3 Microparasites, communities and ecosystems . . . . .	5
1.3.1 Environmental Forcing . . . . .	6
1.3.2 Trophic cascades . . . . .	7
1.3.3 The trophic cascade hypothesis for HPS outbreaks . . . . .	8
1.4 Microparasites can shape evolutionary histories . . . . .	13
1.5 Approach . . . . .	13
1.5.1 Capture-mark-recapture statistical modeling using Program MARK . . . . .	16
1.6 Conclusions . . . . .	20
<b>Chapter 2</b>	
<b>The effect of seasonality, density and climate on the population         dynamics of Montana deer mice, important reservoir         hosts for Sin Nombre hantavirus</b>	<b>21</b>
2.1 Abstract . . . . .	21
2.2 Introduction . . . . .	22
2.3 Methods . . . . .	24
2.3.1 Study site and field methods . . . . .	24

2.3.2	Climatic and vegetation data . . . . .	25
2.3.3	Estimating density and demographic parameters . . . . .	26
2.3.4	Population Model . . . . .	27
2.4	Results . . . . .	28
2.4.1	Demographic Rates . . . . .	29
2.4.2	Population Model . . . . .	32
2.5	Discussion . . . . .	34
2.6	Acknowledgements . . . . .	37
2.7	Notes . . . . .	37
 <b>Chapter 3</b>		
	<b>Sin Nombre Hantavirus Decreases Survival of Male Deer Mice</b>	<b>38</b>
3.1	Abstract . . . . .	38
3.2	Introduction . . . . .	39
3.3	Methods . . . . .	41
3.3.1	Field Site and Animal Processing . . . . .	41
3.3.2	Capture-Mark-Recapture Analysis . . . . .	41
3.4	Results . . . . .	42
3.5	Discussion . . . . .	44
3.6	Acknowledgments . . . . .	47
3.7	Notes . . . . .	47
 <b>Chapter 4</b>		
	<b>A Stage-Structured Model for Sin Nombre Hantavirus</b>	<b>48</b>
4.1	Introduction . . . . .	48
4.2	A mathematical model . . . . .	51
4.2.1	Density dependent demographics . . . . .	51
4.2.2	The stage structured SI Model with density dependent demographics . . . . .	52
4.2.3	$R_0$ , threshold criteria, and equilibria . . . . .	53
4.2.4	Data . . . . .	55
4.2.5	Parameter Estimation . . . . .	56
4.2.6	Analysis . . . . .	57
4.3	Results . . . . .	57
4.4	Discussion . . . . .	60
4.5	Notes . . . . .	67
 <b>Chapter 5</b>		
	<b>Hibernation patterns in mammals: a role for bacterial growth?</b>	<b>68</b>
5.1	Abstract . . . . .	68

5.2	Introduction . . . . .	69
5.3	Methods . . . . .	71
5.3.1	Model and Data . . . . .	71
5.3.2	Analysis . . . . .	73
5.4	Results . . . . .	74
5.5	Discussion . . . . .	76
5.6	Acknowledgements . . . . .	81
5.7	Notes . . . . .	81
<b>Appendix A</b>		
	<b>Supplemental Figures and Tables to Chapter 2</b>	<b>82</b>
A.1	Robust Design Capture-Mark-Recapture	
	Model Comparisons . . . . .	82
A.2	Multistrata Capture-Mark-Recapture	
	Model Comparisons . . . . .	84
<b>Appendix B</b>		
	<b>Supplemental Equations for Chapter 2 Mark-Recapture Models</b>	<b>90</b>
<b>Bibliography</b>		<b>94</b>

## List of Figures

1.1	An example multistrata capture history format. Each row represents one mouse, and each column a monthly trapping occasion. Entries are coded as follows: 0=not captured, 1=juvenile susceptible, 2=juvenile antibody positive, 3=sub-adult susceptible, 4=sub-adult positive, 5=adult susceptible, 6=adult positive. The group information (here sex) can be noted at the end. For example the first row represents a male that was not captured in January or February 2003, but was caught March, April and May, and at each occasion, he was an adult susceptible. . . . .	15
1.2	At each capture occasion, a mouse could be either alive (with probability $\phi$ ) or dead ( $1-\phi$ ), and if alive will be caught with probability, $p$ . Therefore, the probability of seeing an animal will be $\phi p$ . . . . .	16
2.1	Monthly abundance of the deer mouse population from two trapping grids in Cascade county, Montana, represented as minimum number known alive (MNA) and Jolly-Seber estimates . . . . .	25
2.2	Four-step-ahead predictions simulated using demographic parameters estimated in MARK for the best models for survival and recruitment, along with the Jolly-Seber population estimates . . . . .	33
3.1	Monthly probability of deer mouse survival for the model, $S(\sim \text{sex} * \text{antibody status} + \text{month})$ $p(\sim \text{antibody status} + \text{time})$ $\psi(\sim \text{sex} + I_{t-1})$ . . . . .	43
4.1	Abundance of susceptible sub-adults, ( $S_{SA}$ ), infected sub-adults ( $I_{SA}$ ), susceptible adults ( $S_A$ ), and infected adults ( $I_A$ ) over the 15-year study. . . . .	50
4.2	Life cycle diagram for the system. See tables 4.1 for variable and parameter information. . . . .	52
4.3	Minimum number alive, MNA, (light dashed line), carrying capacity, $K$ , (heavy solid line), used to estimate parameters, and simulated abundance from the model (heavy dashed line). . . . .	55

4.4	(a) The prevalence of the virus is determined by the equilibrium population size, $N^*$ , or $K$ . As a result, (b) the regulatory impact of the virus is a function of $N^*$ , shown here as the proportion of the disease free equilibrium population remaining in the presence of the disease. . . . .	57
4.5	Deer mouse abundance (MNA; solid black line) over the study period in relation to the critical host density, $N_c$ (dotted black line), as well as number of infected mice (MNI; red dashed line; scale on the right). . . . .	58
4.6	$R_0$ as a function of equilibrium population density for several values of disease-induced mortality rate, $\mu$ . The heavy line is the estimated $\mu$ , and the dashed line is the threshold quantity, the critical host density, $N_c$ . . . . .	59
4.7	Prevalence appears to be negatively correlated with current density in both (a) the data and (b) the model, although transmission is positively density dependent. . . . .	60
4.8	The strongest correlation between density and prevalence by cross correlation function (CCF) is at a 16 month lag for both (a) the data and (b) the model. . . . .	61
4.9	(a) The lag between a peak in density and the peak in prevalence is negatively correlated with $R_0$ . (b) The number of months it takes to reach 5 infected individuals from 1 initial infection is negatively correlated with the carrying capacity, $K$ . . . . .	62
5.1	Relationship between square root of bacterial growth rate and temperature for <i>Salmonella</i> (Mackey and Kerridge, 1988) and coliform C1 (Baig and Hopton, 1969) . . . . .	75
5.2	Predicted and observed torpor patterns throughout a hibernation season. (a) Predicted expression for a hibernating animal exposed to bacterial pathogens with growth properties similar to <i>Salmonella</i> and (b) coliform C1. (c) Observed torpor patterns in a European ground squirrel in captivity under simulated natural light and ambient temperature conditions (figure 1 from Henning et al., 2002). . . . .	76
5.3	Bacterial parameters ( $b$ and $T_0$ ) that give the best fit of the model to the data, using maximum likelihood estimates. Contours show likelihood test statistics. The six psychrophilic bacteria described by Baig and Hopton (1969) are givsen by circles, and the filled triangle represents the optimal parameter combination. . . . .	78

A.1	Population abundance estimates including Minimum Number Alive (MNA), Jolly-Seber, and Closed Robust Design estimates from August 2004 to May 2009. . . . .	83
-----	--	----

## List of Tables

2.1	The basic set of statistical models tested for variation in survival ( $S$ ) and maturation ( $\psi$ ) probabilities, along with the most parsimonious model with covariates, using multistrata models in Program MARK.	30
2.2	The basic set of statistical models tested for variation in recruitment rates ( $f$ ), along with the most parsimonious model with covariates, using Pradel models.	31
2.3	The effect of precipitation (Prcp) and temperature (Temp), occurring during the given season, on recruitment ( $f$ ) 0-4 months later and survival ( $S$ ) 5 months later based on the most parsimonious MARK models.	32
3.1	Mark-recapture models for probability of recapture, $p$ , using the following models for survival and force of infection: $S(\sim\text{antibody status})$ $\psi(\sim\text{antibody status})$ .	42
3.2	Mark-recapture models for survival, $S$ , and force of infection, $\Psi$ , using the best model for recapture, $p(\sim\text{antibody status}+\text{time})$ accounting for 175 parameters.	44
4.1	Notation used to denote model variables and parameters and their maximum likelihood estimates.	54
5.1	Estimated slope, $b$ , and x-intercept, $T_0$ , for the psychrophilic bacteria in Baig and Hopton (1969) when the square root of the growth rate (divisions per hour) is plotted against temperature (K).	73
A.1	Statistical models tested using Closed Robust Design models to obtain an estimate for abundance at each monthly primary trapping occasion (session), $N(\sim\text{session})$ .	82
A.2	Statistical models tested for variation in recapture rates ( $p$ ), using multistrata models.	84
A.3	Ranking of Multistrata MARK models for survival ( $S$ ), capture probability ( $p$ ), and maturation probability ( $\psi$ ).	85

A.4 Ranking of Pradel MARK models for recruitment rate (f) with the following models for survival,  $\phi$ , and capture probability,  $p$ :  
 $\phi(\sim \text{month} * P_{t-5} + \text{month} * T_{t-5} + \text{month} * P_t + \text{month} * P_t) \quad p(\sim \text{time}). \quad . \quad 89$

## Acknowledgments

I would like to thank my committee, Ottar Bjørnstad, Peter Hudson, Bryan Grenfell, John Fricks, and Rick Douglass for their help and support during my graduate career. I am especially indebted to Ottar and Peter. It is hard to imagine a better advisor than Ottar. I've learned so much from him- mathematical, analytical, statistical, the writing and organizing of presentations, and work-life balance, among many other things. I would like to thank him for his endless support and patience. I am also indebted to Peter, who has been extremely helpful in my scientific development, including developing the ecological questions, critical thinking, and becoming a better writer. I also thank him for supporting me with my decision to change directions when I found my calling in mathematical modeling.

The research presented in this dissertation was done in collaboration with several researchers who have contributed in many ways, from the development of ideas and analysis to the editing of manuscripts. I would like to thank the wonderful people at Montana Tech of the University of Montana, including Rick Douglass, Amy Kuenzi, Scott Carver, and Kevin Hughes, as well as Jim Mills at the Centers for Disease Control and Prevention. They let me play with their amazing data and helped me to understand the ecological system, as well as to get out of the office, get my hands dirty, and fall in love with Montana (in the summer anyway).

Thanks to the members of the Bjørnstad, Grenfell and Hudson labs (past and present) who have offered valuable support, advice and criticism in and out of lab meetings, including: Matt Ferrari, Laura Pomeroy, Jennie Lavine, Lawrence Chien, Lindsay Beck-Johnson, Megan Greischar, Tomas de-Camino-Beck, Petra Klepac, Jamie Lloyd-Smith, Nita Bharti, Shweta Bonsal, Conrad Stack, Jess Metcalf, Ginny Pitzer, Tom Raffel, Isabella Cattadori, Sarah Perkins, Kurt Vandegrift, Jim Sinclair, Lien Luong, Dan Gill, and Dan Gear.

Special thanks to Kat Shea for introducing me to the world of ecological modeling through her great class, Ecological and Environmental Problem Solving. She has been a great mentor for both modeling and teaching.

I've felt lucky to be part of the awesome Ecology Program here at Penn State.

I would like to thank the two chairs of the program during my tenure here, Dave Mortensen and Dave Eissenstat. They have allowed the graduate students to have a great deal of input on many aspects of the program including the seminar series and the program curriculum. They have also supported us in our professional development, encouraging us to organize classes, conferences, and panel discussions. And special thanks to the lifeblood of the program: the motivated, bright and amazing graduate students, who will hopefully remain my colleagues and friends for life.

Thanks to my family for continual love and support (moral and financial) through my many years of higher education. Finally, I would like to thank Mike Turns for endless love, support, and laughs.

# Chapter 1

## Introduction, Overview and Synthesis

Mathematical models and statistical analysis have contributed greatly to our understanding of the role of infectious diseases in population dynamics and observed patterns of disease spread (i.e., Kermack and McKendrick, 1927; Bartlett, 1957; Anderson and May, 1978). However, through much of the last century, parasitism was thought to be a less significant ecological force than predation and competition, and after the discovery of vaccines, antibiotics, and other medical advancements in the last century, many thought that infectious diseases were mostly a concern of the past, at least in developed countries. However, several emerging infectious diseases, such as HIV, West Nile virus, lyssaviruses, hantavirus, prions, and SARS and the emergence of drug-resistance have brought pathogens back to the forefront of the public attention. Furthermore, theoretical ecologists have shown that parasites can be important ecological forces (Anderson and May, 1981; Hudson et al., 1998). In the last decade the US has seen a surge in the study of the ecology of infectious diseases in wildlife.

In this thesis I explore various questions in disease ecology choosing to be taxonomically focused on rodents. Examining diseases in rodents in particular is valuable because they are the reservoirs of many zoonoses (pathogens which are transmitted from animals to humans), from relatively trivial (e.g. cowpox causes skin lesions) to deadly (e.g., Sin Nombre virus causes Hantavirus Pulmonary Syndrome (HPS) in humans and can have up to a 35 to 60% mortality rate), but also because they are a good model for understanding the ecology of infectious diseases because they are readily trapped and monitored.

## 1.1 Microparasite effects on individuals

Microparasites can have various effects on individuals, including mortality and a number of sublethal effects. Historical conventional wisdom has been that parasites should evolve toward being relatively benign, since harming the host may harm their chances of transmission to new hosts, and those that were virulent were a result of recent emergence or cross-over, in which the pathogen has not yet had time to adapt to the new host. However the application of life-history theory has been valuable in explaining patterns of virulence in host-pathogen systems (Antia et al., 1994; Frank, 1996). It is true that pathogens with high virulence may decrease their chances of transmission by decreasing the infectious period either by killing the host or inducing a strong immune response. However, virulence can also be beneficial to the parasite, since it is often correlated with parasite reproduction, and some symptoms can help in transmission (coughing, for example). Therefore, an intermediate level of virulence may be the optimal strategy for the parasite (May, 1983).

Even with this knowledge, some still contend that zoonotic pathogens are mostly avirulent in their reservoir hosts (Begon, 2003). Indeed, in some medical texts, a reservoir host is by definition an asymptomatic carrier (Dorland, 1994). I find the Haydon et al. (2002) definition more appropriate: a reservoir is one or more epidemiologically connected populations in which the pathogen can be permanently maintained and from which infection is transmitted to a defined target population in which the pathogen is not maintained endemically (here, humans). The relationship to a target population should not alter the fact that there should be a range of virulences experienced in reservoir hosts, but often an intermediate level of virulence.

Pathogens can cause mortality directly, or indirectly, through an increase in predation for example. However, sublethal effects of infection can also have important effects on individual lifetime fitness, such as impairment of reproduction. Parasites may affect reproduction directly, causing sterility in the most extreme cases (Alvarez et al., 1995). However, if infection is acute (nonpersistent), it may be the host's optimal strategy to downregulate current reproduction to increase chance of survival and future reproduction. Fighting parasites can be energetically

expensive, and energy that would have gone into reproduction is instead used to fight infection. An infected individual that chooses to reproduce will suffer both the costs of reproduction and mounting an immune response. An individual may maximize its own fitness if it chooses to delay or downregulate reproduction. An example of an infection that reduces fecundity is cowpox infection in bank voles and wood mice. Infected females delay maturity and timing of first litter (Telfer et al., 2005; Feore et al., 1997). This can have a significant impact on their lifetime reproductive fitness.

Seemingly paradoxically, infection has also been linked to increased survival (Telfer et al., 2002; Burns et al., 2005). One possible mechanism can be explained by life history theory. Parasites are by definition detrimental to their hosts, but if only one life history trait is measured, they may appear to have a positive effect on fitness. Physiological tradeoffs in life history traits occur when an individual has a finite amount of energy to devote to two or more processes. Life history tradeoffs exist between survival and reproduction and also between current and future reproduction (as the cowpox example above). If a host chooses to delay reproduction when acutely infected and reproduction is more energetically costly than fighting infection, the remaining energy balance can be used for maintenance, foraging, etc, which may lead to an increase in body condition and could increase survival. Even if fighting infection is as energetically costly as reproduction, delaying reproduction may still increase survival if behaviors required for reproduction increase risk of predation (displaying, calling, increasing movement to find mates, etc).

In chapter 3, I explore the effect of Sin Nombre virus (SNV) on its rodent host. Although SNV is the etiologic agent of hantavirus pulmonary syndrome (HPS) and can have a 40-60% mortality rate in humans, it has traditionally been thought to cause a chronic, avirulent infection in the deer mouse reservoir host (i.e. Calisher et al., 1999; Botten et al., 2000; Easterbrook and Klein, 2008). Using capture-mark-recapture statistical modeling, I found that antibody positive males had a 15.4% decrease in monthly survival probability. This adds to the sparse literature of how chronic infections affect reservoir hosts of zoonotic diseases in nature, and may have important consequences for the persistence and spread of the disease as discussed in section 1.2.

## 1.2 Microparasites and populations

The effects at the individual level described above can impact the dynamics at the population level. If transmission of the microparasite is density dependent (contacts and transmission increase with increased density) and there is disease-induced mortality, decreased survival will occur in a density dependent manner, and may lead to regulation of the host population, holding the number of individuals below the disease free equilibrium, if the disease-induced mortality rate ( $\mu$ ) is greater than the host growth rate (realized birth rate - death rate). In chapter 3, I show that SNV transmission is density dependent rather than frequency dependent (contacts and transmission are independent of density) and causes disease induced mortality. Therefore, SNV has the potential to regulate the deer mouse host population. In chapter 4, I explore this topic further with a stage-structured epidemiological model for SNV dynamics. In a host population experiencing logistic growth with a variable carrying capacity (like SNV in the deer mouse population), the pathogen's ability to regulate the host population will depend not only on  $\mu$  and intrinsic birth and death rates ( $b$  and  $d$ ), but also the abundance of the host population in relation to the equilibrium or carrying capacity,  $K$ , since these determine the realized birth and death rates.

I find that the largest impact of SNV on the population occurs when prevalence is high, which is largely determined by  $K$ . As the environmental carrying capacity increases, mouse density increases, resulting in a nonlinear increase in prevalence (see Fig 4.8). As described in more detail in section 1.3.2 and chapter 4, there is a lag between a peak in host density and a peak in prevalence, so that the greatest prevalence and greatest disease induced mortality can be seen when the population density may already be on the decline because of an environmentally induced reduction in  $K$ , making the disease less likely to persist after an epidemic. Delayed density dependent regulation can lead to destabilization of host population dynamics, and the observed mouse density is far from stable (there are small-scale and large-scale fluctuations through time; see Fig. 4.4). However, in this case, the climatic drivers are the dominant force in this system, which act independent of density, often bringing the population density low enough to cause the virus to go locally extinct.

Population level patterns of microparasites can range from violent epidemics followed by pathogen extinction to stable endemicity. Where a pathogen lies on this axis is determined by pathogen and host characteristics such as virulence, transmission rate, host immunity, and host demographics. In addition to the virulence-transmission tradeoff discussed in section 1.1, there can also be an invasion-persistence tradeoff. Highly acute (virulent or highly immunizing) infections may be more likely to invade and cause a larger epidemic, but then experience deeper troughs and may be more likely to fade-out. On the other hand, less acute or chronic infections may be less likely to take off but more likely to persist and become endemic (Grenfell, 2001; King et al., 2009). The highly acute pathogens can only persist at the metapopulation level.

In chapter 4, I explore how disease induced mortality affects the population dynamics of SNV. Disease induced mortality effectively reduces the infectious period and decreases  $R_0$ , making the virus less likely to invade and more likely to fade-out. The addition of disease induced mortality in the model increases the critical host density necessary to sustain an epidemic,  $N_c$ . Without disease induced mortality (what was previously believed),  $N_c$  would be 19 mice per 2 hectares, whereas with the calculated  $\mu$  of 0.085,  $N_c = 33$  mice per 2 hectares. If  $\mu$  is underestimated (as it may well be; see chapter 3), then  $N_c$  may be even higher.

### 1.3 Microparasites, communities and ecosystems

Host population dynamics can have strong impacts on disease dynamics, particularly for diseases with density dependent transmission. Anything that affects the density of hosts will affect contact rates and disease transmission. Since the host population dynamics can be affected by many intrinsic and extrinsic factors, such as environmental forcing, disturbance, availability of resources, competition, and other food web interactions, these can all have strong influences on the persistence and spread of a pathogen in the host population.

Not only do community interactions affect pathogen dynamics, but the reverse is true as well. If a pathogen affects its host's population dynamics, it may have cascading effects through the ecosystem and affect other interactions in the community. Even if the pathogen has a negligible effect on the host population

dynamics, pathogen spillover or cross-species transmission to other hosts in the community can alter interactions between species. In this section I will discuss ecosystem and community interactions that may impact pathogen dynamics, with particular interest to SNV dynamics.

### 1.3.1 Environmental Forcing

Organisms live in changing environments, yet most epidemiological models assume static conditions. This may be a reasonable assumption when the processes being modeled are short relative to environmental changes or demographic processes of the host, like for example during the course of a rapid epidemic in a long lived host, such as a local flu epidemic in humans. However, in many cases, we are interested in modeling the long-term dynamics, and the inclusion of host population dynamics can have a great impact on the disease dynamics.

When background host population dynamics are considered in epidemiological models, they are typically very simple. Human populations in developing countries are relatively stable and are commonly modeled with a constant birth rate balanced by death rate. In developing countries the population is often increasing, and background host dynamics are often modeled as growing exponentially. The effect this has on the disease dynamics will depend on the assumption of how the number of contacts changes with host density. For diseases with density dependent transmission, as population size grows, infection rates increase,  $R_0$  increases, and the average age at infection decreases (Anderson and May, 1991).

One type of external forcing that has been fairly well studied is seasonality (Altizer et al., 2006). Birth, death, or disease transmission rates can vary seasonally and have a strong effect on the dynamics. Transmission rates can vary seasonally because of changes in behavior. For example, children have increased contact rates during school terms, and animals may have increased contacts rates during the mating season or around water sources in the dry season. Hosts and vectors can also have strongly seasonal birth and death rates. Seasonal forcing can change dynamics from damped oscillations to sustained oscillations, can give rise to regular cycles each year (harmonic oscillations, where the interepidemic period is the same as the forcing), multiple year cycles (subharmonic resonance, where the interepidemic

period is a multiple of the forcing period), or even chaos (Dietz, 1976; Keeling et al., 2001; Hosseini et al., 2004).

Other sources of environmental forcing, such as stochastic climatic fluctuations, large scale oscillations (like El Nino) and trends, have received less attention historically, but with recent interest in climate change research, interest is beginning to surge. Climate is known to be an important factor for vector-borne diseases, such as malaria and dengue fever, by altering the abundance and/or distribution of vector hosts (Hopp and Foley, 2003; Pascual et al., 2006), as well as for water-borne diseases, such as cholera, through an increase in environmental reservoirs (de Magny et al., 2008). However, less studied is the effect of climate on vertebrate reservoir hosts of zoonotic diseases, through changes in demography, distribution or abundance. In chapters 2 through 4, I examine how changing environmental conditions can affect host demography and in turn, affect the disease dynamics.

### **1.3.2 Trophic cascades**

These environmental and other ecological forces which affect one trophic level can have cascading effects through the ecosystem. Trophic cascades can be defined as reciprocal consumer-resource effects that alter the abundance, biomass or productivity of a population, community or trophic level across more than one link in a food web (Pace et al., 1999). Trophic cascades can be top-down or bottom-up. Top-down or consumer-driven trophic cascades, occur when for example, predators keep herbivore prey populations at levels below the population size that would be observed in the absence of predators, which allows for an increase in primary productivity due to a release of herbivory. Bottom-up or resource-driven trophic cascades can occur when factors such as food and/or habitat availability are the main drivers explaining population fluctuations, and these in turn affect higher trophic levels. With top-down trophic cascades, the direction of effects between adjacent trophic levels is usually in opposite directions (e.g., an increase in predators leads to a decrease in prey). In contrast, responses between trophic levels are typically in the same direction with bottom-up cascades (e.g., an increase in plants leads to an increase in herbivores). There can be a time lag in response of bottom-up effects (Gratton and Denno, 2003; Bjorkman et al., 2004). This means

that given a change in a lower trophic level, there may be time to predict and possibly mitigate effects at the higher trophic levels.

A handful of studies have examined the role of disease in trophic cascades (Lafferty, 2004; Wilmers et al., 2006; Holdo et al., 2009). Parasites are often overlooked in food webs, but with the effects on the host population as described earlier, they could have cascading top-down effects through the ecosystem. A great example of a top-down disease-mediated trophic cascade is from the Serengeti (Holdo et al., 2009). Until its eradication in the 1960s, rinderpest regulated the wildebeest on the savannah. After rinderpest eradication, an irruption of wildebeest led to greater grazing pressure, and a decrease in fire extent. This led to an increase in tree density, causing the savannah ecosystem to change from a carbon source to a carbon sink (Holdo et al., 2009).

Evidence of disease outbreaks resulting from bottom-up trophic cascades is even more rare. However, there is some evidence for climate affecting plague outbreaks in black-tailed prairie dogs, possibly through interactions with arthropod vectors and hosts (Collinge et al., 2005), as well as some previous evidence qualitatively linking an increase in precipitation to human hantavirus cases in the Southwest (Engelthaler et al., 1999). In chapters 2 through 4, using 15 years of data from central Montana, I quantitatively explore the bottom-up trophic cascade hypothesis for Sin Nombre hantavirus outbreaks.

### 1.3.3 The trophic cascade hypothesis for HPS outbreaks

During the spring and summer of 1993, thirteen people mysteriously died from acute respiratory distress in the Four Corners region of southwestern U.S. Soon thereafter, the Centers for Disease Control and Prevention (CDC) discovered that the cause was a previously unknown hantavirus, named Sin Nombre virus (SNV). Since the discovery, there have been approximately 500 human cases of Hantavirus Pulmonary Syndrome (HPS), with a 35-60% mortality rate. The main reservoir host for SNV is the deer mouse (*Peromyscus maniculatus*), an omnivorous generalist whose range spans most of North America. Humans contract this deadly disease when they come into contact with an infected mouse's excreta or saliva.

The original outbreak in the Four Corners Region was preceded by an El Nino

Southern Oscillation event, which brought increased precipitation to this usually arid region. A bottom-up trophic cascade hypothesis was proposed to explain the HPS outbreak (Mills et al., 1999a; Parmenter et al., 1993), in which increased precipitation would lead to increased primary productivity and a greater abundance of food for the deer mouse. Increases in resources would lead to higher population density and increased transmission and prevalence of SNV in the deer mice, and therefore a greater chance of spillover to humans. There is no effective treatment or vaccine for HPS, therefore the most effective strategy is to take preventative measures. Understanding the environmental risk factors associated with epidemics in the reservoir hosts and increased human risk may allow public health officials to predict outbreaks and effectively target prevention strategies.

Since the original outbreak in 1993, longitudinal studies sponsored by the CDC have monitored the population dynamics and infection status of rodent populations in the southwestern U.S. and Montana (Mills et al., 1999b). The studies in the southwestern U.S. have indeed demonstrated a qualitative correlation among precipitation, rodent population size, incidence of hantavirus infection in rodent populations, and consequent risk of hantavirus infection in humans (Mills et al., 1999b; Abbott et al., 1999; Engelthaler et al., 1999). A quantitative understanding of how these environmental factors affect the mouse demography and lead to outbreaks is key in creating a predictive model and effectively preventing human infection. Relatively simple epidemiological models have been shown to be effective at predicting epidemics if key ecological processes, including the essence of transmission and demography, are included in the model (for example, Bjørnstad et al., 2002; Grenfell et al., 2002).

The bulk of my thesis was done in collaboration with Richard Douglass at Montana Tech of the University of Montana and James Mills at the CDC. For the last 15 years they have been conducting monthly year-round monitoring of the small mammal population in Cascade county, central Montana, in which deer mice account for over 85% of the small mammal assemblage (Douglass et al., 2001). Each mouse caught is tagged with an individual ear-tag, allowing for individual capture histories in which the mouse's capture status (caught/ not caught), breeding status, body mass, and prevalence of antibody to hantavirus can be noted for each monthly capture occasion. This is the largest hantavirus dataset of its kind, including

more monthly mouse captures and higher seroprevalence than seen in studies in the southwestern U.S. We also have precipitation and temperature data from a meteorological tower less than 1 km from the field site.

In chapters 2-4, I examine the role of environmental factors, specifically the impact of seasonality, precipitation and temperature, on hantavirus dynamics in the deer mouse and create population and epidemiological models including key climatic variables, of hantavirus dynamics in the deer mouse population.

In chapter 2, I explore the first part of the trophic cascade hypothesis, that precipitation and temperature affect the mouse population dynamics. Using capture-mark-recapture statistical methods, I estimated deer mouse survival, maturation and birth rates and tested the relative importance of seasonality, population density and local climate in explaining temporal variation in these deer mouse demographic rates. From these estimates I designed a population model to simulate deer mouse population dynamics given climatic variables and compared the model to observed patterns. Month, precipitation 5 months previously, temperature 5 months previously, and to a lesser extent precipitation and temperature in the current month, are important in determining deer mouse survival. Month and the sum of both precipitation and temperature over the last 4 months are important in determining birth and immigration rates. These results are consistent with the trophic cascade hypothesis; the climatic factors are most likely affecting primary productivity, but it is not as simple as the more-rain-equals-more-food-equals-more-mice hypothesis. The effects of precipitation and temperature depend on the month. For example, higher temperatures and more precipitation during the summer through early winter were correlated with increased survival and recruitment, but not during the spring, perhaps because of an overabundance of water already present in the form of melting snow. While climatic drivers appear to have a complex influence on dynamics, the models forecasting ability is quite good, explaining 79% of the variation seen in mouse abundance, predicting 4 months ahead.

Although studies of SNV in deer mice have been conducted since the original outbreak, there were still several key questions to be answered before creating an epidemiological model. In chapter 3, I ask a) Is there disease induced mortality in the mice? and b) Does transmission depend on the density of the mouse population? Other field studies have revealed either no effect or marginally signif-

icant effects of SNV on the deer mouse reservoir host (i.e., Calisher et al., 1999; Douglass et al., 2001). Using more advanced capture-mark-recapture statistical methods than previously used, I have discovered that SNV does indeed decrease survival of infected deer mice, but surprisingly only in males. Infected male deer mice experience a 15.4% reduction in survival. This substantial reduction in lifespan could have a significant effect on the dynamics of the virus in the host as described in section 1.2. Transmission of the virus was also found to be density dependent, so there is a greater chance of transmission of the virus among the mouse population and a greater chance of an epidemic as the number of mice increases.

In chapter 4, including the density dependent transmission and disease induced mortality discovered in chapter 3, I created an age-structured SI (or Susceptible-Infected) model for hantavirus in the deer mouse reservoir. This is a model in which individuals are grouped into categories reflecting their infection status: susceptible (uninfected) or infected, and categories reflecting their age: juvenile, subadult, or adult. The model includes density dependent population growth in which the number of mice supported varies with changing environmental conditions. Using maximum likelihood, I estimated the remaining parameters for this epidemiological model and calculated 2 important threshold values, the basic reproductive rate,  $R_0$ , and the critical host density necessary to sustain an epidemic,  $N_c$ .  $R_0$ , is the average number of cases resulting from one infected individual in a fully susceptible population. When  $R_0 > 1$  the disease can invade and cause an epidemic, and when  $R_0 < 1$ , it cannot invade and will fade out. The critical host density is the density of hosts necessary for  $R_0 = 1$ . The analysis revealed that approximately 17 mice per hectare are necessary to get an outbreak, and 52% of the time the population was below this critical threshold. This finding helps explain some of the previously unexplained patterns seen in the SNV-deer mouse system, such as the sporadic disappearance of the virus and reintroductions of the virus just resulting in only a few infected individuals, rather than an epidemic. SNV in deer mice appears to be at the edge of local persistence. There is local extinction followed by reintroduction by infected immigrants from other populations; the virus must persist at the regional rather than local scale.

A key finding in the epidemiological model is that an increase in the carrying capacity (from favorable environmental conditions) and the resulting increase in

mouse density leads to a delayed increase in prevalence (if the population is above the critical host density). This can help explain another puzzling pattern seen in the data- seemingly inverse density dependence. Typically, directly transmitted diseases have density dependent transmission, and the analysis in chapter 3 indicates that SNV does. However, diseases with density dependent transmission should increase in prevalence at increased density, yet the SNV data reveals either no correlation between current density and current prevalence or sometimes a negative one. Our model reveals that we were looking at the wrong time scale. The increase in prevalence happens slowly for this slowly circulating disease, which is often on the edge of local persistence. In the data there was an approximately 16 month lag between the peak in mouse abundance in 2002 and the subsequent peak in prevalence. With the epidemiological model we can explore what conditions affect the length of this lag. It appears to be correlated to  $R_0$ , which is a function of all the demographic and epidemiological parameters, including the carrying capacity, as defined in chapter 4. In the same way that diseases with a lower  $R_0$  have a higher age at first infection (Anderson and May, 1991), this slowly circulating virus may take a number of months to build to a maximum prevalence. Therefore, the finding that older mice are more likely to be infected may not only be due to the probable transmission mechanism of aggressive contacts which occur mostly in reproductive individuals, but also because the virus has a low  $R_0$  and is slowly circulating.

There are several possible future directions for this research. I would like to estimate a more refined approximation of  $K$ , the carrying capacity of the environment, from temperature and precipitation data from chapter 2. I would also like to use transfer functions (Nisbet and Gurney, 1982) to help describe how interactions in demography and transmission amplify or dampen stochastic changes in  $K$  and provide a measure of lag between environmental perturbation and the responses of population and disease dynamics. It would also be interesting to examine the models' applicability to other field sites in Montana. A preliminary look at the field data from another site in Montana, reveals that the dominant lag there between density and prevalence is about 8 months. It would be interesting to see how the demographic rates, transmission rates, etc, are different between the 2 sites and how that affects the dynamics.

## 1.4 Microparasites can shape evolutionary histories

With all the interactions described above, parasites and hosts are sure to have strong evolutionary pressures on each other. There are many known instances of coevolution between host and parasite. Parasites evolve to optimize reproduction, transmission, and infection of new hosts, thereby increasing their fitness. Although it occurs on a much slower time scale, the hosts can also evolve better strategies to fight the parasites and increase their own fitness.

In chapter 5, I explore the hypothesis that microparasites may have shaped mammalian hibernation patterns. In order to conserve energy when resources are scarce, hibernating mammals experience torpor in which their body temperature and heart rate decrease dramatically, and many other physiological functions slow down or are effectively shut off. These torpor bouts are punctuated by periodic arousal from torpor in which their body temperature and other physiological functions return to almost normal levels. These periodic arousals from hibernation use up to 80% of their stored energy reserves (Kayser, 1953; Wang, 1978), but their function remains unclear. There are many hypotheses for why these periodic arousals occur. One hypothesis is that immune stimulation could be an important factor (Prendergast et al., 2002). While in torpor the immune response is effectively turned off and periodic arousals may be necessary to check for and combat any itinerant infection. Using a simple mathematical model of the general dynamics of bacterial abundance at body temperatures experienced during hibernation, I ask if bacterial infection could be a factor in shaping observed hibernation patterns, using data from European ground squirrels. Using maximum likelihood to estimate model parameters, our analyses suggest that indeed, there are some pathogenic bacteria that can grow at low body temperatures, and they may be a selective force on torpor behavior.

## 1.5 Approach

An interesting area of personal development during my graduate research has been on the relationship between theoretical models and data. In my thesis, I took

two main approaches. In chapters 2 and 3, I use capture-mark-recapture (CMR) statistical modeling, as discussed in section 1.5.1, to estimate demographic and epidemiological rates. These methods take advantage of more of the data than just the time series of abundance. By tracking individual histories, it is possible to separate out survival and recapture, as well as births (or recruitment) and deaths, which can be difficult when estimating parameters from time series. CMR statistical modeling is an area that has seen exciting new developments in the last decade, combining Jolly-Seber models (Jolly, 1965; Seber, 1965) with generalized linear models (White and Burnham, 1999). Parameters may be specified as a function of covariates. The data determines the formulation of the model, but it is constrained within the generalized linear model framework. Although the processes being modeled may be continuous (e.g., animals are not all born or die at the beginning of every month), the data is invariably collected at discrete time intervals, and the parameters estimated using these methods are discrete (e.g., the probability of surviving one month).

The other approach taken in chapter 4 was to create a mechanistic theoretical model with *a priori* assumptions (e.g the carrying capacity formulation) and parameterize it using the time series of abundances of the different classes of individuals through time (juvenile, sub-adult susceptible, sub-adult infected, adult susceptible, adult infected). I used maximum likelihood estimation combined with numerical integration of ordinary differential equations to estimate parameters of these mechanistic models and explore the model's dynamics. The advantage of these models is that they are more flexible, more realistic, and can be analytically more tractable. We can look at equilibrium conditions and threshold criteria, etc. The disadvantage of this approach is that there is much less information in the time series data and there can be problems with collinearity when estimating parameters.

A complication of using these 2 different types of models in conjunction is that it can be difficult to move between them. The CMR estimates are for discrete time parameters, and the more flexible theoretical models are in continuous time. Parameters and external covariates that change through time (e.g., coefficients for how seasonality affects survival, and the external covariates precipitation and temperature) need to be smoothed so that they are continuous and C2 differen-

tiable (i.e. have finite and continuous first and second derivatives) in order to be useful in the continuous-time framework. However, external covariates may not be amenable to a smoothing spline without losing a lot of variation. For example, precipitation and temperature measurements are not continuous and are very stochastic and jagged. Smoothing may lead to a loss of the signal. For these reasons, I have been unable thus far, to write a continuous time model including precipitation and temperature that shows the temporal variability and fit of the discrete time model.

Another problem is that since the CMR statistical models are constrained within the generalized linear model framework, the parameters may not be the same. For instance, with the CMR population model I could form an expression for how monthly precipitation and temperature influence survival and recruitment, yet, with the continuous time ODE epidemiological model, I wanted to use a more commonly used formulation of how environmental forces affect density through a carrying capacity,  $K$ . Therefore, the birth and death rate parameters are not the same between the two models.

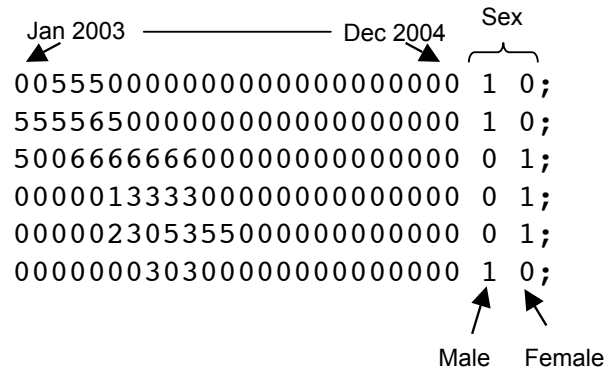


**Figure 1.1.** An example multistrata capture history format. Each row represents one mouse, and each column a monthly trapping occasion. Entries are coded as follows: 0=not captured, 1=juvenile susceptible, 2=juvenile antibody positive, 3=sub-adult susceptible, 4=sub-adult positive, 5=adult susceptible, 6=adult positive. The group information (here sex) can be noted at the end. For example the first row represents a male that was not captured in January or February 2003, but was caught March, April and May, and at each occasion, he was an adult susceptible.

### 1.5.1 Capture-mark-recapture statistical modeling using Program MARK

Since a large part of chapters 2 and 3 is dedicated to estimating population and epidemiological parameters from field data using Program MARK (White and Burnham, 1999), I will give an overview of the theory behind capture-mark-recapture statistical modeling and the nomenclature used.

The 15 years of deer mouse field data contain a great deal of information. Animals were live-caught monthly on permanent grids and each animal was tagged with an individual ear tag, which allows us to follow individuals through time, and note at each capture occasion if the animal was captured, its sex, weight (which can be used to estimate age), whether the animal was in breeding condition, as well as take a blood sample to test for presence of antibodies to SNV. All these data can be represented in a multistrata capture history format, as in Fig 1.1. The different strata could be age classes, breeding condition, SNV status, or a combination, and are denoted with a unique character in the capture histories. From these data we can estimate recapture probability, survival probability, recruitment rate, abundance, and probability of changing strata (e.g. from juvenile to adult, or uninfected to infected), among other things. These parameters can be specified as constant, time varying or a function of serostatus, age, sex, or other covariates, such as month, precipitation, or temperature.

To illustrate the theory, we can look at a simple example in which we want to estimate time varying recapture and survival probabilities. At each capture

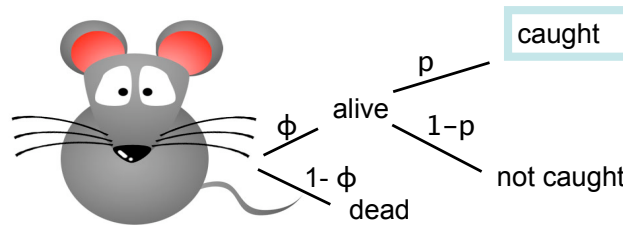


**Figure 1.2.** At each capture occasion, a mouse could be either alive (with probability  $\phi$ ) or dead ( $1-\phi$ ), and if alive will be caught with probability,  $p$ . Therefore, the probability of seeing an animal will be  $\phi p$ .

occasion, a mouse could be either alive (with probability  $\phi$ ) or dead ( $1-\phi$ ), and if alive will be caught with probability,  $p$ . Therefore, the probability of seeing an animal at any occasion will be  $\phi p$  (Fig 1.2). If an animal was not caught in a particular period, but was caught previously and at a later occasion, we know that it was alive for that period, yet not caught,  $\phi(1-p)$ . However if an animal was not caught at the occasion or any later occasion, we don't know if the animal was alive and not caught, or if it was dead, therefore we add the possible probabilities together,  $\phi(1-p)+(1-\phi)$ . For a simple example with 3 capture occasions with time dependent parameters, there are 2 survival parameters:  $\phi_1$  (probability of surviving from occasion 1 to 2) and  $\phi_2$  (between occasion 2 and 3) and 2 recapture parameters,  $p_2$  and  $p_3$  (recapture at occasion 2 and 3 respectively). The following table shows some sample capture histories, the number of individuals with those capture histories, along with the probability of seeing that capture history.

capture history	probability	freq obs
111	$\phi_1 p_2 \phi_2 p_3$	7
110	$\phi_1 p_2 (1 - \phi_2 p_3)$	13
101	$\phi_1 (1 - p_2) \phi_2 p_3$	6
100	$1 - \phi_1 p_2 - \phi_1 (1 - p_2) \phi_2 p_3$	29

The likelihood of observing these different capture histories follows a multinomial distribution. The multinomial likelihood function for this example is

$$L = (\phi_1 p_2 \phi_2 p_3)^7 \times (\phi_1 p_2 (1 - \phi_2 p_3))^{13} \times (\phi_1 (1 - p_2) \phi_2 p_3)^6 \times (1 - \phi_1 p_2 - \phi_1 (1 - p_2) \phi_2 p_3)^{29}.$$

MARK estimates these 4 parameters ( $\phi_1, \phi_2, p_2$ , and  $p_3$ ) to maximize this likelihood,  $L$ .

The parameters can be transformed so that they are ensured to be positive using a log link, or ensured to lie between 0 and 1 (for all the parameters that are probabilities: recapture, survival, maturation, becoming seropositive, etc) using a logit link:  $\log\left(\frac{x}{1-x}\right)$ . On the link scale, parameters can also be defined to be a function of 1 or more covariates (as per the GLM formalism), for example:

$$\text{logit}(p) = \beta_0 + \beta_1 X_1 + \beta_2 X_2$$

where  $X_1$  and  $X_2$  are 2 vectors of covariates such as temperature and precipitation over the study period. Here, the  $\beta$  coefficients are the parameters that are estimated by MARK.

Different models (ones with time varying parameters, seasonal parameters, constant parameters, etc) can be compared by their  $AIC_c$  values (Akaike's information criterion adjusted for differences in effective sample size).  $AIC_c$  assesses fit of the model to the data, penalizing models with more parameters. It is calculated for a particular model as

$$AIC_c = -2\log L + 2K + \frac{2K(K+1)}{M-K-1},$$

where  $L$  is the likelihood,  $K$  is the number of parameters in the model, and  $M$  is the effective sample size (the total number of captures). The most parsimonious model is the one with the lowest  $AIC_c$ .

If the most parameterized model does not fit the data well by a goodness of fit (GOF) test, this typically indicates that 1 of 2 assumptions is violated: that every marked animal present in the population (or group) at time (t) has the same probability of recapture ( $p_t$ ), or that every marked animal in the population (or group) immediately after time (t) has the same probability of surviving to time (t+1). If there is a lack of fit, a correction factor,  $\hat{c}$  can be estimated, which is the GOF  $\chi^2$  divided by the degrees of freedom. The  $AIC_c$  will become  $QAIC_c$ , in which the term  $-2\log L$  is divided by  $\hat{c}$ . Values of  $\hat{c}$  significantly larger than one will penalize models more for having more parameters. This can indicate the need to include more groups in the analysis; for example in chapter 2, I did not include sex or SNV antibody status in the capture history data (because of computing limitations with the large dataset), and these were found to be important in survival and recapture rates in chapter 3. GOF tests revealed a lack of fit for the models in chapter 2, and I needed to use the  $QAIC_c$  and  $\hat{c}$ . However, with the addition of these groups, it was not necessary in chapter 3.

Using RMark (Laake, 2007), a package for the R software (R Development Core Team, 2005), models can be specified using the same nomenclature as for generalized linear models, e.g.  $\phi(\sim \text{time}) p(\sim 1)$  is a model in which  $\phi$  is a function of time, and  $p$  is constant. Covariates and interactions can be included,

e.g.  $\phi(\sim \text{sex})p(\sim \text{month*age class})$  is a model in which 2  $\phi$  values are estimated, one for each sex, and  $p$  is a function of month and age class and their interaction.

The results are typically presented in a table with the candidate models ranked by  $\text{AIC}_c$  (or  $\text{QAIC}_c$ ), along with the number of parameters, and their Akaike weights, which are relative likelihoods for each model in the candidate set. The weights are calculated as

$$w_i = \frac{\exp\left(\frac{-\Delta\text{AIC}}{2}\right)}{\sum\{\exp\left(\frac{-\Delta\text{AIC}}{2}\right)\}},$$

where  $\Delta\text{AIC}$  is the difference in AIC between model  $i$  and the model with the lowest AIC value. The denominator is the sum of this expression for all the models, which allows the weights to sum to 1.

The results are presented in a table, such as

model	# parameters	$\text{AIC}_c$	weight
$\phi(\sim 1)p(\sim 1)$	2	322.6	0.96003
$\phi(\sim \text{time})p(\sim 1)$	7	330.1	0.02253
$\phi(\sim 1)p(\sim \text{time})$	7	330.7	0.01650
$\phi(\sim \text{time})p(\sim \text{time})$	11	336.4	0.00093

Although Program MARK is a powerful tool for estimating demographic rates and identifying factors that may be important in determining them, it has its limitations, particularly with large datasets. The Montana SNV dataset is much larger than typically used in this kind of analysis (large number of individuals and number of trapping occasions as well as several individual and temporal covariates). The specification of covariates for a dataset this large was impossible before the advent of RMark (Laake, 2007). However, even with RMark, running these models challenges our desktop computers (with modern specs) to their limits of memory and processing power. It is often necessary to leave out some important information when forming the data. For example, when forming the data by age in chapter 2, I was unable to also include information about sex or infection status, because of computational constraints.

## 1.6 Conclusions

A combination of statistical analysis and mathematical models can be a powerful tool for understanding observed ecological patterns and helping forecast dynamics. The models developed in this thesis can help us to understand how external forcing, such as from climate and seasonality, can drive population and disease dynamics, and since there may be a delay between climatic events and their corresponding effects, this can add to our forecasting abilities. In the case of SNV, we may have up to 20 months or more advance warning of increased human risk of HPS, after sufficient climatic conditions. The interaction of external forcing along with disease pressures can also affect the host's population dynamics, physiology and behavior. Models presented here can help explain how disease can regulate the host population, but only with sufficient climatic conditions, and how disease along with seasonality may lead to the observed patterns in hibernation physiology and behavior.

## **The effect of seasonality, density and climate on the population dynamics of Montana deer mice, important reservoir hosts for Sin Nombre hantavirus**

### **2.1 Abstract**

Since Sin Nombre virus was discovered in the U.S. in 1993, longitudinal studies of the rodent reservoir host, the deer mouse (*Peromyscus maniculatus*) have demonstrated a qualitative correlation among mouse population dynamics and risk of hantavirus pulmonary syndrome (HPS) in humans, indicating the importance of understanding deer mouse population dynamics for evaluating risk of HPS. Using capture-mark-recapture statistical methods on a fifteen-year dataset from Montana, we estimated deer mouse survival, maturation and recruitment rates and tested the relative importance of seasonality, population density and local climate in explaining temporal variation in deer mouse demography. From these estimates we designed a population model to simulate deer mouse population dynamics given climatic variables and compared the model to observed patterns. Month, precipitation 5 months previously, temperature 5 months previously and to a lesser extent precipitation and temperature in the current month, were important in determining deer mouse survival. Month, the sum of precipitation over the last 4 months, and the sum of the temperature over the last 4 months were important in determining recruitment rates. Survival was more important in determining the growth rate of the population than recruitment. While climatic drivers appear to

have a complex influence on dynamics, our forecasts were good. Our quantitative model may allow public health officials to better predict increased human risk from basic climatic data.

## 2.2 Introduction

It is becoming increasingly more apparent that climate can have significant impacts on infectious disease dynamics (Harvell et al., 2002; Patz et al., 2005). Understanding the influence of climatic drivers on disease emergence and incidence can help in forecasting and prevention and is becoming more urgent in this era of climate change. Climate can affect vector-borne diseases, such as malaria and dengue fever, by altering the abundance and/or distribution of vector hosts (Hopp and Foley, 2003; Pascual et al., 2006), as well as the occurrence of water-borne diseases, such as cholera, through an increase in environmental reservoirs (de Magny et al., 2008). Less studied is the effect of climate on vertebrate reservoir hosts of zoonotic diseases, through changes in demography, distribution or abundance. One zoonotic pathogen for which climate appears to affect reservoir host demography is Sin Nombre hantavirus.

The main reservoir host for Sin Nombre virus (SNV), the primary etiologic agent of hantavirus pulmonary syndrome (HPS), is the deer mouse, *Peromyscus maniculatus*, an omnivorous generalist whose range spans most of North America. The first recognized outbreak of HPS in 1993 in the Four Corners region of the southwestern U.S. (where the states of Arizona, New Mexico, Colorado and Utah adjoin) was preceded by an El Niño Southern Oscillation (ENSO) event, which brought increased precipitation to this normally arid region. Parmenter et al. (1993) proposed a bottom-up trophic cascade hypothesis to explain the epidemic of HPS in which increased precipitation would lead to increased primary productivity, and greater abundance of preferred food items of the deer mouse. Increases in resources would allow the mice to survive and reproduce which would lead to higher population density. This increase in density has been hypothesized to lead to increased transmission and prevalence of SNV in the deer mice and therefore a greater chance of spillover to humans (Mills et al., 1999a; Yates et al., 2002). The length of the cascade leads to the prediction that there should be a delay between

the climatic triggers and increased risk to humans.

Since the original outbreak in the Four Corners region, longitudinal studies sponsored by the U.S. Centers for Disease Control and Prevention (CDC) have monitored the population dynamics and infection status of rodent populations in the southwestern U.S. and Montana (Douglass et al., 1996, 2001; Mills et al., 1999b). Some of these studies have demonstrated a correlation among precipitation, rodent population size, prevalence of SNV antibody in rodent populations, and consequent risk of HPS in humans (Abbott et al., 1999; Engelthaler et al., 1999; Glass et al., 2000; Mills et al., 1999a; Yates et al., 2002). A few novel studies have taken a more quantitative approach with satellite imagery (Glass et al., 2000, 2002). However, we still lack a clear understanding of how changing climatic conditions lead to changes in host demography (survival, maturation and birth rates) and increase the risk of disease outbreaks. Several recent studies have highlighted the importance of reservoir demography on human risk. Because hantaviruses cause chronic (often life-long) infection in their natural hosts, antibody is often used as a marker of infection (Mills et al., 1999b). Madhav et al. (2007) demonstrated delayed density dependence in antibody prevalence, and Calisher et al. (2001) demonstrated that populations with an older age structure have higher antibody prevalence.

Reservoir demography can be affected by both density-dependent and independent processes. Understanding both processes and their interaction may be needed in order to fully understand reservoir demography and what leads to outbreaks. There is now a broad consensus that both density-dependent and independent factors are important in population ecology, but their relative importance may vary among and within species (Higgins et al., 1997; Lewellen and Vessey, 1998b; Lima et al., 2001; Merritt et al., 2001). This is illustrated by the wealth of studies of population dynamics of rodents. Northern Fennoscandian rodent populations, for example, undergo regular cycles thought to be due to delayed density dependence mediated by specialist predators and competition (Stenseth et al., 1996). These populations are therefore thought to be predominantly under density dependent controls. In contrast, populations of the muroid genera *Peromyscus* in North America and its sister genus, *Apodemus*, in Eurasia, while showing evidence of density dependent competition for space (e.g., Saitoh et al., 1999), are significantly influ-

enced by external drivers. These drivers include large scale climatic oscillations (Brown and Heske, 1990; Glass et al., 2002; Stapp and Polis, 2003) and more local scale fluctuations in productivity such as acorn mast (Ostfeld et al., 2006; Shimada and Saitoh, 2006; Wolff, 1996) and periodic emergence of insects (e.g., cicadas and gypsy moths; Elkinton et al., 2004; Marcello et al., 2008).

Since there is no effective treatment or vaccine for HPS, the most effective strategy is prevention. Since human risk is linked to mouse density and demography, in order to understand what leads to spillover, we need to dissect deer mouse population dynamics to determine the relative contributions of endogenous and exogenous factors. A quantitative understanding of how environmental factors affect mouse demography and human risk may allow public health officials to better predict outbreaks and more effectively target prevention strategies.

Using a capture-mark-recapture dataset spanning fifteen years (Douglass et al., 1996, 2001), we evaluated the seasonal and interannual variation in survival, maturation rates and recruitment rates and explored the relative importance of environmental versus density dependent factors on deer mouse demography and dynamics. Because the bottom-up trophic cascade model postulates a delayed response to climate, we carefully evaluated evidence of lagged effects of climatic drivers. We then formulated a population model including climatic drivers to capture the key dynamics of this system and tested its predictive capabilities. Through our capture-mark-recapture analyses we discovered a high level of predictability to the dynamics once key environmental drivers and their lags were taken into account.

## 2.3 Methods

### 2.3.1 Study site and field methods

Long-term studies of deer mice have been conducted in Cascade County, central Montana since June of 1994. The study site is grassland supporting an active cattle ranch where deer mice typically account for over 85% of the small mammal assemblage (Douglass et al., 2001). It is a highly seasonal environment which receives about 36 cm of precipitation a year, mostly in spring. Often this spring precipitation is in the form of snow, which may persist for 2-3 months or last only

a few days, depending on wind and temperature. Temperatures also fluctuate widely; one January it may be  $-37^{\circ}\text{C}$  and next year  $10^{\circ}\text{C}$ , and temperatures in the summer may range from  $1^{\circ}\text{C}$  in the morning to  $35^{\circ}\text{C}$  in the afternoon.

Live trapping was conducted for three consecutive nights each month on two grids (3 km apart) from June 1994 through May 2009. Grids consisted of 100 trap stations equally spaced (10 meters apart) in a square of 0.81 ha with one Sherman live trap per station. Since the mouse abundances on the two grids were significantly correlated (Pearsons product moment correlation test on minimum number alive (MNA);  $R=0.77$ ,  $p < 0.001$ ), we analyzed the capture histories from the two grids jointly. Each captured mouse was tagged with a uniquely numbered ear-tag, its breeding status, body mass and presence of scars noted, and a blood sample taken to test for hantavirus antibody. For a detailed description of the field methods see Douglass et al. (1996).

### 2.3.2 Climatic and vegetation data

Climatic data, including mean temperature and summed precipitation, were obtained from the Western Regional Climate Center ([www.wrcc.dri.edu](http://www.wrcc.dri.edu)). Data were collected from a meteorological tower less than 1 km from the study site (Cascade 20 SSE, Station number 241557). Normalized difference vegetation indices (NDVI) for the study area from 2000 through 2004 were obtained from MODIS satellite

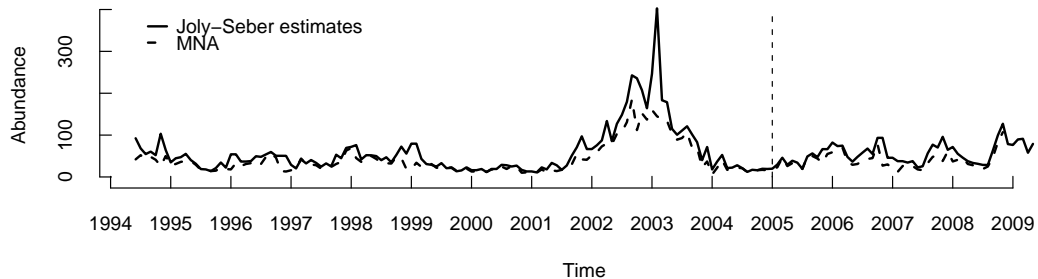


**Figure 2.1.** Monthly abundance of the deer mouse population from two trapping grids in Cascade county, Montana, represented as minimum number known alive (MNA) and Jolly-Seber estimates

data (<http://www.modis.ornl.gov/modis/index.cfm>).

### 2.3.3 Estimating density and demographic parameters

Models were formulated from capture-mark-recapture data from June 1994 through 2004 and were tested against data through May 2009. These data were used to estimate density and demographic rates. Individuals were classified into age classes at each capture occasion based on mass according to the definitions of Fairbairn (1977): juveniles  $< 14\text{g}$ , subadults  $> 14$  and  $< 17\text{g}$ , and adults  $> 17\text{g}$ . For the purposes of this study, we combined juveniles and subadults, because they represent the non-reproductive portion of the mouse population, hereafter called juveniles. For analysis, the data for the three consecutive trapping days were collapsed into one primary trapping occasion, which resulted in 127 monthly primary trapping occasions for the demographic rate analyses, from June 1994 to December 2004, and 180 monthly occasions for the density analysis, through May 2009. We did not use robust design models (Pollock, 1982) because the data for the secondary occasions were not recorded for most of the study. Goodness of fit tests were performed on both the multistrata capture histories (stratum for each age class) and the single stratum histories (without separating juveniles and adults) (Pradel et al., 2003), as implemented in U-CARE (Choquet et al., 2005).

The POPAN formulation (Schwarz and Arnason, 1996) of Jolly-Seber models (Jolly, 1965; Seber, 1965) was used to estimate population density, as implemented in Program MARK (White and Burnham, 1999). We estimated survival ( $S$ ) and maturation ( $\phi$ ) probabilities using multi-strata models (Nichols et al., 1992) and recruitment rates ( $f$ ) using Pradel models (Pradel, 1996), as implemented in Program MARK. We evaluated the appropriateness of including covariates (age class, month, season, year, precipitation, temperature, density, including at several lags) using quasi-Akaike's information criterion ( $\text{QAIC}_c$ ). Covariates were included in models by altering the design matrix using RMark (Laake, 2007), a package for the R software (R Development Core Team, 2005) with an interface to Program MARK. The demographic parameters were essentially modeled as a function of these covariates assuming multinomial errors and a generalized linear framework (McCullagh and Nelder, 1989). The link function was logit for the recapture, sur-

vival and maturation analyses, and log for recruitment. In the capture history data, survival is confounded with emigration and births are confounded with immigration, so the parameters estimated here are apparent survival (hereafter called survival) and recruitment.

For the three demographic parameters, we initially explored a basic set of models, which included constant, age class dependent, monthly, seasonal, yearly and fully time-dependent models, without density and environmental covariates. A large suite of models was subsequently tested, in order to test for significant seasonality, density dependence and climatic forcing, including those containing covariates for month, temperature and precipitation deviation from monthly means and density, at various time lags. We looked at precipitation and temperature lags up to six months; such lags have been shown to affect both grassland primary productivity and small mammal abundance (Collins and Weaver, 1978; Lewellen and Vessey, 1998a; Perry, 1976). Models were ranked based on their QAIC<sub>c</sub> values.

We also estimated seniority probabilities ( $\gamma$ ) for our best model in order to explore the possible contribution of survival versus recruitment on the population growth rate (Nichols et al., 2000). Seniority probability ( $\gamma$ ) is the probability that an individual in the population at the current time step was also there at the previous time step, equivalent to reversing the capture histories and calculating survivorship (Pradel, 1996). From the seniority estimates ( $\gamma$ ), we can determine the relative contribution of survivors and new recruits to the population growth rate,  $\lambda$ , equivalent to elasticities (Caswell and Trevisan, 1994). If  $\gamma < 0.5$ , then recruitment is more important. If  $\gamma > 0.5$ , survivorship is more important.

### 2.3.4 Population Model

To simulate the mouse population dynamics we developed a discrete-time population model with monthly time steps. The model is:

$$N_{t+1} = (S[s, c, d] + f[s, c, d])N_t \quad (2.1)$$

where  $N$  is mouse abundance, and  $t$  is time in months, therefore  $N_{t+1}$  and  $N_t$  refer to the mouse abundance in the next month and the current month, respectively.  $S$  is the probability of survival to the next month, and  $f$  is the recruitment rate per

individual at month  $t$ . Both parameters may be a function of covariates,  $[s, c, d]$ : season (or month), climate and density. To test the predictive power of the model, we used the Pearsons product moment correlation between abundance predicted by the model four months ahead (parameterized from the data through 2004) and MNA or Jolly-Seber abundance estimates (for the full time series through May 2009), using the following equation:

$$Npred_{t+4} = (S_t + f_t)(S_{t+1} + f_{t+1})(S_{t+2} + f_{t+2})(S_{t+3} + f_{t+3})Nobs_t \quad (2.2)$$

where  $Npred$  is the predicted abundance and  $Nobs$  is the observed abundance. We use both MNA and Jolly-Seber estimates because we feel neither is ideal. The MNA estimates do not account for low trappability, whereas the Jolly-Seber estimates were calculated using Program Mark and are not fully independent of the demographic rate estimates. (Robust design models would give population estimates with minimal sampling correlation to vital rates (Kendall and Pollock, 1992), however, the secondary trapping information was not recorded for most of the study. We compared the different population estimates for dates in which we had the additional data, from August 2004 through May 2009, and found that the population estimates using a closed robust design gave estimates very similar to MNA (Pearsons product-moment correlation,  $R=0.93$ ); See Appendix Fig. A1 and Table A1). Formulating the population model from the demographic estimates and comparing the output to the data allows us to test the accuracy of the estimates and test the predictive power of the model.

## 2.4 Results

There was a total of 4288 captures representing 2036 individuals on the two grids over the study period from June 1994 to December 2004 and 5930 captures representing 2770 individuals over the study through May 2009. Minimum number known alive (MNA) as well as Jolly-Seber estimates of abundance were used as indices of population density (Fig. 2.1). Goodness of fit tests on the fully time-dependent mark-recapture statistical models revealed some evidence of lack of fit ( $p < 0.001$ ). There appeared to be a significant number of transients seen

(animals that were passing through the study site en route to other locations;  $\chi^2 = 189.2, df = 114, p < 0.001$ ) as well as some trap-dependence (i.e. trap-happy animals;  $\chi^2 = 318.5, df = 102, p < 0.001$ ). To accommodate the lack of fit, we estimated the correction factor,  $\hat{c}$ , for the QAIC<sub>c</sub>. (As  $\hat{c}$  or lack of fit increases, models with fewer parameters are favored.)  $\hat{c}$  was calculated to be 1.796 for the single stratum capture history data and 1.28 for the multistrata data.

### 2.4.1 Demographic Rates

First we explored the basic suite of mark-recapture models for the demographic rates that did not include covariates (i.e. density, precipitation and temperature). For recapture probability ( $p$ ), the fully time-dependent and age class-dependent model (i.e.  $p \sim \text{age class} + \text{time}$ ) was the most parsimonious (Appendix Table A2). For survival and maturation probabilities, models calculating a separate probability for each month were the best models (according to QAIC<sub>c</sub> values) in the basic suite of models (Table 2.1), demonstrating that seasonality is important for these demographic parameters. For recruitment rates, the year model (an estimate for each of the eleven years of trapping) was the best model (Table 2.2). To explore if precipitation, temperature and/or density could explain some additional variation, we evaluated a large suite of candidate models (Appendix Tables A3 and A4), including covariates, such as precipitation and temperature variables as well as density, at several time lags.

The most parsimonious models were

$$\text{logit}(\text{Survival}_t) \sim \text{month} * \text{Prctp}_{t-5} + \text{month} * \text{Temp}_{t-5} + \text{month} * \text{Prctp}_t + \text{month} * \text{Temp}_t$$

$$\text{logit}(\text{Maturation}_t) \sim \text{month}$$

$$\text{log}(\text{Recruitment}_t) \sim \text{month} * \text{sum}(\text{Prctp}_{t \rightarrow t-4}) + \text{month} * \text{sum}(\text{Temp}_{t \rightarrow t-4})$$

where Prcp is precipitation, Temp is temperature,  $t - 5$  indicates 5 months previously,  $t$  indicates the current month,  $t \rightarrow t - 4$  indicates the current month through 4 months previously, and  $*$  indicates the interaction of two terms in the model (as well as the individual terms). (Tables 2.1 and 2.2 show these models in relation to the basic suite of models, and Appendix Tables A3 and A4 show all the models considered.) Precipitation, temperature and seasonality were important factors ex-

**Table 2.1.** The basic set of statistical models tested for variation in survival ( $S$ ) and maturation ( $\psi$ ) probabilities, along with the most parsimonious model with covariates, using multistrata models in Program MARK.

Model	Npar	QAIC <sub>c</sub>	Weight	QDev
$S(\text{month} * P_{t-5} + \text{month} * T_{t-5} + \text{month} * P_t + \text{month} * T_t) \psi(\text{month})$	211	8056.5	1	3408.9
$S(\sim \text{month}) \psi(\sim \text{month})$	163	8079.9	0	3537.1
$S(\sim \text{age class} + \text{month}) \psi(\sim \text{month})$	164	8081.9	0	3536.9
$S(\sim \text{year}) \psi(\sim \text{month})$	162	8087.3	0	3546.6
$S(\sim \text{age class} * \text{month}) \psi(\sim \text{month})$	175	8088.3	0	3519.4
$S(\sim \text{age class}) \psi(\sim \text{month})$	153	8137.4	0	3616.1
$S(\sim \text{month}) \psi(\sim \text{year})$	161	8138.5	0	3600.0
$S(\sim \text{time}) \psi(\sim \text{month})$	277	8142.7	0	3246.2
$S(\sim \text{year}) \psi(\sim \text{year})$	160	8145.5	0	3609.1
$S(\sim \text{time}) \psi(\sim 1)$	255	8221.5	0	3475.1
$S(\sim \text{month}) \psi(\sim \text{time})$	391	8395.7	0	3330.6

(Npar is the number of estimable parameters. QAIC<sub>c</sub> is the estimated quasi-Akaike's information criterion, using the correction factor,  $\hat{c}=1.28$ , to adjust for lack-of-fit. Weight gives the statistical weight of that model compared to the other candidate models, and QDev is the model deviance. P and T denote precipitation and temperature, respectively; t-5 indicates 5 months previously; t indicates the current month; time denotes the full time-specific variation with 126 values estimated, one for each capture occasion; month denotes 12 values estimated, one for each month of the year; age class denotes 2 values estimated, one for juveniles and one for adults; a one denotes no time-specific variation, which is a single value estimated for all capture occasions; and \* indicates the interaction of two terms as well as the individual terms. For all models capture probabilities were  $p(\sim \text{age class} + \text{time})$  accounting for 127 parameters.)

plaining variation in survival and recruitment rates. Climatic variables important in determining survival were precipitation and temperature in the current month and 5 months previously, whereas the sum of precipitation over the last 4 months and the sum of temperature over the last 4 months were important for recruitment rates. Full equations are given in the appendix (Eqns B1-3). These survival and recruitment models did significantly better (had a lower QAIC<sub>c</sub> value) than the best model in the basic suite of models that did not consider covariates (Tables 2.1 and 2.2). Survival did not appear to be age specific (i.e. models which estimated a separate survivorship for juveniles and adults had higher QAIC<sub>c</sub> values than those

**Table 2.2.** The basic set of statistical models tested for variation in recruitment rates ( $f$ ), along with the most parsimonious model with covariates, using Pradel models.

Model	npar	AICc	Weight	QDev
$f(\sim \text{month} * P_{t \rightarrow t-4} + \text{month} * T_{t \rightarrow t-4})$	175	15232.3	1	1765.7
$f(\sim \text{year})$	150	15259.4	0	1846.8
$f(\sim \text{time})$	265	15334.3	0	1667.5
$f(\sim \text{season})$	143	15587.9	0	2190.3
$f(\sim \text{month})$	151	15591.1	0	2176.3
$f(\sim 1)$	140	15603.2	0	2212.1

(See footnote for Table 2.1.  $P_{t \rightarrow t-4}$  and  $T_{t \rightarrow t-4}$  denote the sum of precipitation and the sum of temperature, respectively, from the current month through 4 months previously. For all models capture probabilities,  $p$ , were fully time-dependent, and survival probabilities,  $\phi$ , were monthly, i.e.  $\phi(\text{month})p(\text{time})$ , accounting for 131 of the parameters.  $\hat{c} = 1.796$ .)

which did not). For comparison, we found that NDVI for the study area from 2000 through 2004 was best explained by month, precipitation 2 months ago, and temperature 3 months ago, and their interactions.

The estimates of monthly population growth rates ( $S + f$ ) ranged from 0.51 to 2.10 with a mean overall growth rate ( $\lambda$ ) of 1.02 (standard deviation ( $sd$ ) = 0.27). Seniority estimates ( $\gamma$ ) for our mouse population ranged from 0.23 to 1.0, with a mean of 0.66 ( $sd$  = 0.15), suggesting considerable variability in the importance of recruitment versus survivorship. However, for 110 out of 126 months,  $\gamma$  was greater than 0.5, indicating that most often, survivorship is more important than recruitment in determining the growth rate of the mouse population.

Seasonality was important for all three demographic rates. Under mean precipitation and temperature conditions, survival was highest in December and January, decreased in the early spring and slowly increased through the summer and fall. Recruitment generally increased through the spring, peaked in the summer, and declined through the fall with another small peak in January. Maturation was low in late fall, increased to a peak in spring, and declined through mid summer with another small peak during late summer. For survival and recruitment rates, the interactions between month and the climatic variables were important, meaning that precipitation and temperature had different effects in different months.

From these models we can describe some likely general trends of the effect

**Table 2.3.** The effect of precipitation (Prpc) and temperature (Temp), occurring during the given season, on recruitment ( $f$ ) 0-4 months later and survival ( $S$ ) 5 months later based on the most parsimonious MARK models.

Season	Effect on demographic rates	
	More Prpc	Warmer Temp
Early spring	$\downarrow f$	$\downarrow f, \downarrow S$
Late spring	$\downarrow f, \downarrow S$	$\downarrow f, \uparrow S$
early summer	$\uparrow f, \downarrow S$	$\uparrow f, \downarrow S$
late summer	$\uparrow f, \uparrow S$	$\uparrow f, \uparrow S$
early fall	$\uparrow f, \uparrow S$	$\uparrow f, \uparrow S$
late fall	$\uparrow f, \uparrow S$	$\uparrow f, \uparrow S$
early winter	$\uparrow f, \uparrow S$	$\downarrow f, \uparrow S$
late winter	$\downarrow f$	$\downarrow f, \uparrow S$

(Up and down arrows indicate an increase or decrease, respectively, in recruitment rate or survival probability. Prpc had mixed to no effect on survival late winter and early spring. The effects were reversed for less Prpc and cooler Temp.)

of precipitation and temperature on demographic rates. The effects of precipitation and temperature on recruitment rates and survival 5 months into the future were fairly consistent across seasons and between other similar models. Recruitment rate was positively correlated with cooler temperatures December through June, warmer temperatures July through October, less precipitation from February through May, and more precipitation July through December (Table 2.3). More precipitation occurring from August through January, less precipitation February and May through July, higher temperatures September through February, and May and June, and lower temperatures April and July through August were positively correlated with Survival 5 months in the future (Table 2.3).

## 2.4.2 Population Model

The above models are more parsimonious than all the other models tested based on QAIC<sub>c</sub>-rankings. It is however important to ask the extent to which they have predictive power relative to long-term population dynamics. To investigate this, we combined the demographic estimates from the best models with our population model (Eqn 2.1), and predicted the abundance for each time point. We used the estimates from the mark-recapture models to predict abundance for the data that

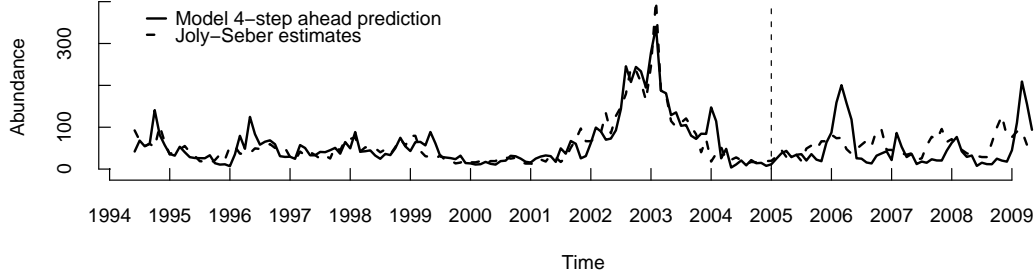


**Figure 2.2.** Four-step-ahead predictions simulated using demographic parameters estimated in MARK for the best models for survival and recruitment, along with the Jolly-Seber population estimates

was not used in the mark-recapture analysis (January 2005 through May 2009). We did 4-step ahead predictions (Eqn 2.2) and then compared the model results with our density indices (MNA and Jolly-Seber estimates), over the study period.

The recruitment rates predicted in this manner contained a few values that were unreasonably high ( $> 1000$ ). These abnormally large values corresponded to several December months. Because of low trappability, the data were particularly sparse for several of the December months, resulting in a large standard error for the  $\beta$  coefficient for the effect of precipitation for December. In order to correct for this sparseness in the data, we averaged the recruitment rates for December through 2003, and used this average,  $f = 0.27$ , for the recruitment rate for December 2004, 2005, 2006 and 2008.

The simulated abundance from the population model predicted 4 months ahead (Eqn 2.2) for the sample data (June 1994 - December 2004) was highly correlated to MNA ( $R=0.85$ ) and to Jolly-Seber estimates ( $R=0.89$ ) (Fig. 2.2). The model did not fit the out-of-sample data as well ( $R=0.26$ ), though the correct range in abundance was predicted. For the whole time series, the model was correlated to the data with  $R=0.79$  for Jolly-Seber estimates and  $R=0.77$  for MNA. The data points for which there was the biggest discrepancy were winter months and these are the months when the data are the sparsest.

## 2.5 Discussion

The objective of our study was to evaluate the importance of seasonality, population density and climate on population dynamics of the deer mouse and formulate population models that can describe the dynamics and forecast abundance. A large amount of the variation seen in the population dynamics of the deer mouse was explained by seasonality, precipitation, and temperature, confirming the importance of density independent forces, and lending significant predictability to this system. Given the current and previous months' precipitation and temperature, we were able to reasonably predict population dynamics several months in advance. Several studies of the effect of food supplementation, acorn masting or periodical cicadas on *Peromyscus* found an increase in population density with increased food availability (Gilbert and Krebs, 1981; Hansen and Batzli, 1978; Marcello et al., 2008; Shimada and Saitoh, 2006; Smith, 1971; Sullivan and Sullivan, 2004; Taitt, 1981; Yunger, 2002), suggesting that many *Peromyscus* populations may be limited by food or at least high quality food. Increasing food items such as the introduced biocontrol agent, gall flies, for knapweed, caused an increase in deer mouse population density in Montana and increased SNV antibody prevalence (Pearson and Callaway, 2006), although other areas in Montana have shown significant increases in density without knapweed (Douglass et al., 2001). If deer mouse populations are often limited by food, increasing primary productivity may increase population density, either directly through an increase in seeds, nuts and fruits, or indirectly through insects.

The time lags between changes in environmental variables and changes in demographic rates indicated by our models (0-5 months) are consistent with those for primary productivity. NDVI was best explained by precipitation at a 2-month lag and temperature at a 3-month lag. So, there was another few months after primary productivity was affected until mouse demography was affected. This lag might be due to time for plants to set seed, for insects to respond, and for mice to reproduce and for their progeny to enter the trappable population. Since environmental variables appear to affect primary productivity and deer mouse demography with a time lag, our study lends support to a bottom-up trophic phenomenon. However, the relationship for our system is not as simple as the more-rain-equals-more-food-

equals-more-mice hypothesis. The effects of precipitation and temperature depend on the month and for some months were not as we had predicted; higher temperatures and more precipitation during the summer through early winter (not in the spring) were correlated to increased survival and recruitment. Previous studies have shown that spring precipitation best predicts grass production, but fall-through-summer precipitation better predicts total forage production (Noller, 1968; Whitman and Haugse, 1972). Our results are not unlike those reported for deer mouse populations in Colorado where populations responded favorably to rainfall during warm periods, but crashed when high rainfall occurred during cold periods (Calisher et al., 2005a; Mills, 2005).

In our analysis, juvenile survival was not significantly different from adult survival. Conventional wisdom is that *Peromyscus* juveniles have a higher mortality rate than adults (Myers and Master, 1983; Terman, 1968). We speculate that the juveniles we captured had already survived the period of high mortality (in the nest or while dispersing) before entering the trappable population. The finding that recruitment is affected by environmental factors from the current month through 4 months previously suggests that we are detecting a combination of immigration and in situ reproduction, since gestation and growth of offspring before leaving the nest would take approximately two months. The small peak in recruitment in January under mean environmental conditions is most likely due to immigration, given the well-known seasonality in reproduction in the deer mouse (Douglass et al., 2001).

Our population model formulated with the most parsimonious MARK models for survival and recruitment accounted for most of the variation seen in mouse abundance for the sample data, but a significant amount of unexplained variation was seen in the out-of-sample data. Some of this reduction in the correlation coefficient can be explained by the restricted range of mouse abundances observed during the out-of-sample period. (As is well known, the statistical  $R$  is both a function of the overall predictability of any given system and the range of observed values along the abscissa.) If we, for example consider the in-sample predictability of abundances that covers the range of the out-of-sample forecast (0-100 individuals), the in-sample  $R$  is reduced by about half to 0.46, more comparable to our out-of-sample predictability of 0.26. There were a large number of models tested, so it is

possible that some associations could occur by chance. However, for the recruitment analysis, most models containing precipitation and temperature (whatever the lag) did better than time varying, monthly or yearly models, suggesting a real effect of the environmental factors. There may be a number of sources for the remaining unexplained variation. Our models did not consider predation, parasitism or interspecific competition - all factors that have been implicated in deer mouse demography (Grant, 1971, 1972; Kaufman and Kaufman, 1989; Pedersen and Greives, 2008). Furthermore, some of the covariates may have non-linear influences on demographic rates other than those implied by the logit- and log-links associated with the mark-recapture formalism. We also did not consider time lags longer than 6 months; there is evidence that precipitation can have lagged effects of up to 2 years, perhaps by increasing soil moisture or altering nutrient cycling rates (Perry, 1976). Delayed-density dependence of longer lags has been implicated in certain small rodents. However that is typically associated with cyclic populations of voles and lemmings and has not been reported for *Peromyscus* or *Apodemus* (see, for example, Saitoh et al., 1999) for a sympatric comparative analysis). Acorn mast (Elkinton et al., 1996; Jones et al., 1998) and knapweed (Pearson and Callaway, 2006) have been shown to affect *Peromyscus* abundance but were not found at our study site. Another possibility is that environmental factors operated differently during the first part of the study than the last. The inability of the model to predict abundance well for the out-of-sample data suggests that more data collection is necessary in order to fully understand climatic influences on deer mouse population dynamics. The uncertainty in the winter months seems to be particularly important.

Understanding what leads to changes in deer mouse abundance is important for predicting Sin Nombre virus epizootics. Hantaviruses are directly transmitted and thought to have density dependent transmission (Madhav et al., 2007), therefore, mouse abundance affects the possibility and size of epizootics. Several previous studies have suggested qualitative correlations between environmental factors and deer mouse population dynamics. Our study quantitatively described this correlation through changes in demographic rates. While it is true that we found the link to be complex, a significant amount of the variability seen in mouse abundance can be predicted from climatic drivers. This is encouraging because it suggests

that armed with a more precise understanding of the links and time-lags between climatic conditions and deer mouse increases, we may be able to better predict epizootics. This particular model may not apply to the southwestern US, because the climate and habitat types are quite different; a separate analysis may be needed for each region of concern. We are currently testing the model to determine its applicability to other field sites in Montana with different habitat types (i.e. sagebrush and pine forests) and formulating an epidemiological model, with the aim to relate environmental forcing to number or proportion of individuals infected. A better understanding may allow public health officials to enhance HPS prevention strategies, as well as help scientists predict possible effects of climate change on hantavirus-host dynamics.

## 2.6 Acknowledgements

We thank Kent Wagoner for database management and design of specialty software and the private ranch owner, Dr. David Cameron, in Cascade County for the use of his property. Kevin Hughes, Arlene Alvarado, Farrah Arneson, Karoun Bagamian, Jessica Bertoglio, Brent Lonner, Jonnae Lumsden, Bill Semmons, and Amy Skypala provided valuable assistance in the field. Thanks also to Scott Carver for field mentoring and ponderings. Financial support was provided by the National Institutes of Health (NIH) grant P20RR16455-05 from the INBRE BRIN program, the U.S. Centers for Disease Control and Prevention, Atlanta, GA, through cooperative agreement US3/CCU813599, and an Academic Computing Fellowship, Penn State University.

## 2.7 Notes

This chapter was published as Luis et al. (2010) in *Journal of Animal Ecology*. Richard Douglass, James Mills, and Ottar Bjørnstad were coauthors. Richard Douglass oversaw data collection in the field and assisted with my understanding of the ecological system. James Mills assisted in the editing of the manuscript. Ottar Bjørnstad assisted with understanding of general concepts and editing of the manuscript.

## Sin Nombre Hantavirus Decreases Survival of Male Deer Mice

### 3.1 Abstract

How pathogens affect their hosts is a key question in infectious disease ecology, and it can have important influences on the spread and persistence of the pathogen. Sin Nombre virus (SNV) is the etiological agent of hantavirus pulmonary syndrome (HPS) in humans. A better understanding of SNV in its reservoir host, the deer mouse, can help lead to improved prediction of circulation and persistence of the virus in the mouse reservoir and help identify the factors that lead to increased human risk of HPS. Using mark-recapture statistical modeling on longitudinal data collected over 15 years, we found a 15.4% decrease in survival of male deer mice with antibody to SNV compared to uninfected mice. Males were also on average 1.5 times as likely to become infected than females. The data identified that transmission was consistent with density dependent transmission, implying that there may be a critical host density, below which SNV cannot persist. Perhaps these observations coupled with the previously overlooked fatality in the host population can contribute to a better understanding of why SNV often goes extinct locally and only seems to persist at the metapopulation scale and why human spillover is episodic and hard to predict.

## 3.2 Introduction

The effects of a pathogen on its reservoir host can have important consequences on the transmission and persistence of the pathogen. Historically, the conventional wisdom was that well-adapted pathogens should be relatively harmless to their hosts, although current evolutionary tradeoff theory shows that an intermediate level of virulence can be the optimal strategy for directly transmitted pathogens (Frank, 1996). More virulent pathogens may have a shorter infectious period because they may kill the host or induce a strong immune response. However, they are often more transmissible, since increased parasite reproduction and shedding are often correlated to virulence. At the population level, they may be more likely to invade, but experience wider fluctuations in prevalence and are more likely to go extinct or have a higher critical community size (King et al., 2009). Although theory can provide important insights on expected patterns and processes, empirical evidence of how chronic infections affect reservoir hosts of zoonotic diseases in nature is rare (but see Telfer et al., 2002; Kallio et al., 2007). We examine the effect of Sin Nombre virus (SNV) on the reservoir host, the deer mouse (*Peromyscus maniculatus*), using mark-recapture statistical modeling and long-term field data.

Although SNV is the etiologic agent of hantavirus pulmonary syndrome (HPS) and can have a 40-60% mortality rate in humans, it has traditionally been thought to cause a chronic, avirulent infection in its reservoir host, the deer mouse (*Peromyscus maniculatus*) (LeDuc, 1987; Mills et al., 1999a). Both laboratory and field studies have revealed that in the deer mouse reservoir, the virus is horizontally and directly transmitted (Botten et al., 2002; Mills et al., 1999a). Virus is shed in infected rodents urine, feces and saliva, and transmission occurs through inhalation of aerosolized virus or through aggressive encounters among mice (Mills et al., 1999a). Infection appears to be life-long, however recent studies reveal that infected mice may move from an acute phase, in which virus is readily isolated from blood and tissues, to a chronic phase, in which virus is only detected intermittently (Botten et al., 2003; Kuenzi et al., 2005); and infected mice may be most infectious in the first few months after infection (Botten et al., 2000).

Authors of published studies generally assume or claim that there is no effect of SNV on the deer mouse reservoir host (i.e. Calisher et al., 1999; Botten et al.,

2000; Easterbrook and Klein, 2008). Indeed, there has been a long-standing belief that hantaviruses have experienced a long coevolutionary history with their rodent hosts, possibly dating back to the divergence of higher muroid taxa (i.e. Yates et al., 2002; Jackson and Charleston, 2004; Plyusnin and Morzunov, 2001). It has been postulated that during this long coevolutionary history, the rodent hosts may have evolved adaptations to mitigate detrimental effects of infection (Easterbrook and Klein, 2008). However, this conflicts with life history trade-off theory that predicts an intermediate level of virulence is often the evolutionarily favored strategy (Frank, 1996). Regardless, recent phylogenetic studies refute the claim of a long coevolutionary history. The time to most recent common ancestor of hantaviruses in the sub-family Sigmodontinae was found to be only approximately 200 years ago (Ramsden et al., 2008). Finally, mathematical theory broadly predicts that chronic, avirulent pathogens should exhibit a pattern of stable endemicity akin to logistic growth within the host population. This seems at odds with the empirical pattern of sporadic disappearance of the virus and recurrent epidemics seen in the deer mouse reservoir (Douglass et al., 2001). A chronic pathogen at the edge of local persistence however, could also lead to the observed dynamics.

Evidence is slowly mounting that SNV infection in its deer mouse host is not as asymptomatic as previously supposed. Netski et al. (1999) saw changes in lung morphology in infected deer mice, similar to humans with HPS. However, Botten et al. (2000) reported no histopathologic changes even when RNA load was high. Douglass et al. found a decrease in weight gain for newly infected males (2007) and a decrease in persistence on the study site for antibody positive juveniles and subadults (2001). However, probability of capture was not taken into account; it needs to be determined if antibody-positive mice are less likely to be recaptured or less likely to survive.

Using capture-mark-recapture analyses on 15 years of longitudinal data, we examine the hypothesis that there is SNV-induced reduction in survival in deer mice. These data also give us a chance to examine the competing hypotheses of density-dependent transmission (transmission proportional to density of infected individuals) versus frequency-dependent transmission (transmission proportional to the frequency of infected individuals; McCallum et al., 2001), by testing which model for the force of infection (the probability of becoming infected per unit

time) is best supported by the data. This question is of great applied interest because important dynamic properties relating to persistence and circulation of the pathogen depend critically on how transmission scales with population size. A greater understanding of SNV in its reservoir host, including patterns of transmission and possible disease-induced mortality, would lead to a better understanding of emergence and persistence of the virus in the mouse reservoir and human risk. This is particularly important for this deadly pathogen, since there is no effective vaccine or cure; currently, the best strategy is to take preventative measures.

### **3.3 Methods**

#### **3.3.1 Field Site and Animal Processing**

Long-term studies of deer mice have been conducted in Cascade County, central Montana since June of 1994. The study site is agricultural grassland where deer mice typically account for over 85% of the small mammal assemblage (Douglass et al., 2001). Live trapping was conducted for three consecutive nights each month on two grids (3 km apart) from June 1994 through December 2008. Grids consisted of 100 trap stations equally spaced (10 meters apart) in a square of 0.81 ha with one Sherman live trap per station. Since the mouse abundances on the two grids were significantly correlated (Pearsons product moment correlation test on minimum number alive (MNA);  $R=0.77$ ,  $p<0.001$ ), we analyzed the capture histories from the two grids jointly. Each captured mouse was tagged with a uniquely numbered ear-tag, its breeding status, body mass and presence of scars noted, and a blood sample taken. Whole blood samples were tested for IgG antibodies to SNV using an enzyme-linked immunosorbent assay (ELISA) at the Montana Department of Health and Human Services or the Montana State University. For a detailed description of the field methods see Douglass et al. (2001).

#### **3.3.2 Capture-Mark-Recapture Analysis**

We analyzed the capture histories using capture-mark-recapture (CMR) statistical modeling (Lebreton et al., 1992), as implemented in Program MARK (White and Burnham, 1999). We collapsed the three consecutive secondary trapping occa-

sions into one primary trapping occasion, which resulted in 175 monthly trapping occasions. To estimate probability of recapture ( $p$ ), survival ( $S$ ), and force of infection ( $\psi$ , probability of becoming infected over the one month trapping interval), we used multistrata models (Nichols et al., 1992), with two strata, SNV antibody-negative mice and SNV antibody-positive mice. Goodness of fit (GOF) tests were performed on the multistrata capture histories (Pradel et al., 2003) using U-CARE (Choquet et al., 2005). We evaluated the appropriateness of including covariates, such as sex, seasonality (or month), and antibody status, using Akaike's information criterion (AICc). Minimum number known alive (MNA) was used as an index of density and in the same way, minimum number infected (MNI) was calculated and used as an index of number infected. Covariates were included in the models by altering the design matrix using RMark (Laake, 2007), a package for the R software (R Development Core Team, 2005). Probability of recapture, survival, and force of infection were essentially modeled as a function of these covariates, assuming multinomial errors and a generalized linear framework (McCullagh and Nelder, 1989). The link function was logit for all three parameters. In the capture history data, deaths are confounded with emigration, so the parameter estimated here is apparent survival hereafter called survival.

### 3.4 Results

Over the 15-year study period, there were 5,930 captures of 2,770 different mice. GOF tests revealed the most general model fit the data well (males:  $\chi^2$

**Table 3.1.** Mark-recapture models for probability of recapture,  $p$ , using the following models for survival and force of infection:  $S(\sim \text{antibody status})$   $\psi(\sim \text{antibody status})$ .

Model	npar	AICc	Weight
$p(\sim \text{antibody status} + \text{time})$	179	12602.27	0.680
$p(\sim \text{sex} + \text{antibody status} + \text{time})$	180	12604.09	0.274
$p(\sim \text{time})$	178	12608.44	0.031
$p(\sim \text{sex} + \text{time})$	179	12609.94	0.015
$p(\sim \text{month})$	16	13363.39	0.00
$p(\sim \text{antibody status})$	6	13672.59	0.00
$p(\sim \text{antibody status} + \text{sex})$	7	13673.92	0.00

=324.7, d.f.=316, p=0.356; females:  $\chi^2=192.8$ , d.f.=270, p=1.00). The best model (lowest AICc value) for probability of recapture included antibody status and time (a different value for each of the 174 months) (Table 3.1). Antibody-positive individuals were more likely to be recaptured than antibody-negative individuals (mean probability of recapture, 0.74 vs. 0.58). Both sex and antibody status, as well as month, were important for the probability of survival over the one month trapping period. Antibody positive males had on average a 15.4% decrease in survival compared with antibody negative males and females (Fig 3.1). Therefore, the best model by AICc was a model that contained a dummy variable for the interaction between sex and antibody status, in which survival for infected males was estimated separately from females and uninfected males (Table 3.2).

We investigated two types of models for force of infection (probability of becoming infected each month),  $\psi$ : the density dependent model, for which the force of infection is a function of the density of infected individuals in the previous month ( $I_{t-1}$ ), and the frequency dependent model, for which the force of infection is a function of the prevalence of infection ( $I_{t-1}/N_{t-1}$ ). We also tested for sex differences and seasonality (using month as a covariate). The best model for the force of infection included sex and a density dependent formulation (Table 3.2). On average, females had a 0.94% chance of becoming infected (and surviving long enough to develop detectable antibody) each month, and males had a 1.4% chance.

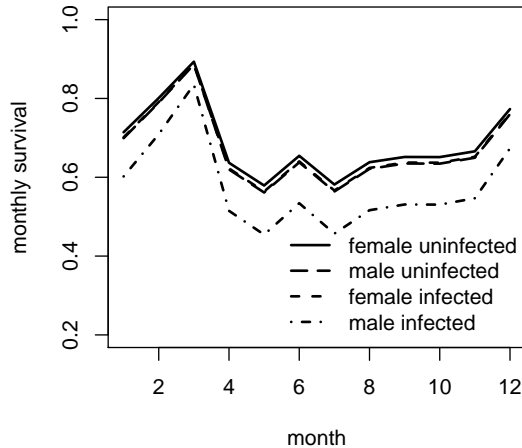


**Figure 3.1.** Monthly probability of deer mouse survival for the model,  $S(\sim \text{sex} * \text{antibody status} + \text{month})$   $p(\sim \text{antibody status} + \text{time})$   $\psi(\sim \text{sex} + I_{t-1})$ .

**Table 3.2.** Mark-recapture models for survival,  $S$ , and force of infection,  $\Psi$ , using the best model for recapture,  $p(\sim\text{antibody status}+\text{time})$  accounting for 175 parameters.

Model	npar	AICc	Weight
$S(\sim\text{dummy} + \text{month}) \psi(\sim\text{sex} + I_{t-1})$	192	12481.16	0.363
$S(\sim\text{dummy} + \text{month}) \psi(\sim I_{t-1})$	191	12481.28	0.342
$S(\sim\text{sex} + \text{antibody status} + \text{month}) \psi(\sim I_{t-1})$	192	12483.21	0.130
$S(\sim\text{sex} * \text{antibody status} + \text{month}) \psi(\sim I_{t-1})$	193	12483.70	0.102
$S(\sim\text{sex} + \text{month}) \psi(\sim I_{t-1})$	191	12485.77	0.036
$S(\sim\text{month}) \psi(\sim I_{t-1})$	190	12486.81	0.021
$S(\sim\text{dummy} + \text{month}) \psi(\sim I_{t-1}/N_{t-1})$	191	12489.83	0.005

### 3.5 Discussion

Although some recent studies have suggested that SNV infection in deer mice may be symptomatic and influence the survival of deer mice, this question has not previously been addressed directly. We addressed this issue by comparing survival of antibody-positive and antibody-negative mice and found a decrease in survival of infected deer mice. Interestingly, this 15.4% decrease in survival was only seen in infected males. Males were also 1.5 times more likely to become infected than females in a given month.

This 15.4% reduction in survival is likely to be an underestimate since we do not know how long after infection animals are likely to experience disease induced mortality. We speculate that the length of the incubation period would be 2 to 4 weeks, since substantial RNA levels can be detected at one week and peaked at 3 weeks post infection (Botten et al., 2000). Unfortunately, we also do not know precisely when many infected individuals acquired infection. Using the presence of antibodies to the virus as a marker of infection means we cannot detect infected individuals until after they develop detectable antibody, which appears to also take approximately 2 to 4 weeks (Botten et al., 2000). Infected mice that experience disease-induced mortality would only be detected if their incubation period is longer than their time to seroconversion. Inter-trapping intervals longer than the time to seroconversion would also decrease detection of infected individuals. If the incubation period is shorter than the one month inter-trapping interval, we may not detect animals experiencing disease-induced mortality, depending on when they became infected in relation to the trapping occasions. Therefore, there

may be higher prevalence and incidence in the reservoir population than the longitudinal data suggest.

Previous research established that, in mammals, males tend to have a greater prevalence and intensity of many micro- and macroparasitic infections than females, possibly through increased exposure or increased susceptibility mediated through sex hormones, such as testosterone (Poulin, 1996; Klein, 2000), or sexual size dimorphism (Moore and Wilson, 2002). Males often have larger home ranges, disperse more, and have more aggressive contacts than females (Klein, 2000), which could increase their exposure to diseases. Male Norway rats infected with Seoul hantavirus tended to have higher circulating testosterone and neurotransmitters that may contribute to aggression and increase the likelihood of transmission through bites (Easterbrook et al., 2007). *Peromyscus sp.* have also been shown to increase social contacts with an increase in testosterone (Gear et al., 2009). Testosterone has been shown to decrease both humoral and cell mediated immune responses (Ahmed et al., 1985; Klein, 2000), and castration of males can increase protection to both micro- and macroparasites relative to that of females (Ahmed et al., 1985). Another possible mechanism for sex-biased parasitism is sexual size dimorphism; the larger sex may be exposed more to infection (because it is a larger target), or there may be an energetic tradeoff between somatic growth and immune function (Moore and Wilson, 2002). Male-biased mortality is common and has been correlated to male-biased parasitism (i.e. Moore and Wilson, 2002; Grobler et al., 1995). If our analyses had not included the SNV data, we would have seen a male bias in overall mortality, although it would be weak (male  $\beta$  coefficient for  $S \sim \text{sex} + \text{month}$ , -0.09, SE=0.05). With the additional data on SNV prevalence we were able to determine that this male biased mortality is associated with infection.

Our results suggest that transmission of the virus is density dependent, rather than frequency dependent. This is a common assumption for directly transmitted pathogens (McCallum et al., 2001), although empirical evidence is equivocal (Smith et al., 2009). Aggressive encounters are thought to be an important transmission mechanism, and fights over mates or territory can increase with increased density (Wolff, 1989). These results may also help shed light on the sporadic disappearance of the virus from the population. For pathogens with density dependent

transmission, there is a critical host density necessary to get disease invasion or persistence. We recently showed that environmental conditions have a strong impact on the population dynamics of the deer mouse (Luis et al., 2010). If the environmental carrying capacity drops below the critical host density, the pathogen cannot persist and will fade-out.

Older males are more likely to be infected with SNV than the rest of the population (Douglass et al., 2001). Therefore, one hypothesis is that infected individuals have a lower survival just because they are older. However, in previous analyses on deer mouse population dynamics, in which we did not consider the infection, we showed that juvenile and adult deer mouse survival were not significantly different in this population (Luis et al., 2010). Furthermore, we also tested a subset of the CMR data used here, including age class in the analysis, and again, models including age class were not significantly better than those without (A. Luis, unpub. data). This suggests that the decrease in survival is not purely a function of age.

With these analyses we are unable to separate mortality and permanent emigration or dispersal. Therefore, the alternative hypothesis is that rather than decrease survival, SNV may make males more likely to emigrate. However, a previous study of dispersal in this mouse population revealed no significant correlation between dispersal and being antibody-positive for SNV (Lonner et al., 2008). Therefore it appears more likely that infection is causing a decrease in survival. Although there was not a significant correlation between dispersal and antibody status, the dispersers were more likely to be adult males with scars, also the subpopulation more likely to be infected (Lonner et al., 2008). If, in fact, infected mice are more likely to emigrate, this could be important for spread and metapopulation persistence of the virus.

Survival is estimated to be high over the winter months, 70-90%, and high survival during winter and low survival in spring have been observed in other rodents (Telfer et al., 2002). In our analyses winter is also when estimated disease-induced reduction in survival is lowest. This is in contrast to the findings of Kallio et al. (2007) that Puumala hantavirus decreased mainly overwinter survival in bank voles. One reason for this discrepancy could be the model structure imposed by the additive survival model,  $S(\sim \text{dummy} + \text{month})$ . If we look at the monthly survival estimates for the model with interactions,  $S(\sim \text{dummy} * \text{month})$ , March and May

were the months with the greatest disease induced reduction in survival. However, the multiplicative model was quite low in the model rankings by AICc (although the deviance was lower, because of the addition of 12 more parameters).

These results, along with those from other studies, should cause us to question the previous belief that SNV causes a chronic, avirulent disease in its reservoir host. It seems more likely that SNV is a moderately virulent virus, with both an acute and a chronic stage. For diseases that cause a reduction in host survival, the infectious period is effectively shortened, which could decrease the spread of the infection and local persistence of the virus. Perhaps the overlooked fatality in infected deer mice along with density dependent transmission can help explain how SNV often goes extinct locally and only seems to persist at the metapopulation scale (Mills et al., 1999a; Kuenzi et al., 1999; Douglass et al., 2001). A quantitative model for the SNV-deer mouse system including disease-induced mortality would be useful for exploring this possibility further.

## 3.6 Acknowledgments

We thank Dave Cameron and Dana Ranch Inc. and the Confederated Salish and Kootenai Tribes at Polson for unlimited access to their properties. K. Hughes, K Coffin, B. Lonner, D. Waltee, R. Van Horn, W. Semmens and T. Wilson provided valuable assistance in the field. S. Zanto provided serologic testing at the Montana State Department of Public Health and Human Services Laboratory; P. Rollin and A. Comer arranged serologic testing at the Special Pathogens Branch Laboratory, US Centers for Disease Control and Prevention. Financial support was provided by the National Institute of Health (NIH) grant P20RR16455-05 from the INBRE BRIN program and the US Centers for Disease Control and Prevention, Atlanta, GA, through cooperative agreement US3/CCU813599.

## 3.7 Notes

This chapter is in review at *Oecologia*. Richard Douglass, Peter Hudson, James Mills, and Ottar Bjørnstad are coauthors. Richard Douglass oversaw data collection in the field. All the authors assisted with editing of the manuscript.

## A Stage-Structured Model for Sin Nombre Hantavirus

### 4.1 Introduction

A new hantavirus named Sin Nombre virus (SNV) was first recognized in 1993 after it caused an outbreak of Hantavirus Pulmonary Syndrome (HPS) in the southwestern U.S. This emerging infectious disease has since been found to occur across most of the U.S., with a majority of cases in the western half of the country. The original outbreak of HPS in the Southwest was preceded by an El Nino Southern Oscillation event which brought increased precipitation to this usually arid region, and it was hypothesized that human infection was the result of an ecological cascade (Parmenter et al., 1993), as follows. Local climatic fluctuations affect primary productivity, altering the food supply for deer mice. An increase in food for the deer mice will increase density and alter the age-structure of the population. This will increase prevalence of SNV in the reservoir population and lead to enhanced human risk of HPS.

Our previous work showed that local climatic fluctuations can have a strong but complex impact on mouse population dynamics in Montana, with temperature, precipitation, and seasonality being strong influences on survival and recruitment rates, accounting for most of the variation seen in deer mouse abundance (Luis et al., 2010). There is also support for this in the southwest (Glass et al., 2002). However, there is still not a clear understanding of how these changing environmental conditions and mouse population dynamics lead to the observed patterns

of SNV infection in the deer mouse reservoir. Nor is it clear how, or if at all, SNV affects rodent demography.

SNV infection dynamics in the deer mouse reservoir host has been notoriously difficult to understand. The virus sporadically disappears from the mouse population and seems to only persist at the metapopulation scale (Mills et al., 1999b; Kuenzi et al., 1999; Douglass et al., 2000; Glass et al., 2002). Most disease models have included a spatial component and posit that there are 'refugia' in which infection is maintained (i.e., Abramson and Kenkre, 2002; Aguirre et al., 2002). When dispersal is included in the models, traveling waves of infection appear (Abramson et al., 2003). The spatial dynamics of these models are difficult to corroborate, since it has not been feasible to carry out field studies at the large spatial scale and the temporal resolution necessary. However, there is evidence of refugia in the Southwest, areas identified as high risk for HPS from satellite imagery, where mouse abundance is greater and with higher prevalences of SNV infection (Glass et al., 2007).

Predicting prevalence in any one area has also been difficult. When the virus is present in a local population, it does not seem to follow typical temporal patterns of incidence or prevalence expected for directly transmitted microparasites. Previous models have assumed that disease transmission is density dependent (increased transmission and prevalence with increased density) (i.e., Abramson and Kenkre, 2002; Aguirre et al., 2002; Abramson et al., 2003; Escudero et al., 2004; Kenkre, 2005), but they have not shown that the data support this. Our previous work indicated that the density dependent formulation for the force of infection (the probability of a susceptible being infected) is better supported by the data than the frequency dependent formulation (Luis, et al. in review; see chapter 3). However, with density dependent transmission one should see increased prevalence with increased density, and the data show either no relationship (Mills et al., 1997; Calisher et al., 1999) or inverse density dependence with higher prevalences at lower densities (Douglass et al., 2001; Calisher et al., 2005b; see Fig 4.5a).

There is evidence of delayed density dependence in prevalence. Madhav et al. (2007) found that antibody prevalence in May was correlated to deer mouse density the previous September. They cited a hypothesis with a 3 step mechanism, as follows (Mills et al., 1999a): Recruitment of uninfected juveniles following the

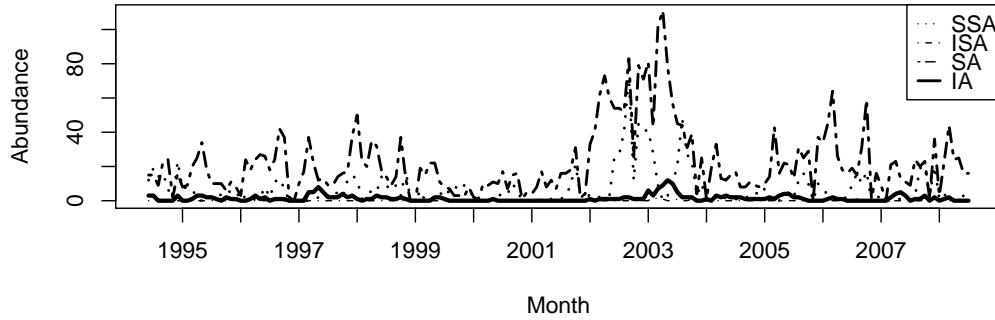


**Figure 4.1.** Abundance of susceptible sub-adults, ( $S_{SA}$ ), infected sub-adults ( $I_{SA}$ ), susceptible adults ( $S_A$ ), and infected adults ( $I_A$ ) over the 15-year study.

spring/summer breeding period results in high densities but low prevalence in the fall. Recruitment halts and cumulative virus transmission and over-winter mortality result in lower population density and high infection prevalence the following spring. Increased crowding over the fall and winter facilitates transmission, and antibody prevalence in the spring is correlated to density the previous fall. Furthermore, Adler et al. (2008) showed that host population dynamics can lead to delayed density dependent prevalence; prevalence in Yates et al. (2002) is correlated to density with an approximately 15 month lag (Adler et al., 2008).

To help understand and predict dynamics, we created a stage structured SI (Susceptible-Infected) model for SNV in the deer mouse reservoir host, which was parameterized from 15 years of field data. We explored how climatic forcing of demographic rates affects the pathogen dynamics, how the pathogen affects the host population dynamics, and conditions required for circulation and persistence of the virus. We estimated age-structured demographic and epidemiological parameters, including transmission rates,  $R_0$ , and critical host density and showed how altering the carrying capacity of the environment can lead to delayed density dependence in prevalence of SNV infection (with a lag of up to 16 months or more) in the mouse population and intermittent crossing of the critical host density necessary for hantavirus endemicity. We also demonstrate that SNV has the ability to regulate the host population, at as much as 25% below the carrying capacity in a high density endemic setting.

## 4.2 A mathematical model

With our stage-structured SI model for SNV infection in the deer mouse, we would like to address these specific questions: Is there a critical host density necessary to get disease invasion? If so, what is this threshold density, and can it help explain the SNV population level patterns we see? Can we get delayed density dependence in prevalence? If so, what affects this delay? Can SNV regulate the deer mouse host population?

### 4.2.1 Density dependent demographics

Our epidemiological model includes background host population dynamics with logistic growth, where the host population experiences density dependence in both birth and death rates. The root of which is the well-known logistic growth equation:

$$\frac{dN}{dt} = rN \left( 1 - \frac{N}{K} \right), \quad (4.1)$$

where  $N$  is the total population size,  $K$  is the carrying capacity of the environment, and  $r$  is the intrinsic growth rate of the population (birth rate,  $b$ , minus death rate,  $d$ ).

In order to separate births and deaths for our age structured population we used this modified logistic formulation, after Gao and Hethcote (1992):

$$\frac{dN}{dt} = N \left( b - ar \frac{N}{K} \right) - N \left( d + (1 - a)r \frac{N}{K} \right), \quad (4.2)$$

where  $a$  is the proportion of density dependence due to density dependence in birth rates. If  $a = 0$ , then birth rates are density independent, and all the density dependence seen is due to density dependence in the death rates, and conversely, if  $a = 1$ , then all the density dependence is in the birth rates. Note that equation 4.2 collapses to 4.1 and that the non-trivial equilibrium is still  $K$ .

We found previously, using capture-mark-recapture statistical analysis, that realized survival and recruitment rates are a function of precipitation and temperature (Luis et al., 2010, chapter 2). We believe that the mouse population growth is strongly density dependent and that precipitation and temperature are moving

the carrying capacity up and down, affecting the realized demographic rates.

#### 4.2.2 The stage structured SI Model with density dependent demographics

In the stage-structured epidemiological model, the mouse population is classified into 3 functional age classes, juveniles ( $J$ ), sub-adults ( $SA$ ), and adults ( $A$ ). We find that juveniles with SNV antibodies become antibody negative over time. Their positive result is most likely due to maternal antibodies, which wane over time (Borucki et al., 2000). Therefore, in the model, the juveniles are not considered susceptible to disease. This assumption will depend on the prevalence of maternal antibodies in the population, but our qualitative conclusions are robust to this assumption. Since SNV infection is chronic and life-long, sub-adults and adults are either susceptible ( $S$ ) or infected ( $I$ ). This leads to 5 classes of mice, juveniles ( $J$ ), susceptible sub-adults ( $S_{SA}$ ), infected sub-adults ( $I_{SA}$ ), susceptible adults ( $S_A$ ), and infected adults ( $I_A$ ). (See figure 4.2 for a life cycle diagram.) Transmission is assumed to be density dependent (see Luis, et al. in review; chapter 3 for the empirical evidence of this), meaning that as density increases, contacts between susceptible and infected individuals increase. Birth and death rates are

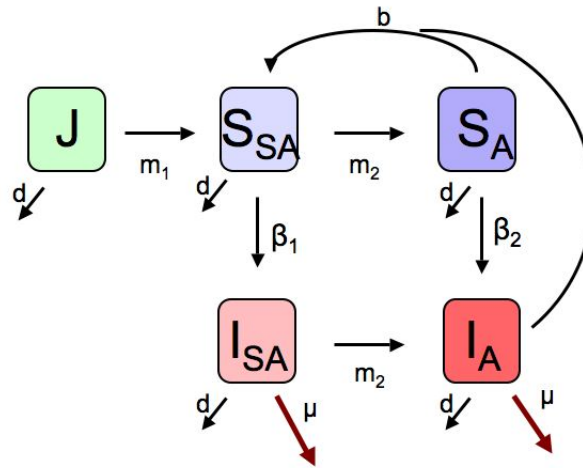


**Figure 4.2.** Life cycle diagram for the system. See tables 4.1 for variable and parameter information.

assumed density dependent as in Eqn 4.2. Maturation from juveniles to sub-adults is constant ( $m_1$ ), but maturation from sub-adult to adult depends on the density of adults, where  $m_2$  is the maximum maturation rate (in the absence of adults). We used this formulation because the presence of adults is known to inhibit sub-adults from maturing and becoming reproductive (Millar, 1989). Since we recently documented that SNV decreases survival, we included a parameter for disease induced mortality ( $\mu$ ) (Luis et al., in review, chapter 3, Douglass et al., 2001). The resulting set of equations is:

$$\begin{aligned}
\frac{dJ}{dt} &= A \left( b - ar \frac{N}{K} \right) - J \left( d + (1-a)r \frac{N}{K} \right) - Jm_1 \\
\frac{dS_{SA}}{dt} &= Jm_1 - S_{SA} \left( d + (1-a)r \frac{N}{K} \right) - \beta_1 S_{SA} I - S_{SA} m_2 \left( 1 - \frac{A}{K} \right) \\
\frac{dI_{SA}}{dt} &= \beta_1 S_{SA} I - I_{SA} \left( \mu + d + (1-a)r \frac{N}{K} \right) - I_{SA} m_2 \left( 1 - \frac{A}{K} \right) \\
\frac{dS_A}{dt} &= S_{SA} m_2 \left( 1 - \frac{A}{K} \right) - S_A \left( d + (1-a)r \frac{N}{K} \right) - \beta_2 S_A I \\
\frac{dI_A}{dt} &= \beta_2 S_A I + I_{SA} m_2 \left( 1 - \frac{A}{K} \right) - I_A \left( \mu + d + (1-a)r \frac{N}{K} \right),
\end{aligned} \tag{4.3}$$

where,  $\beta_1$  is the transmission rate for sub-adults, and  $\beta_2$  is the transmission rate for adults. (See table 4.1 for a list of variables, parameters and their descriptions.) All the parameters can be estimated using the field data as described below. We follow the convention of using Roman letters for demographic parameters and Greek letters for epidemiological parameters. For the statistical estimation (see below) we assume that all of the parameters are nonnegative, and  $a$  to be a proportion, constrained to the interval  $[0,1]$ .

### 4.2.3 $R_0$ , threshold criteria, and equilibria

In the absence of disease, the equilibrium population ( $N^*$ ) will not be  $K$ , but a proportion,  $p$ , of  $K$ .  $N^* = pK$ , where  $p$  is a lengthy function of the demographic parameters, which we estimated numerically. The reason it is not  $K$  is that in this model only adults reproduce. If juveniles and sub-adults also reproduced, the other parameters would cancel out and result in  $N^* = K$ . From this model, we can

**Table 4.1.** Notation used to denote model variables and parameters and their maximum likelihood estimates.

	Estimate	Description
Variables		
$J$		number of juveniles
$S_{SA}$		number of susceptible sub-adults
$I_{SA}$		number of infected sub-adults
$S_A$		number of susceptible adults
$I_A$		number of infected adults
$A$		total number of adults
$I$		total number of infected individuals
$N$		total number of individuals
$K$		carrying capacity
Parameters		
$b$	0.315	maximum birth rate (when $N = 0$ )
$d$	$3.66 \times 10^{-5}$	minimum death rate (when $N = 0$ )
$r$	0.3149	$b - d$
$a$	0.614	proportion of the density dependence attributable to births
$m_1$	2.12	maturation rate from juvenile to sub-adult
$m_2$	1.05	maximum maturation rate (when $A = 0$ ) from sub-adult to adult
$p$	0.879	proportion of $K$ that is the disease-free equilibrium ( $N^* = pK$ )
$\beta_1$	$1.94 \times 10^{-3}$	transmission rate for sub-adults
$\beta_2$	$7.50 \times 10^{-3}$	transmission rate for adults
$\mu$	0.085	disease-induced mortality rate (Luis et al., in review; chapter 3)
$D_{SA}$	0.215	proportion of the population made up of sub-adults at the disease-free equilibrium
$D_A$	0.737	proportion of the population made up of adults at the disease-free equilibrium

derive an expression for the basic reproductive number,  $R_0$ . Where, as always,  $R_0$  is the expected number of secondary cases from a single case in a fully susceptible population. If  $R_0 > 1$ , then a single case will, on average, result in more than one secondary case, and the disease can invade and cause an epidemic. If  $R_0 < 1$ , the disease cannot invade and will fade out. For our model:

$$R_0 = \frac{\beta_1 N^* D_{SA} + \beta_2 N^* D_A}{\mu + d + (1 - a)rp}, \quad (4.4)$$

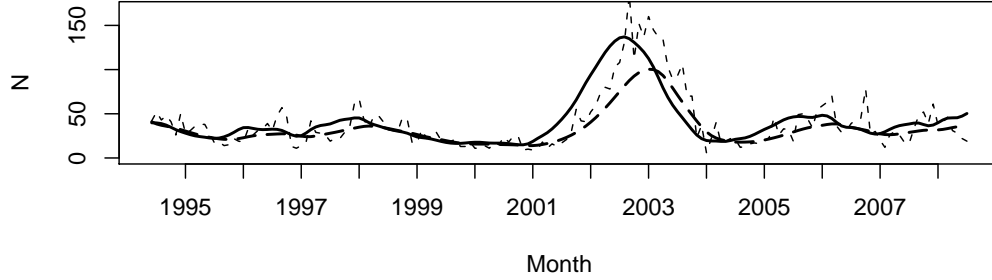


**Figure 4.3.** Minimum number alive, MNA, (light dashed line), carrying capacity,  $K$ , (heavy solid line), used to estimate parameters, and simulated abundance from the model (heavy dashed line).

where  $D$  is the stable age distribution, so that  $D_{SA}$  and  $D_A$  are the proportion of the population that is made up of sub-adults and adults, respectively.

Because the virus has density dependent transmission, and  $R_0$  is a function of density, there will be a critical host density below which the virus cannot invade, (e.g. Anderson et al., 1981). This critical host density,  $N_c$ , is the density at which  $R_0 = 1$ . If the density falls below this threshold,  $R_0$  will drop below one and the disease cannot invade. If the density increases above this threshold, an epidemic is possible. For our model, the critical host density is

$$N_c = \frac{\mu + d + (1 - a)rp}{\beta_1 D_{SA} + \beta_2 D_A}. \quad (4.5)$$

If environmental conditions are favorable,  $K$  increases, the equilibrium density increases, and the mouse population increases above  $N_c$ . If SNV is present, it can persist and cause an epidemic.

#### 4.2.4 Data

To parameterize the model, we used 15 years of mark-recapture data from two trapping grids (3 km apart) in Cascade County, central Montana from June 1994 through December 2008. Deer mice accounted for over 85% of the small mammal assemblage (Douglass et al., 2001). Live-trapping occurred for three consecutive nights each month. Grids consisted of 100 trap stations equally spaced (10 meters apart) in a square of 0.81 ha with one Sherman live trap per station. Individu-

als were tagged with uniquely numbered ear tags and classified into age classes based on weight according to the definitions of Fairbairn (1977): juveniles  $<14$ g, subadults  $>14$  and  $<17$ g, and adults  $\geq 17$ g. Since the mouse abundances on the two grids were significantly correlated (Pearsons product moment correlation test on minimum number alive (MNA);  $R=0.77$ ,  $p= 2.2 \times 10^{16}$ ; Luis et al, 2010), we analyzed the capture histories from the two grids jointly. Individuals were considered infected if they had detectable antibodies to SNV (except for juveniles, as explained above) by enzyme-linked immunosorbent assay (ELISA) at the Montana Department of Health and Human Services or at Special Pathogens Branch, Centers for Disease Control and Prevention, Atlanta, Georgia (Feldmann et al., 1993). For a detailed description of the field methods see Douglass et al. (2001).

#### 4.2.5 Parameter Estimation

We used mouse captures on the two grids as an index for density of the 5 classes. The disease-induced reduction in monthly survival probability for infected deer mice was estimated using mark-recapture statistical modeling as described previously (Luis et al. in review, chapter 3). This probability was converted to a rate for the estimate of disease-induced mortality,  $\mu$ , which was an average of the female and male rates (according to  $\text{rate} = -\log(1 - \text{probability})$ ). We numerically integrated the first-order ordinary differential equations (eq 4.3) as implemented in the 'lsoda' function from the *odesolve* package for R software (R Development Core Team, 2005). Although we do not have an independent measurement of the time varying  $K$  for the system at this time, we use the simplifying scenario that density lags behind  $K$  by a few months. The implicit assumption is that demographic change is relatively fast compared to environmental change. We set  $K$  equal to a smoothed spline of the MNA 4 months ahead. We used these time varying  $K$  values to estimate the remaining parameters in the model using maximum likelihood (e.g., Bolker, 2008). For this, we numerically minimized the negative log-likelihood between the model and the vectors of abundance for the 5 classes over the whole trajectory assuming Poisson errors and using the Nelder-Mead algorithm implemented in the 'optim' function.

### 4.2.6 Analysis

To analyze the lags between density and prevalence, we used the cross correlation function to find the lag which gave the largest correlation for both the data and model. We also ran simulations to determine the effect of the different parameters on the dynamics. Using a push disturbance, from  $K = 50$  to  $K = 120$ , we varied all the model parameters individually ( $b$ ,  $d$ ,  $m_1$ ,  $m_2$ ,  $\beta_1$ ,  $\beta_2$ ,  $a$ , and  $\mu$ ), and determined the lag between maximum density and maximum prevalence, and compared this lag to  $R_0$  for the given parameter values. We ran simulations with different values of  $K$  and determined the time lag between maximum density and maximum prevalence. Also, for different values of  $K$ , starting from equilibrium in the absence of infected individuals, we determined how long it took to reach 5 infected individuals from 1 initial infection.

## 4.3 Results

This relatively simple stage structured SI model has interesting dynamical properties. In the absence of disease, the population reaches disease free equilibrium,  $N^* = pK$ . In the presence of disease, the model shows stable endemic dynamics

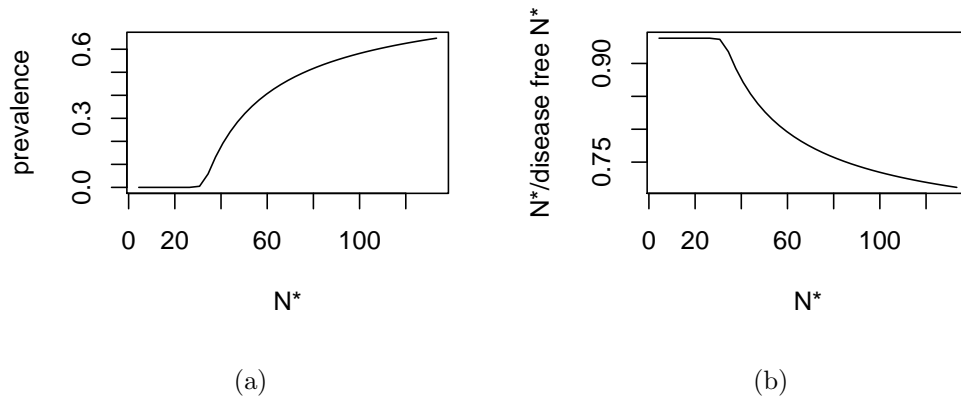


**Figure 4.4.** (a) The prevalence of the virus is determined by the equilibrium population size,  $N^*$ , or  $K$ . As a result, (b) the regulatory impact of the virus is a function of  $N^*$ , shown here as the proportion of the disease free equilibrium population remaining in the presence of the disease.

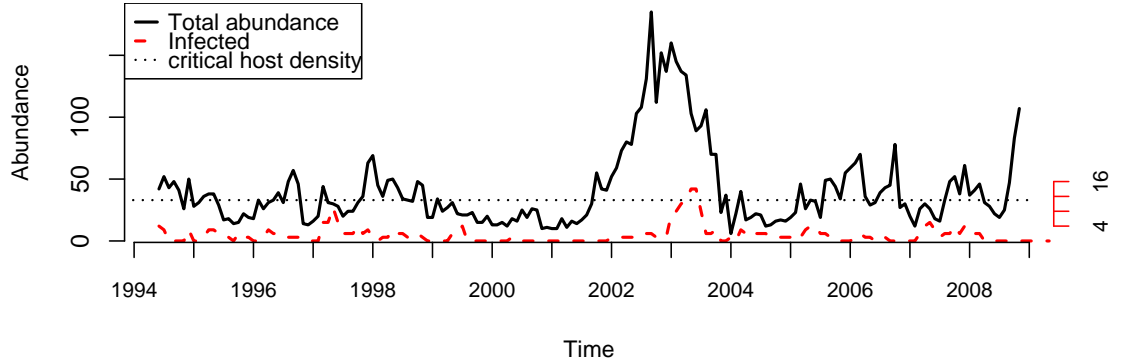


**Figure 4.5.** Deer mouse abundance (MNA; solid black line) over the study period in relation to the critical host density,  $N_c$  (dotted black line), as well as number of infected mice (MNI; red dashed line; scale on the right).

when  $R_0 > 1$ . Increasing  $K$  leads to a linear increase in  $R_0$  and a nonlinear increase in the equilibrium prevalence once the critical host density,  $N_c$  is exceeded (Fig 4.4a).

All maximum likelihood estimates for the model parameters are given in table 4.1. The stable age distribution of the model and the mean age distribution of the data were similar (model:  $J = 0.05$ ,  $SA = 0.21$ ,  $A = 0.74$ ; data:  $J = 0.05$ ,  $SA = 0.19$ ,  $A = 0.76$ ). Using these estimates and assuming the stable age distribution for the model, the critical host density,  $N_c$ , was 33 mice (per 2 ha). We find that in the data, the population was below this critical threshold 52% of the time (Fig 4.5).  $R_0$  ranged from 0.19 to 5.73 in the best environmental conditions, with a mean=1.27, and median=0.96. If we use the number of sub-adults and adults present, rather than the model predicted stable age distribution,  $R_0$  was estimated to be below one 64% of the time.

Disease-induced mortality was estimated from the mark-recapture data as described in Luis et al. (submitted; chapter 3), and as we discussed there, this is likely to be an underestimate. Therefore, we explored the effect of varying  $\mu$  on the pathogen dynamics. The disease-induced mortality affects both  $R_0$  and the critical host density. With the estimated parameters, if there was no disease-induced mortality, the critical host density would be as low as 19 mice; increasing  $\mu$  to 0.2 would increase the critical host density to 53 mice (Fig 4.6).

Although our previous work shows support for density dependent transmission (chapter 3), the prevalence is not predicted to increase with density if looking at the current month (Fig 4.7). Instead, there is clear evidence of delayed density dependence in prevalence. The dominant lag between a peak in abundance and a peak in prevalence was 16 months for both the data ( $R=0.367$ ,  $p < 0.0001$ ,  $CCF=0.348$ ) and the model ( $R=0.90$ ,  $p < 0.0001$ ,  $CCF=0.737$ ) (Fig 4.6). This lag can be seen in the large increase in density in 2002 and the subsequent peak in prevalence in 2003 (see Fig 4.8).

To explore what affects this lag between density and prevalence, we ran simulations individually varying the carrying capacity and model parameters. All the model parameters affected this lag to some extent. By individually varying  $b$ ,  $d$ ,  $m_1$ ,  $m_2$ ,  $\beta_1$ ,  $\beta_2$ ,  $a$ , and  $\mu$ , and calculating both the lag and the  $R_0$  associated with these parameter values, we found that the lag between a peak in density and a peak in prevalence is negatively correlated with  $R_0$  (Fig 4.9a).

We also looked at the effect of  $K$  on this lag. With higher  $K$  values, the population reached equilibrium and maximum prevalence faster, because of increased transmission. To illustrate, for various  $K$  values, starting from equilibrium in the absence of infected individuals, we looked at how long it took to reach 5 infected individuals from 1 initial infection (Fig 4.9b). For a  $K$  value of 50 (near the mean of the data), it took 37 months to reach only 5 infected individuals. With  $K = 150$ , it took 4 months. If the population is not starting from equilibrium, (if  $K$  has just increased), it will take even longer to equilibrate and reach the maximum density and maximum prevalence.

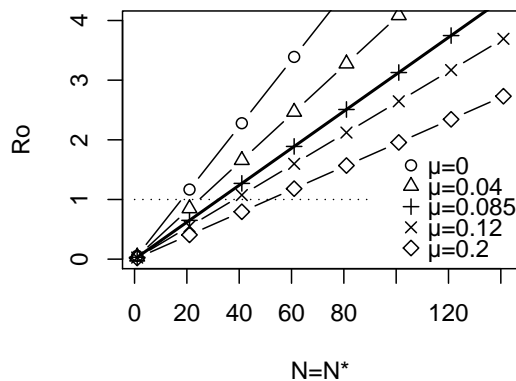


**Figure 4.6.**  $R_0$  as a function of equilibrium population density for several values of disease-induced mortality rate,  $\mu$ . The heavy line is the estimated  $\mu$ , and the dashed line is the threshold quantity, the critical host density,  $N_c$ .

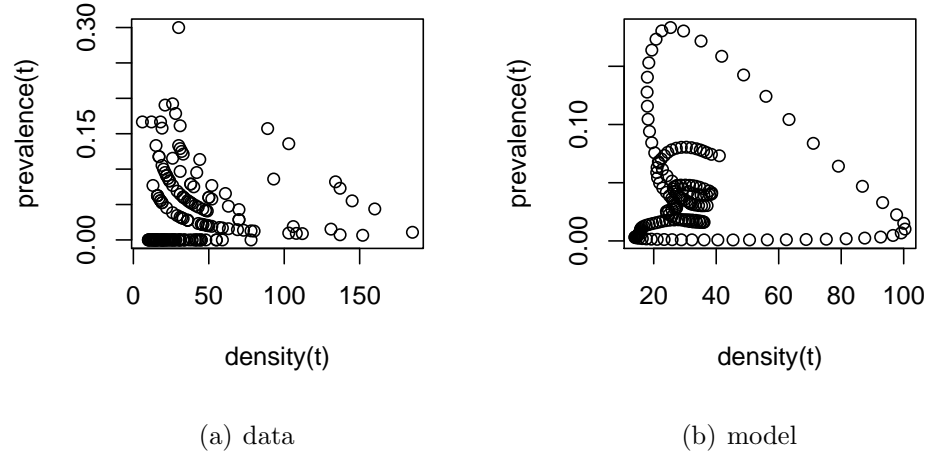


**Figure 4.7.** Prevalence appears to be negatively correlated with current density in both (a) the data and (b) the model, although transmission is positively density dependent.

Since SNV causes disease-induced mortality, it has the potential to regulate the deer mouse population (Luis et al., in review; chapter 3). The strength of the impact on the population is largely determined by the prevalence, which as discussed above, is a function of previous density or carrying capacity as shown in Fig 4.4. For example, for the estimated disease-induced mortality, when prevalence is at 30% (as seen in the study) the population is reduced to 18% below the disease-free equilibrium density (shown in Fig 4.4a as 82% remaining in the presence of disease).

## 4.4 Discussion

This is the most comprehensive study to date of SNV and deer mouse population dynamics, including age-structured demographic and epidemiological parameter estimates, transmission rates,  $R_0$ , critical host density, and impact on the host population dynamics, using detailed long-term demographic data. Several aspects of the observed patterns of SNV infection in deer mice are explained with this simple age-structured SI model. The analysis revealed that approximately 33 mice per 2 hectares are necessary for invasion, and 52% of the time the population

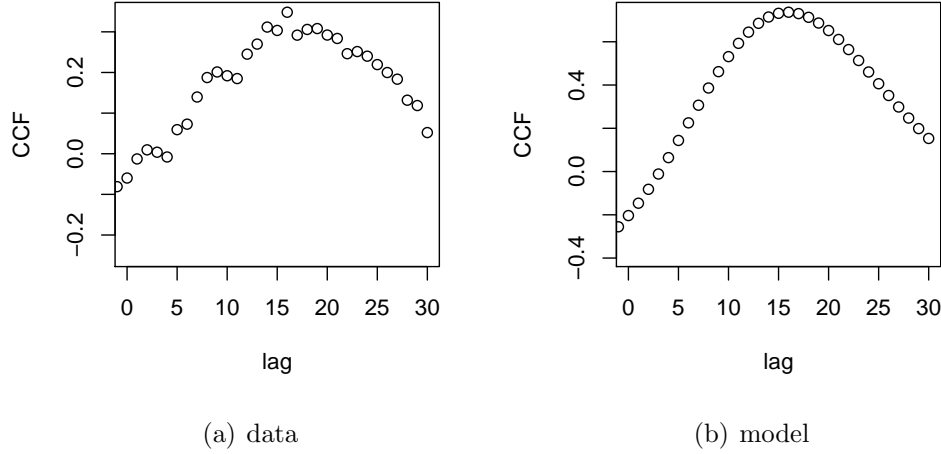


**Figure 4.8.** The strongest correlation between density and prevalence by cross correlation function (CCF) is at a 16 month lag for both (a) the data and (b) the model.

was below this critical threshold. This finding explains the sporadic disappearance of the virus and reintroductions of the virus resulting in only a few infected individuals, rather than an epidemic. SNV in deer mice appears to be at the edge of local persistence. There is local extinction followed by reintroduction by infected immigrants from other populations; the virus must persist at the regional rather than local scale (similar to that described by Glass et al., 2000).

Another pattern elucidated is the relationship between density and prevalence. The two most commonly used formulations for disease transmission are density dependent and frequency dependent transmission (McCallum et al., 2001). One way to determine if transmission is density dependent or frequency dependent is to look at the prevalence of the infection in relation to the density of hosts. If prevalence increases with host density, the infection is said to have density dependent transmission. If prevalence remains roughly the same with increased density the infection is said to have frequency dependent or density independent transmission. The results presented here suggest that the time scale at which this relationship is investigated is important. The current or previous month's density does not appear to be positively correlated to the prevalence of SNV. This may lead one to assume that transmission is not density dependent. However, after

an increase in the carrying capacity and an increase in mouse density, this slowly circulating virus can take months to reach a maximum in prevalence, by which time, the population density may have begun to decline again from a decrease in the carrying capacity. The lag at which a positive correlation between density and prevalence would be found depends on all the demographic and epidemiological parameters, and appears to be longer for pathogens with lower  $R_0$ . In the same way that diseases with a lower  $R_0$  have a higher age at first infection (Anderson and May, 1991), a more slowly circulating virus may take a number of months to build to a maximum prevalence after an increase in density. Another complication is that this lag may not always be the same, even in the same population, because it also depends on the carrying capacity which may be constantly changing. Therefore, even within one time series, determining if the infection is density dependent or independent may be difficult.

A consistent finding in SNV field studies is that older, heavier mice are more likely to be infected (i.e., Abbott et al., 1999; Bennett et al., 1999; Mills et al., 1999b; Douglass et al., 2001). Our results concur; the rate at which adults became infected was almost 4 times greater than that for subadults ( $\beta_2=7.50 \times 10^{-3}$  and  $\beta_1=1.94 \times 10^{-3}$ , respectively). This is fitting since much of the transmission is

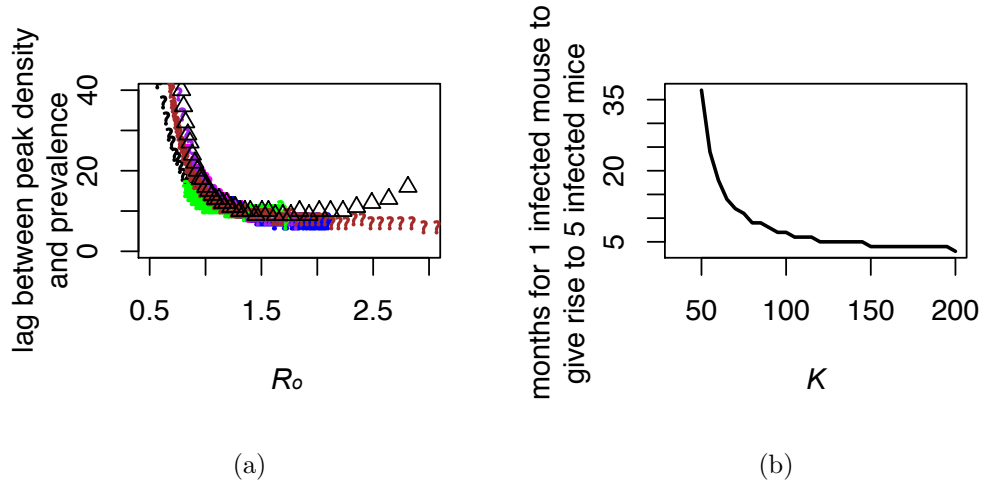


**Figure 4.9.** (a) The lag between a peak in density and the peak in prevalence is negatively correlated with  $R_0$ . (b) The number of months it takes to reach 5 infected individuals from 1 initial infection is negatively correlated with the carrying capacity,  $K$ .

thought to occur through aggressive contacts, which are more common in reproductive individuals (Glass et al., 1988; Mills et al., 1997). However, these findings also suggest that another reason for a higher age at infection is that the virus has a low  $R_0$  and is slowly circulating.

As discussed above, Madhav et al. (2007) found a positive correlation between density in September and prevalence the following May. Since our model did not include seasonality, the delayed-density dependence is not simply due to strong seasonality in birth rates and transmission, although this may explain why prevalence often peaks in the spring (Douglass et al., 2001; Kuenzi et al., 2005; Madhav et al., 2007). Another mechanism proposed by Madhav et al. (2007) and Mills et al. (1999a), dilution by new recruits, appears to be one important mechanism for this delay. An increase in density through an increase in birth rate when environmental conditions are favorable leads to more uninfected mice (since there is no vertical transmission), and a number of months may be necessary for enough transmission to increase the prevalence significantly. A portion of the data used in this study was also used in their study along with data from other field sites in Montana. Madhav et al. (2007) reported an 8 month lag, however in that study they did not examine months other than September and May or different lag times. Our findings suggest that the delay between density and prevalence may vary between field sites if certain demographic and epidemiological rates and environmental drivers differ between habitat types. This is an important area for future study.

Although we were able to explain the SNV epizootic in 2003 after the mouse irruption in 2002, we were not able to explain all other smaller fluctuations in prevalence that occurred when  $N < N_c$ . In these cases, mouse densities were insufficient to sustain a chain of transmission and infections were most likely introduced from an infected immigrant or two which resulted in a stuttering chain of transmission before fading out. This means that we only have data on a single robust outbreak in which the population was above  $N_c$  for a significant amount of time. There were times when  $N$  increased to slightly above  $N_c$  for a few months. However, a much longer time or much larger change in density is needed to cause a significant outbreak. For example, if  $K$  increased to 50, density would increase to 44 mice (which is above  $N_c$ ), and if one infected mouse was introduced it would take 37 months to get enough transmission to give rise to 5 infected mice, because

contact rates and transmission are still low for this density. Long before that time,  $K$  would likely have decreased again and the density fallen to below  $N_c$ , causing the infection to fade out. Therefore, it appears that the 4 or fewer individuals infected at any one month through the rest of the study, were likely stochastic immigration events. Therefore, the largest problem with prediction is the large amount of stochasticity. Although we are not able to predict these smaller fluctuations, the largest threat of HPS to humans probably occurs when  $R_0$  is above one. In support of this, the most human cases per year in Montana (5) occurred in 2003 (unpublished data from the Montana State Department of Public Health and Human Services).

The infected immigrants must be coming from some location where  $R_0$  is greater than 1. SNV studies in the U.S. Southwest have concentrated on finding these 'refugia', small patches of suitable habitat that can support a high enough density of mice to support transmission, even when environmental conditions are unfavorable elsewhere. Using satellite imagery, Glass et al. (2002, 2007) have identified some probable refugia sites in the Southwest, which are characterized by deciduous or mixed forest land cover on moderate to steep slopes above 2130 m elevation and tended to be near water bodies or on mesas or mountains. The refugia sites could be very different in Montana, and more research is needed to try to identify possible habitat characteristics associated with densities above  $N_c$ , where disease can persist.

Previous SNV models assume no disease-induced mortality (i.e., Abramson and Kenkre, 2002; Aguirre et al., 2002; Abramson et al., 2003; Buceta et al., 2004; Escudero et al., 2004; Adler et al., 2008). We estimated the disease-induced mortality rate,  $\mu$ , to be 0.085 (chapter 3), which has important effects on the disease dynamics as well as the host population dynamics. Having disease-induced mortality effectively reduces the infectious period and decreases  $R_0$ , making the virus less likely to invade and more likely to fade-out. The addition of disease-induced mortality in the model increases the critical host density necessary to sustain an epidemic,  $N_c$ . Without disease induced mortality,  $N_c$  would be 19 mice per 2 hectares, whereas with the calculated  $\mu$  of 0.085,  $N_c = 33$  mice per 2 hectares. If  $\mu$  is underestimated (as it may well be; see chapter 3), then it may increase our estimate for  $N_c$ .

Since SNV causes disease induced mortality (chapter 3), it has the potential to regulate the host population. Here, the strength of regulation largely depends on the prevalence of the virus, which is determined by the carrying capacity. During the study, prevalence reached as high as 30%, and during that time, the population may have been regulated to 18% below the disease-free equilibrium. Since there is a delay between an increase in density and an increase in prevalence and the subsequent effect on host population dynamics, this can lead to delayed density dependent regulation, which can lead to destabilization of the host population dynamics (Xiao et al., 2009). However, in this case, the climatic drivers are the dominant force in determining prevalence in this system, which act independent of density, often bringing the population density low enough to cause the virus to go locally extinct.

There is evidence that in rodents, disease transmission may be a saturating function of density, with density dependent transmission at low population densities and frequency dependent at high densities (Smith et al., 2009). This could be explored by replacing the density dependent force of infection,  $\beta SI$ , with a more flexible force of infection,  $\frac{\beta SI}{N^q}$ , which could include frequency dependent transmission (if  $q = 1$ ), density dependent transmission (if  $q = 0$ ), or other relationships between host density and transmission (other values of  $q$ ) (Smith et al., 2009). We explored this question of how SNV transmission scales with deer mouse density, by using the more flexible force of infection, and the maximum likelihood estimate for  $q$  was  $< 0.0001$  (data not shown), indicating that density dependent transmission, as presented here, was appropriate.

Since  $a$  was estimated to be 0.614, this means that density dependence was slightly stronger in birth rates than in death rates. This does not necessarily mean that litter sizes changed with density. Since the birth rate,  $b$ , is estimated from the number of juveniles trapped per adult, it is a combination of litter sizes, number of litters, and nestling survival until entering the trappable juvenile population, as well as early immigration.

Previously, models of SNV have demonstrated interesting theoretical dynamical properties, some of which are described here, such as increasing prevalence with increased density and the presence of a critical host density, which could lead to local extinction after environmental conditions decreased the carrying capacity.

However, only two previous studies have compared or fit their models to field data of SNV infection in deer mice (Peixoto and Abramson, 2006; Adler et al., 2008). Abramson and Peixoto fit a non-age-structured SI model to data from Yates et al. (2002) from Zuni, New Mexico and estimated the critical host density to be 2 mice per hectare (Abramson, 2004; Peixoto and Abramson, 2006). They fit parameters for birth, death, and transmission rates from small subsets of the full dataset, and say to take their estimates "cum grano salis." The time series of density and prevalence confirms a low critical host density; there were infected mice present at densities as low as 2 mice per hectare (Yates et al., 2002). It is interesting how much lower this value is than our  $N_c = 16.5$  mice per hectare. Even without disease-induced mortality, the critical host density for our study would be 9.5 mice per hectare. It is possible that the way in which mouse contact rates vary with density differs between the Southwest and Montana, and transmission is not density dependent in their study. Adler et al. (2008) also fit a non-age-structured model to the data from Yates et al. (2002). They did not calculate a critical host density. There was no carrying capacity in this model; instead, birth and death rates were modeled in two different ways, constant birth rate with time varying death rate or vice versa. The baseline values for birth and death rates were not estimated from those data, but from previously published studies elsewhere. Transmission rates were estimated from the data to match the prevalence seen. Adler et al. (2008) showed that a peak in the density of mice lead to a peak in prevalence 15 months later, very similar to our data. Our study builds on these by giving precise estimates of parameters and the critical host density from detailed long-term field data, exploring what affects the lag between a peak in density and a peak in prevalence, and showing that SNV has the potential to regulate the deer mouse host population.

This relatively simple deterministic model neglects several factors that may be important in the dynamics. Demographic stochasticity could make a difference, when most often  $I < 10$ . However, our deterministic model allowed for fractions of infected individuals, which made intermittent immigration of infected individuals unnecessary. We did not include sex even though males are more likely to be infected (Mills et al., 1999b; Douglass et al., 2001) and experience higher disease-induced mortality (chapter 3). The disease-induced mortality rate used here was an

average of that for males and females, therefore the model had less male deaths and more female deaths than expected in the natural system. It is difficult to surmise what affect this would have on the population since both male and female mice can be promiscuous (Wolff, 1989). However, it is likely that removing males from the population will have less of an impact on the population than removing females, since males can inseminate many females. There is some evidence for increased infectiousness in the first few months after infection (Botten et al., 2000), which could affect the dynamics.

Since there is no effective treatment or vaccine for HPS, the most effective strategy is to take preventative measures. This quantitative understanding of the lags between environmental conditions and prevalence of infection may allow us advance warning (up to 20 months or more) of increased risk to humans. Even without knowledge of what environmental conditions are necessary to raise the carrying capacity, monitoring the density of mice may provide several months warning of a significant increase in prevalence of infection in rodent populations and increased human risk.

## 4.5 Notes

This chapter will be submitted for publication with Richard J. Douglass, James N. Mills, and Ottar N. Bjørnstad as coauthors.

## Hibernation patterns in mammals: a role for bacterial growth?

### 5.1 Abstract

To examine the hypothesis that stimulation of immune function plays a role in periodic arousal from hibernation, bacterial growth during hibernation was estimated using a simple mathematical model of the general dynamics of bacterial abundance at body temperatures experienced during hibernation. In the model, periodic arousals were important for animals infected with *Salmonella* at body temperatures above 7°C, but not below. In contrast, periodic arousals appeared to be important at all temperatures examined when infected with several species of coliform bacteria and *Pseudomonas sp.*, species which grow well at low temperatures. The modeled outputs were compared to torpor patterns seen in captive European ground squirrels, *Spermophilus citellus*, under natural light and temperature conditions. We used maximum likelihood to estimate model parameters and show that the six bacterial species examined are consistent with the immune stimulation hypothesis. Our analyses suggest that bacterial infection could be a selective force on torpor behavior and warrants further experimental investigation.

## 5.2 Introduction

Hibernation is an adaptive strategy used by endotherms when periods of reduced food availability coincide with low winter temperatures and result in increased demand for metabolic energy to maintain body temperature (Karmanova, 1995). Torpid hibernators are thermo-conforming over a wide range of ambient temperatures and allow their body temperature to drop to 1-2°C above the ambient temperature and drastically decrease their cardiac, respiratory and metabolic rates (Geiser and Kenagy, 1988). Indeed, every physiological system seems to be affected (Lyman, 1958; Nedergaard and Cannon, 1990; Karmanova, 1995). The adaptive value of hibernation is to conserve energy, although hibernating animals periodically emerge and their body temperature and cardiac, respiratory and metabolic rates return to normal for a period of usually less than 24 hours (Pengelley and Fisher, 1961; Willis, 1982; Geiser et al., 1990). These periodic arousals can cost animals up to 80% of their stored energy resources (Kayser, 1953; Wang, 1978), but the true function remains unclear and indeed may be multi-factorial. Several hypotheses have been considered to explain these arousals, including, restoration of electrolyte balance, regeneration of gonads, prevention of muscular atrophy, elimination of metabolic wastes, evaporative water loss, replenishment of blood glucose, and elimination of sleep debt (Fisher, 1964; Fisher and Manery, 1967; Galster and Morrison, 1970; Barnes et al., 1986; Wickler et al., 1987; Daan et al., 1991; Thomas and Geiser, 1997). However, several of these hypotheses have been challenged (Willis, 1982), and the true function of periodic arousals remains uncertain.

One additional hypothesis is that periodic arousals are necessary for mounting an immune response to tackle pathogens that invade the host prior to or during torpor (Prendergast et al., 2002). Energetically the immune system is very costly to maintain (Lochmiller and Deerenberg, 2000). Furuse and Yokota (1984) showed that germ free birds fed a diet with limited protein, grew 78% faster than birds with normal gut bacteria. Since hibernation is primarily an adaptation for conserving energy, and the immune system is energetically costly then we would expect hibernators to reduce their response during torpor but to reactivate the dormant immune system by exhibiting periodic arousals that would test the infection status

of the host (Prendergast et al., 2002). Although the effect of hibernation on the immune system has received little attention, a few studies have demonstrated that the activation of lymphocytes, production of antibodies, and the acute phase response to lipopolysaccharide (LPS) are arrested during torpor (McKenna and Musacchi, 1968; Maniero, 2000; Prendergast et al., 2002), so it appears that arousals may be needed to mount an effective immune response.

Hibernating animals may not be able to determine their infection status while in torpor (Prendergast et al., 2002), consequently, they would need to arouse periodically to check for infections. Given the high energetic cost of arousal we should ask how often animals should arouse from torpor. The natural torpor patterns expressed by hibernating animals vary between species and even among individuals of the same species, but some general patterns are observed. For instance, torpor bouts are shortest at the onset of hibernation and become longer as the hibernation season progresses, until prior to emergence when they once again shorten (Geiser and Brigham, 2000; Henning et al., 2002; Hut et al., 2002; Zervanos and Salsbury, 2003). There is good evidence that torpor bout varies with ambient temperature (Ransome, 1971; Geiser and Kenagy, 1988; Geiser et al., 1990; Park et al., 2000). In this study we ask if these patterns could be explained by bacterial dynamics. Presumably, hibernating animals expressing the optimal torpor bout length will be selected for, since if the torpor bout is too long, rampant infection could cause host damage or mortality. On the other hand, if the torpor bouts are too short, the animal would waste critical energy reserves which may lead to reduced condition in the spring or even mortality.

To examine the hypothesis that bacterial infection could account for host torpor patterns, we designed a mathematical model of the optimal torpor patterns that incorporated bacterial growth rates at different host temperatures and then compared outputs with observed torpor arousal data. We asked two specific questions: What torpor patterns could we expect if the function of arousals is to control bacterial infection? Can we explain the torpor patterns observed in European ground squirrels, *Spermophilus citellus*, with our simple mechanistic model? Modeling predicted torpor patterns in relation to bacterial growth could provide insights to direct further experimentation needed to address this hypothesis.

## 5.3 Methods

### 5.3.1 Model and Data

Bacterial growth rates in relation to temperature were estimated using the equation from Ratkowsky et al. (1982):

$$\sqrt{r} = b(T - T_0) \quad (5.1)$$

where,  $r$  is the bacterial growth rate and  $T$  is the temperature. When the square root of the growth rate ( $\sqrt{r}$ ) is plotted against temperature ( $T$ ),  $b$  is the slope of the regression line, and  $T_0$  is the x-intercept. Initially, two representative bacterial species were selected, based on availability of growth rate data in relation to temperature. *Salmonella enterica* data were obtained from Mackey and Kerridge (1988), and a Coliform species (C1) from Baig and Hopton (1969) (Fig. 5.1). Bacterial population growth inside a hibernating animal was examined assuming that bacteria continue to divide at a constant rate with no density dependent food or space constraint. This was described using the doubling equation:

$$N_{t+1} = 2^r N_t \quad (5.2)$$

where,  $N$  is the bacterial population size, and  $r$  is the growth rate of the bacteria ( $\approx 1/\text{generation time}$ ).

When infected during torpor we assume that the bacteria grow exponentially at a rate determined by the host body temperature, until they either damage or kill the host. The immune stimulation hypothesis postulates that there would be a selective advantage amongst those individuals that terminate a torpor bout to let the immune system check and combat any itinerant infection before it causes damage. For this model, we assumed arousal and immune function should occur when the bacteria population reaches  $10^9$ . Although this number is essentially arbitrary, we know that for at least some bacterial pathogens (i.e., *Salmonella enterica*), when numbers increase above  $10^9$ , the host becomes septicemic and may die (Vazquez-Torres et al., 2004). We used this figure as a starting point and then undertook a sensitivity analysis to determine the sensitivity of any conclusions to

this amount. We also assumed that the bacteria infect the host at the beginning of hibernation and that the initial inoculum size is 100 bacteria.

Antibody production during hibernation is insignificant and even during periods of arousal is significantly less than in non-hibernating animals, and takes much longer to reach detectable levels such that it takes several periods of arousal for the acquired immune response to rise (Dempster et al., 1966; McKenna and Musacchi, 1968; Burton and Reichman, 1999). In the model we therefore assume the animals produce no antibodies, and consequently there is no clearance of the bacteria, so the innate immune response is the principle mechanism for controlling infection. The innate response acts to reduce the bacterial population to  $10^5$ , an arbitrary level, but one based on the innate control of bacterial numbers in wildtype mice recorded in both *Salmonella* and *Bordetella bronchiseptica* (Vazquez-Torres et al., 2004; Mann, 2005). We then explored the significance of this level on our final conclusions using a sensitivity analysis. In the model, the animal remains euthermic for 18 hours, which is a typical length of an arousal episode, including re-warming, euthermic period, and cooling below  $30^\circ\text{C}$  (Hut et al., 2002). After 18 hours, the animal returns to torpor, allowing the bacterial numbers to increase again from  $10^5$ .

Next, how the ambient temperature in the hibernaculum and minimum torpor body temperature changed during a hibernation season were considered. A representative profile of minimum body temperature throughout hibernation was recorded in the European ground squirrel by Henning *et al.* (2002; Fig. 5.2c). This temperature profile can be represented over 4320 hours or a 6 month hibernation period by the equation:

$$y = 2 \times 10^{-6}x^2 - 0.0105x + 15.011 \quad (5.3)$$

where,  $y$  is the temperature ( $^\circ\text{C}$ ), and  $x$  is the time (hours). Since the rate of bacterial growth changes with temperature, torpor bout length becomes dynamic using this changing temperature profile in the model. Torpor patterns over an entire hibernation season were predicted with respect to *Salmonella* and coliform C1 bacterial growth, and subsequently other psychrophilic bacteria (after Baig and Hopton) including coliform species designated C4 and EBT and *Pseudomonas*

**Table 5.1.** Estimated slope,  $b$ , and x-intercept,  $T_0$ , for the psychrophilic bacteria in Baig and Hopton (1969) when the square root of the growth rate (divisions per hour) is plotted against temperature (K).

Bacterium	$b$	$T_0$
Coliform species		
C1	0.020	264.77
C4	0.019	265.77
EBT	0.019	264.74
Pseudomonad species		
P11	0.017	264.74
P14	0.022	265.50
P26	0.019	264.55

species P11, P14 and P26 (1969).

The model outputs were compared to observed torpor patterns and corresponding minimum body temperatures collected for six European ground squirrels held in captivity in outdoor enclosures under natural light and ambient temperature conditions from Hut et al. (2002) and one European ground squirrel in the laboratory under simulated natural conditions from Henning et al. (2002).

### 5.3.2 Analysis

In the model, torpor bout length is determined by body temperature throughout the bout. The relationship between minimum body temperature during a torpor bout and torpor bout length for European ground squirrels was explored and compared to the modeled outputs for the six psychrophilic bacteria from Baig and Hopton (1969). Given the European ground squirrel data (Henning et al., 2002; Hut et al., 2002) and our model (equations 5.1 and 5.2), we used maximum likelihood techniques to estimate what parameters for bacterial growth ( $b$  and  $T_0$ ) would be consistent with the immune stimulation hypothesis. We assumed Gaussian likelihoods for the torpor lengths, such that the negative log likelihood is equal to  $(1/n) \log SS$  (e.g., McCullagh and Nelder, 1989), where  $SS$  is the squared difference between the observed and model predicted torpor lengths. Unique maximum likelihood estimates for  $b$  and  $T_0$  were found using the Nelder-Mead algorithm

as implemented in the `optim` function in R (R Development Core Team, 2005). However, because of the strong colinearity between  $b$  and  $T_0$ , there is a range of parameter combinations with almost identical likelihoods. We therefore used two dimensional profile likelihood to map the set of near optimal parameter combinations. We used likelihood ratios assuming  $\chi^2$  distributions with 1 degree of freedom (e.g. McCullagh and Nelder, 1989) to compare the observed bacterial growth data with those expected based on the maximum likelihood estimates. All calculations were done using R version 2.0.1 (R Development Core Team, 2005).

## 5.4 Results

From known temperature dependent growth rates of bacteria, we extrapolated growth rates using equation (5.1) from Ratkowsky et al. (1982) (Table 5.1). Initially, we examined the growth rates of *Salmonella enterica* (Mackey and Kerridge, 1988), and a coliform species (C1 from Baig and Hopton (1969)). At temperatures above 11.5°C, *Salmonella* grows better than coliform, but below 11.5°C, coliform grows better than *Salmonella* (Fig. 5.1).

We examined bacterial growth rates in a hibernating animal with a body temperature of 10°C. For *Salmonella*, which has a growth rate of 0.1074 divisions per hour at 10°C, the initial torpor bout lasted approximately 9 days, and the subsequent torpor bouts were approximately 5.3 days until bacterial numbers reached  $10^9$ . Coliform bacteria have a higher growth rate ( $r = 0.1354$ ) at 10°C than *Salmonella*, and, subsequently, this species reached  $10^9$  faster than *Salmonella*. The model predicted an initial torpor bout of approximately 7.2 days and subsequent torpor bouts of 4.2 days, for this bacterial species.

Running the model using the minimum body temperatures during hibernation described by equation (5.3) gives two distinct sets of torpor patterns for the two bacterial species, *Salmonella* and coliform (Figs 5.2a and b, respectively). Since *Salmonella* does not grow well at temperatures below 7°C, the optimal torpor bouts lengthen since it now takes much longer for the bacteria to reach  $10^9$ . However, since coliform bacteria grow well at these low temperatures, the torpor bout durations only moderately lengthen (Fig. 5.2b). Running the model with other psychrophilic bacteria, coliform species C4 and EBT and *Pseudomonas sp.*

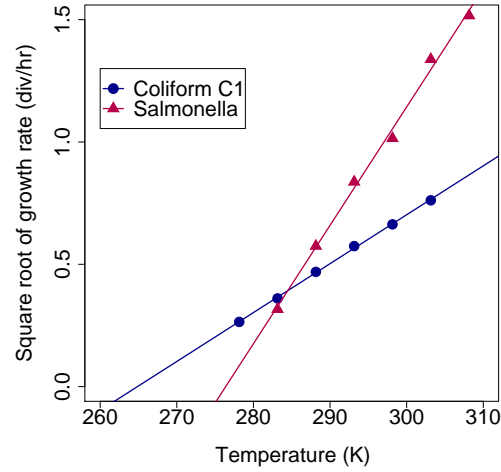


**Figure 5.1.** Relationship between square root of bacterial growth rate and temperature for *Salmonella* (Mackey and Kerridge, 1988) and coliform C1 (Baig and Hopton, 1969)

P11, P14, and P26 (Baig and Hopton, 1969), gives similar patterns as C1 (data not shown). Data from a representative European ground squirrel (figure 1 from Henning et al., 2002) are presented for comparison (Fig. 5.2c).

Using maximum likelihood, bacterial parameters ( $b$  and  $T_0$ ) that give the best fit of the model to the data were calculated as:  $b = 0.0119$  and  $T_0 = 256.700$ . Using these optimal bacterial parameters, torpor bout length was predicted for the body temperatures from European ground squirrels and compared to the corresponding torpor bout lengths recorded. Linear regression gives an  $R^2$  of 0.57. Due to the co-linearity of the model parameters, the result is a ridge in likelihood space (Fig. 5.3). All six bacterial species from Baig and Hopton (1969) (C1, C4, EBT, P11, P14 and P26) are within the 0.01 likelihood ratio statistic, which corresponds to  $p = 0.92$  (1 df).

A sensitivity analysis on the threshold values of  $10^5$  and  $10^9$  revealed that changing these parameters by 10 fold changed the likelihood ratio by just 0.01, which is still highly significant ( $p > 0.85$ ) and makes no substantive differences to the findings of this model.

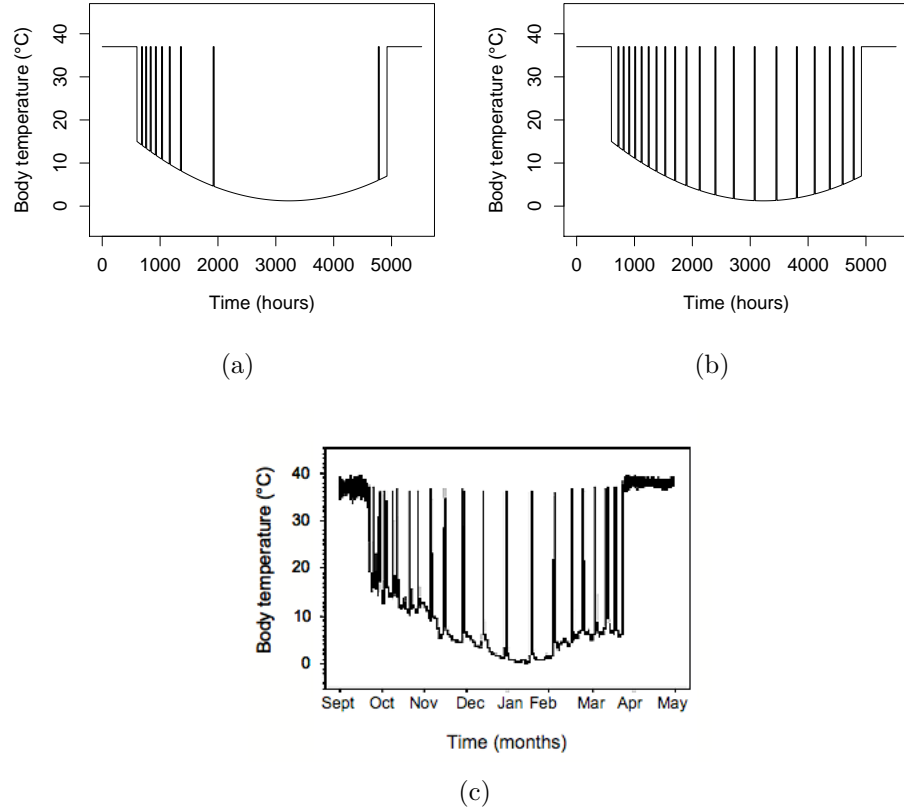


**Figure 5.2.** Predicted and observed torpor patterns throughout a hibernation season. (a) Predicted expression for a hibernating animal exposed to bacterial pathogens with growth properties similar to *Salmonella* and (b) coliform C1. (c) Observed torpor patterns in a European ground squirrel in captivity under simulated natural light and ambient temperature conditions (figure 1 from Henning et al., 2002).

## 5.5 Discussion

We explored the hypothesis proposed by Prendergast et al. (2002) that bacterial infection is an important selective force on torpor patterns because the immune system is impaired during torpor, and periodic arousals are necessary to initiate control of any itinerant infections. Specifically, we asked: What torpor patterns would we expect to see if the function of arousals is to control bacterial infection? How do these predicted torpor patterns compare to observed patterns? Through modeling we found that the predicted torpor patterns are dependent on the growth

properties of the bacterium in relation to temperature. Although bacterial growth rates are much slower at temperatures experienced during mammalian hibernation, some bacteria are able to replicate at temperatures as low as  $-20^{\circ}\text{C}$  (Deming, 2002). If animals are exposed to pathogenic bacteria with growth properties similar to *Salmonella*, periodic arousal to control infection would be an important adaptation at temperatures above  $7^{\circ}\text{C}$ , but not below  $7^{\circ}\text{C}$  because, pathogenic bacteria with these growth properties do not grow well at low temperatures. However, if animals are exposed to pathogenic bacteria that are able to grow well at low temperatures, like the psychrophilic coliform and *Pseudomonas sp.* described by Baig and Hopton (1969), periodic arousals would be important throughout hibernation at all the temperatures examined.

Fitting optimal bacterial parameters to the model results in a ridge in likelihood space in which the six bacteria described from Baig and Hopton (1969) fit within the 0.01 likelihood test statistic. Therefore, 92% of the time we would see data this extreme if the model fit the data. From this, we conclude that several species of psychrophilic bacteria could produce the torpor patterns observed. Furthermore, this simple model that considers only bacterial growth rates at different temperatures, offers a parsimonious explanation for the general torpor patterns observed in some hibernating animals. These findings do not suggest that all animals arouse because they are infected, but that the animals that express these torpor patterns may have been selected for because they were able to deal with bacteria that are able to grow well at low temperatures, such as some coliform and *Pseudomonas* species. This approach provides support for the hypothesis because the data are consistent with the model but experimental studies are needed to test the hypothesis.

An interesting discrepancy between the model and the data is that in nature, hibernating animals generally do not have a longer first torpor bout than subsequent bouts, whereas the model shows this to be the case. However, in the model the length of the first bout is determined by the bacterial inoculum size, whereas subsequent bouts are not, so the length of the first bout is a consequence of the initial infection size while subsequent ones are not. In nature, some hibernators display a shorter first torpor bout in which they experience shallow decreases in body temperature, called test drops. These animals may be re-setting their hy-

pothalamic thermostat which may help to acclimate cellular functions to the onset of low body temperature (Hammel, 1967; Zervanos and Salsbury, 2003).

Hibernators thermo-conform over a wide range of ambient temperatures, however, when ambient temperature ( $T_a$ ), drops below a threshold, body temperature ( $T_b$ ) remains constant. This threshold is the body temperature set point ( $T_{bset}$ ). As  $T_a$  decreases below  $T_{bset}$ , the animal thermoregulates and maintains  $T_b$  at  $T_{bset}$  to avoid a lethal decline in  $T_b$  (Geiser and Kenagy, 1988; Buck and Barnes, 2000). If considered at all temperatures, our model would predict that torpor bout length always increases as  $T_b$  decreases. However, in hibernating animals this is only observed when  $T_b$  is above  $T_{bset}$ . When  $T_b$  drops below  $T_{bset}$ , the torpor bout lengths decrease (Geiser and Kenagy, 1988; Buck and Barnes, 2000).

Other hypotheses have been proposed to explain the function of arousals and may explain this phenomenon. Several of these can be grouped under metabolism effects, such as reduction of energy substrates and accumulation of metabolic wastes. Metabolic rate decreases with  $T_a$  until it drops below  $T_{bset}$  therefore, these metabolic effects would occur at a slower rate as ambient temperature de-

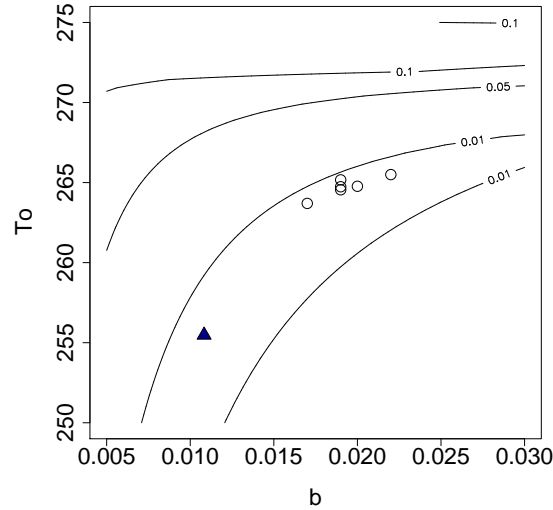


**Figure 5.3.** Bacterial parameters ( $b$  and  $T_0$ ) that give the best fit of the model to the data, using maximum likelihood estimates. Contours show likelihood test statistics. The six psychrophilic bacteria described by Baig and Hopton (1969) are given by circles, and the filled triangle represents the optimal parameter combination.

clines to  $T_{bset}$ , allowing for longer torpor bouts (Geiser and Kenagy, 1988; Geiser and Brigham, 2000), also producing the inverse relationship of torpor bout lengths and  $T_a$  as predicted from other temperature dependent processes such as bacterial growth. However, regression analyses by Geiser et al. (1990) suggest that torpor bout lengths at  $T_a$ s above  $T_{bset}$  are more strongly correlated with  $T_b$  than metabolism, as measured by consumed volume of  $O_2$ , lending some credence to the immune stimulation hypothesis. However, at  $T_a$ s below  $T_{bset}$ , metabolic rate increases as the animal thermoregulates. Therefore, the relationship between torpor bout length and temperature at temperatures below  $T_{bset}$  is consistent with metabolic rate hypotheses for the function of arousals (Buck and Barnes, 2000). However, since at  $T_a$ s above  $T_{bset}$ , torpor bout length is more strongly correlated with  $T_b$  than metabolic rate (Geiser et al., 1990; Buck and Barnes, 2000), it appears there may be two different arousal triggers, one for  $T_a$ s below  $T_{bset}$  and another for above  $T_{bset}$ . Buck and Barnes (2000) speculated that animals may need to arouse more often at  $T_a$ s below  $T_{bset}$  due to an increase in metabolism, to replenish glycogen stores, whereas above  $T_{bset}$ , a temperature sensitive timing mechanism may operate. This hypothesis is consistent with our model. Nevertheless, none of these hypotheses for periodic arousals are mutually exclusive and these processes may, in fact, act in concert.

Burton and Reichman (1999) argued that most pathogens are not able to replicate at low temperatures. Mitosis at low temperatures has been shown to lead to damage caused by disrupted microtubulin polymerization in some organisms (Roth, 1967; Nagasawa and Dewey, 1972). However, each bacterial species has different growth properties. Some are better at growth at low temperatures than others and may be able to grow at temperatures lower than  $5^\circ\text{C}$ , although at slower rates (Baig and Hopton, 1969). So these bacteria could be an important selective pressure that influences torpor patterns.

Different species of hibernating animals show large variations in their maximum torpor bout lengths. For example, the edible dormouse has a reported maximum torpor bout length of 792 hours, and the Turkish hamster has a reported maximum torpor bout length of only 130 hours. In terms of the immune stimulation hypothesis, this could be explained by differences in bacteria that these different species have been exposed to. Furthermore, other microorganisms follow the growth rela-

tionship described by equation (5.3) including fungi (Ratkowsky et al., 1982). In fact, fungal pathogens often grow better at low temperatures (such as those  $T_b$ s experienced by hibernating animals) as compared to bacteria (Ratkowsky et al., 1982). Differences in maximum torpor bout length may be a result of exposure to different bacterial or fungal pathogens. Furthermore, as mentioned earlier, none of the hypotheses for the function of periodic arousal are mutually exclusive and torpor patterns may result from a combination of factors.

Key simplifying assumptions were made in the model. One assumption is that bacterial growth is not density dependent. We believe this is a reasonable assumption since we are considering time points early in the growth process. We also assume that bacterial growth and immunity rates are immediate and rise to maximum, and the animal enters and arouses from torpor such that its body temperature rises quickly to 37°C. Although we know that animals may take less than an hour to a few hours to arouse from torpor and longer to enter torpor, increasing or decreasing their body temperatures between euthermic and ambient temperatures (Hut et al., 2002; Park et al., 2000), no studies that we are aware of have addressed the question of when during this re-warming process the immune system begins to function effectively and when during cooling it ceases to function effectively. Therefore, adding cooling and re-warming phases does nothing to improve the model. To date, no experiments have characterized bacterial growth rates in a hibernating animal, so the data for bacterial growth used in this model came from experiments on minced beef (Mackey and Kerridge, 1988) and in culture (Baig and Hopton, 1969).

The model indicates that hibernators exposed to bacterial pathogens would benefit from periodic arousals, however several studies suggest that hibernators exposed to viruses may not. Viral studies performed on hibernating animals indicate that viral replication is undetectable during torpor, yet may occur during periods of arousal (Sulkin et al., 1960; Dempster et al., 1966; Sulkin et al., 1966; Main, 1979; Herbold et al., 1983). Dempster et al. (1966) also found that Cocksackie B-3 virus was able to reach higher titers faster in animals recently aroused from torpor, whether infected during torpor or 48 hours after arousal, and caused more severe pathology than seen in non-hibernating animals. This would imply that there are immunological trade-offs involved in periodic arousals, not only between

conserving resources and immunological defense, but also between the optimal immune responses for viruses and bacteria.

Understanding host-pathogen interactions in wildlife reservoirs is important if we are to obtain insight into the emergence and spread of zoonotic diseases. Some wildlife disease reservoirs are hibernating animals, such as bats, but relatively little is known about disease dynamics in hibernators. Furthermore, with the increased attention to hibernation for medical applications, such as preservation of tissue at low temperature and reduction of physiological damage caused from trauma and ischemia (Carey et al., 2003), understanding bacterial and immune dynamics at these decreased temperatures could have important implications for human health.

## 5.6 Acknowledgements

We would like to thank Ottar Bjørnstad for his valuable help with the analysis and Bryan Grenfell for his constructive comments on the manuscript. A.L. would like to thank Kat Shea for her guidance during the development of the model and Tom Raffel and Isa Cattadori for their useful input.

## 5.7 Notes

This chapter was published as Luis and Hudson (2006) in *Functional Ecology*. Peter Hudson was a coauthor and assisted with the editing of the manuscript.

# Appendix A

## Supplemental Figures and Tables to Chapter 2

### A.1 Robust Design Capture-Mark-Recapture Model Comparisons

**Table A.1.** Statistical models tested using Closed Robust Design models to obtain an estimate for abundance at each monthly primary trapping occasion (session),  $N(\sim\text{session})$ .

Model	npar	AICc	Weight
$S(\sim\text{time})\gamma''(\sim 1)\gamma'(\sim 1)p(\sim\text{session}*\text{time})c(\sim\text{session})$	297	-2526.7	1
$S(\sim\text{time})\gamma''(\sim 1)\gamma'(\sim 1)p(\sim\text{session}*\text{time})c(\sim 1)$	242	-2492.9	0
$S(\sim\text{time})\gamma''(\sim\text{time})\gamma'(\sim\text{time})p(\sim\text{session}*\text{time})c(\sim\text{session})$	412	-2372.4	0
$S(\sim\text{time})\gamma''(\sim 1)\gamma'(\sim 1)p(\sim\text{session})c(\sim\text{session})$	237	-2046.6	0

(npar is number of estimable parameters,  $S$  is survivorship,  $\gamma$  is the probability of an individual that was available for encounter during the last primary session temporarily emigrating between the previous and current session,  $\gamma'$  is the probability of remaining outside the study area,  $p$  is probability of first capture, and  $c$  is the probability of recapture.  $S(\sim\text{time})$  means that an estimate for survivorship is calculated for each primary trapping session (month).  $\sim 1$  means a single value is estimated. Session means an estimate for each primary trapping session.  $\sim\text{session}*\text{time}$  for  $p$  means an estimate for each trapping occasion, primary or secondary. Since we saw some emigration during the primary period we pooled the second and third sampling occasions into one (Kendall, 1999))

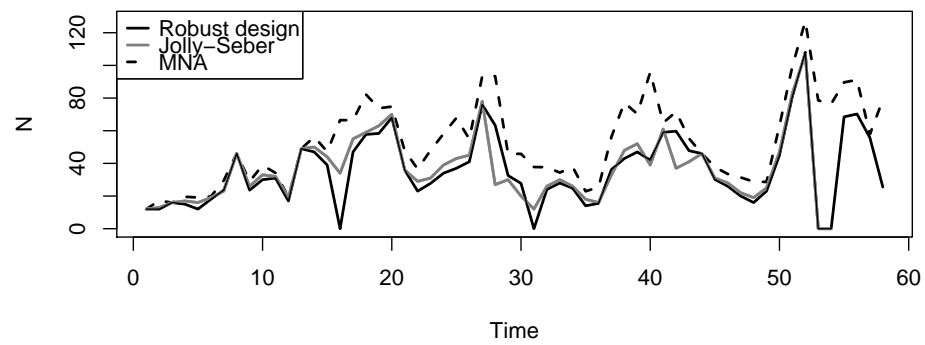


**Figure A.1.** Population abundance estimates including Minimum Number Alive (MNA), Jolly-Seber, and Closed Robust Design estimates from August 2004 to May 2009.

## A.2 Multistrata Capture-Mark-Recapture Model Comparisons

**Table A.2.** Statistical models tested for variation in recapture rates ( $p$ ), using multi-strata models.

Model	npar	QAICc	Weight
$p(\sim \text{age class} + \text{time})$	163	8079.9	0.987
$p(\sim \text{time})$	162	8088.6	0.013
$p(\sim \text{month})$	48	8363.0	0.000
$p(\sim \text{season})$	40	8389.2	0.000
$p(\sim \text{age class})$	38	8506.2	0.000
$p(\sim 1)$	37	8538.5	0.000

(npar is number of estimable parameters, age classes (strata) are juvenile and adult based on weight, time denotes the full time-specific variation with 126 values estimated, one for each capture occasion, month denotes 12 values estimated, one for each month of the year, year denotes 11 values estimated, one for each year of the study, season denotes 4 values estimated, one for each of the seasons, and a one denotes no time-specific variation, which is a single value estimated for all capture occasions. For all models survival ( $S$ ) and maturation ( $\psi$ ) models were the best of the basic models tested, i.e.  $S(\sim \text{month})$   $\psi(\sim \text{stratum} * \text{month})$ , accounting for 36 of the parameters. QAICc is the estimated quasi-Akaike information criterion, using the correction factor,  $\hat{c}=1.28$ , to adjust for lack-of-fit. Weight gives the statistical weight of that model compared to the other candidate models.)

**Table A.3.** Ranking of Multistrata MARK models for survival ( $S$ ), capture probability ( $p$ ), and maturation probability ( $\psi$ ).

Model	npar	QAICc	Weight
$S(\sim \text{month} * P_{t-5} + \text{month} * T_{t-5} + \text{month} * P_t + \text{month} * T_t) p(\sim \text{stratum} + \text{time}) \psi(\sim \text{stratum} * \text{month})$	211	8056.56	0.757
$S(\sim \text{stratum} + \text{month} * P_{t-5} + \text{month} * T_{t-5} + \text{month} * P_t + \text{month} * T_t) p(\sim \text{stratum} + \text{time}) \psi(\sim \text{stratum} * \text{month})$	212	8058.89	0.236
$S(\sim \text{month} * P_{t-5} + \text{month} * T_{t-5} + \text{month} * P_t + \text{month} * T_t) p(\sim \text{time}) \psi(\sim \text{stratum} * \text{month})$	210	8067.284	0.0035
$S(\sim \text{month} * P_{t-5} + \text{month} * T_{t-5} + \text{month} * P_t + \text{month} * T_t) p(\sim P_t + \text{time}) \psi(\sim \text{stratum} * \text{month})$	211	8069.5	0.0012
$S(\sim \text{month} * P_{t-5} + \text{month} * T_{t-5} + \text{month} * P_t + \text{month} * T_t) p(\sim T_t + \text{time}) \psi(\sim \text{stratum} * \text{month})$	211	8069.5	0.0012
$S(\sim \text{month} * P_{t-5} + \text{month} * T_{t-5} + \text{month} * P_t) p(\sim \text{time}) \psi(\sim \text{stratum} * \text{month})$	198	8071.911	0.00035
$S(\sim \text{month} * P_{t-5} + \text{month} * T_{t-5} + \text{month} * T_t) p(\sim \text{time}) \psi(\sim \text{stratum} * \text{month})$	198	8072.480	0.00026
$S(\sim \text{month} * P_{t-5} * T_{t-5}) p(\sim \text{time}) \psi(\sim \text{stratum} * \text{month})$	198	8080.430	0.00000
$S(\sim \text{month} * P_{t-5} + \text{month} * T_{t-5}) p(\sim \text{time}) \psi(\sim \text{stratum} * \text{month})$	186	8082.026	0.00000
$S(\sim \text{month} * P_{t-5} + \text{month} * T_{t-5} + \text{MNA}_{t-1}) p(\sim \text{time}) \psi(\sim \text{stratum} * \text{month})$	187	8084.152	0.00000
$S(\sim \text{month}) p(\sim \text{time}) \psi(\sim \text{stratum} * \text{month})$	162	8088.6	0.00000
$S(\sim \text{month} * P_{t-5} + \text{month} * T_{t-5} + \text{month} * P_t + \text{month} * T_t) p(\sim \text{time}) \psi(\sim \text{stratum} * \text{month})$	260	8089.591	0.00000
$*P_{t-5} + \text{stratum} * \text{month} * T_{t-5} + \text{stratum} * \text{MNA}_{t-1})$			
$S(\sim \text{stratum} + \text{month}) p(\sim \text{time}) \psi(\sim \text{stratum} * \text{month})$	163	8090.4	0.00000
$S(\sim \text{month} * P_{t-5} + \text{month} * T_{t-5} + \text{month} * P_t + \text{month} * T_t + \text{MNA}_{t-1}) p(\sim \text{time}) \psi(\sim \text{stratum} * \text{month} * \text{MNA}_{t-1})$	261	8090.705	0.00000
$S(\sim \text{year}) p(\sim \text{time}) \psi(\sim \text{stratum} * \text{month})$	161	8098.9	0.00000
$S(\sim \text{month} * P_{t-5} + \text{month} * T_{t-5} + \text{month} * P_t + \text{month} * T_t) p(\sim \text{time}) \psi(\sim \text{stratum} * \text{month} * P_{t-5} + \text{stratum} * \text{month} * T_{t-5})$	258	8104.639	0.00000
$S(\sim \text{month} * P_{t-5} + \text{month} * T_{t-5} + \text{MNA}_{t-1}) p(\sim \text{time}) \psi(\sim \text{stratum} * \text{month} * P_{t-5} + \text{stratum} * \text{month} * T_{t-5} + \text{stratum} * \text{MNA}_{t-1})$	237	8107.736	0.00000
$S(\sim \text{month} * P_{t-5} + \text{month} * T_{t-5} + \text{month} * P_t + \text{month} * T_t) p(\sim \text{time}) \psi(\sim \text{stratum} * \text{month} * P_{t-5} + \text{stratum} * \text{month} * T_{t-5} + \text{stratum} * \text{MNA}_{t-1})$	282	8118.270	0.00000
$S(\sim \text{month} * P_{t-5} + \text{month} * T_{t-5} + \text{month} * P_t + \text{month} * T_t) p(\sim \text{time}) \psi(\sim \text{stratum} * \text{month} * P_{t-5} + \text{stratum} * \text{month} * T_{t-5} + \text{stratum} * \text{MNA}_{t-1})$	233	8118.5	0.00000
$S(\sim \text{month} * P_{t-5} + \text{month} * T_{t-5} + \text{month} * P_t + \text{month} * T_t) p(\sim \text{month} * P_t + \text{time}) \psi(\sim \text{stratum} * \text{month})$	289	8134.078	0.00000
$S(\sim \text{month} * P_{t-5} * T_{t-5} * \text{MNA}_{t-1}) p(\sim \text{month} * P_{t-5} * T_{t-5} * \text{MNA}_{t-1}) \psi(\sim \text{stratum} * \text{month} * P_{t-2} * T_{t-2} + \text{MNA}_{t-1})$			
$S(\sim \text{month} * P_{t-5} * T_{t-5}) p(\sim \text{time}) \psi(\sim \text{stratum} * \text{month} * P_{t-5} * T_{t-5})$	270	8134.110	0.00000
$S(\sim \text{stratum}) p(\sim \text{time}) \psi(\sim \text{stratum} * \text{month})$	152	8143.0	0.00000

**Table A.3.** continued.

Model	npar	QAICc	Weight
$S(\sim \text{month} * P_{t-5})p(\sim \text{month} * P_{t-5} * T_{t-5})\psi(\sim \text{stratum} * \text{month})$	96	8144.578	0
$S(\sim \text{month} * P_{t-5} + \text{month} * T_{t-5})p(\sim \text{month} * P_{t-5} * T_{t-5})\psi(\sim \text{stratum} * \text{month})$	108	8146.082	0
$S(\sim \text{month} * P_{t-5} * T_{t-5} * \text{MNA}_{t-1})p(\sim \text{month} * P_{t-5} * T_{t-5})\psi(\sim \text{stratum} * \text{month})$	168	8148.129	0
$S(\sim \text{month} * P_{t-5} * T_{t-5} + \text{MNA})p(\sim \text{month} * P_{t-5} * T_{t-5})\psi(\sim \text{stratum} * \text{month})$	121	8149.654	0
$S(\sim \text{month} * P_{t-5} * T_{t-5})p(\sim \text{month} * P_{t-5} * T_{t-5})\psi(\sim \text{stratum} * \text{month})$	120	8150.663	0
$S(\sim \text{month} * P_{t-5} * T_{t-5} * \text{MNA})p(\sim \text{month} * P_{t-5} * T_{t-5})\psi(\sim \text{stratum} * \text{month})$	168	8151.795	0
$S(\sim \text{month} * P_{t-7} * T_{t-7} * \text{MNA}_{t-1})p(\sim \text{month} * P_{t-5} * T_{t-5})\psi(\sim \text{stratum} * \text{month})$	168	8152.983	0
$S(\sim \text{month} * P_{t-5} * T_{t-5} * \text{MNA}_{t-2})p(\sim \text{month} * P_{t-5} * T_{t-5})\psi(\sim \text{stratum} * \text{month})$	168	8155.419	0
$S(\sim \text{month} * P_{t-4} * T_{t-4})p(\sim \text{month} * P_{t-4} * T_{t-4})\psi(\sim \text{stratum} * \text{month})$	120	8158.901	0
$S(\sim \text{month} * P_{t-5} * T_{t-5} * \text{MNA}.A)p(\sim \text{month} * P_{t-5} * T_{t-5})\psi(\sim \text{stratum} * \text{month})$	168	8159.972	0
$S(\sim \text{month} * T_{t-5})p(\sim \text{month} * P_{t-5} * T_{t-5})\psi(\sim \text{stratum} * \text{month})$	96	8161.937	0
$S(\sim \text{month} * P_{t-6} * T_{t-6} * \text{MNA}_{t-1})p(\sim \text{month} * P_{t-5} * T_{t-5})\psi(\sim \text{stratum} * \text{month})$	168	8168.655	0
$S(\sim \text{month} * P_{t-5} * T_{t-5} * \text{MNA})p(\sim \text{month} * P_{t-5} * T_{t-5})\psi(\sim \text{stratum} * \text{month} * \text{MNA})$	192	8174.406	0
$S(\sim \text{month} * P_{t-3} * T_{t-3})p(\sim \text{month} * P_{t-3} * T_{t-3})\psi(\sim \text{stratum} * \text{month})$	120	8175.266	0
$S(\sim \text{month} + P_{t-5} + T_{t-5} + \text{MNA}_{t-1})p(\sim \text{time})\psi(\sim \text{stratum} + \text{month} + P_{t-5} + T_{t-5} + \text{MNA}_{t-1})$	157	8190.419	0
$S(\sim \text{month} * P_{t-5} * T_{t-5} * \text{MNA}_{t-1})p(\sim \text{month} * P_{t-1} * T_{t-1})\psi(\sim \text{stratum} * \text{month})$	168	8194.516	0
$S(\sim \text{month} * P_{t-5} * T_{t-5} * \text{MNA}_{t-1})p(\sim \text{month} * P_{t-5} * T_{t-5})\psi(\sim \text{stratum} * \text{month} * P_{t-2} * T_{t-2})$	240	8195.249	0
$S(\sim \text{month} * P_{t-5} * T_{t-5} * \text{MNA}_{t-1})p(\sim \text{month} * P_{t-5} * T_{t-5})\psi(\sim \text{stratum} * \text{month} * P_{t-5} * T_{t-5})$	240	8197.650	0
$S(\sim \text{month} * P_{t-3} * T_{t-3})p(\sim \text{month} * P_{t-3} * T_{t-3})\psi(\sim \text{stratum} * \text{month})$	120	8197.965	0
$S(\sim \text{month} * P_{t-5} * T_{t-5} * \text{MNA})p(\sim \text{month} * P_{t-5} * T_{t-5})\psi(\sim \text{stratum} * \text{month} * P_{t-5} * T_{t-5})$	240	8201.289	0
$S(\sim \text{month} * P_{t-1} * T_{t-1})p(\sim \text{month} * P_{t-1} * T_{t-1})\psi(\sim \text{stratum} * \text{month})$	120	8203.719	0
$S(\sim \text{month} * P_{t-2} * T_{t-2})p(\sim \text{month} * P_{t-2} * T_{t-2})\psi(\sim \text{stratum} * \text{month})$	120	8207.483	0
$S(\sim \text{month} * P_t * T_t)p(\sim \text{month} * P_t * T_t)\psi(\sim \text{stratum} * \text{month})$	120	8225.957	0
$S(\sim \text{stratum} * \text{month} * P_{t-3} * T_{t-3})p(\sim \text{month} * P_{t-3} * T_{t-3})\psi(\sim \text{stratum} * \text{month})$	168	8229.165	0
$S(\sim \text{month} * \text{PrCp})p(\sim \text{month} * P_t * T_t)\psi(\sim \text{stratum} * \text{month})$	96	8234.580	0
$S(\sim \text{month} * P_{t-1} * T_t)p(\sim \text{month} * P_{t-1} * T_t)\psi(\sim \text{stratum} * \text{month})$	120	8237.964	0
$S(\sim \text{month} * P_t * T_t)p(\sim \text{month} + P_t + T_t)\psi(\sim \text{stratum} * \text{month})$	86	8238.344	0
$S(\sim \text{month} * \text{PrCp}_{t-1})p(\sim \text{month} * P_t * T_t)\psi(\sim \text{stratum} * \text{month})$	96	8240.903	0
$S(\sim \text{month} * P_{t-5} * T_{t-5})p(\sim \text{month} * P_t * T_t)\psi(\sim \text{stratum} * \text{month})$	120	8242.951	0

**Table A.3.** continued.

Model	npar	QAICc	Weight
$S(\sim \text{month} * P_{t-5} * \text{MNA}_{t-1})p(\sim \text{time})\psi(\sim \text{stratum} * \text{month} * P_{t-5} * T_{t-5} * \text{MNA}_{t-1})$	366	8243.936	0
$S(\sim \text{month} * P_t * T_t)p(\sim \text{month} * P_t)\psi(\sim \text{stratum} * \text{month})$	96	8253.423	0
$S(\sim \text{month} * P_{t-1} * T_{t-1})p(\sim \text{month} * P_{t-1} * T_{t-1})\psi(\sim \text{stratum} * \text{month} * P_{t-1} * T_{t-1})$	192	8257.736	0
$S(\sim \text{month} * P_{t-5} * T_{t-5} + \text{MNA}_{t-1})p(\sim \text{month} * P_{t-5} * T_{t-5} * \text{MNA}_{t-1})\psi(\sim \text{stratum} * \text{month} * P_{t-2} * T_{t-2} * \text{MNA}_{t-1})$	337	8261.697	0
$S(\sim \text{month} * P_{t-2} * T_t)p(\sim \text{month} * P_{t-2} * T_t)\psi(\sim \text{stratum} * \text{month})$	120	8269.700	0
$S(\sim \text{month} * P_{t-5} * \text{SumCdd}_{t-5} * \text{MNA}_{t-1})p(\sim \text{time})\psi(\sim \text{stratum} * \text{month} * P_{t-5} * T_{t-5} * \text{MNA}_{t-1})$	390	8272.373	0
$S(\sim \text{month} * P_{t-5} + \text{month} * T_{t-5})p(\sim \text{time})\psi(\sim \text{stratum} * \text{month} * P_{t-5} * T_{t-5} * \text{MNA}_{t-1})$	354	8276.185	0
$S(\sim \text{month} * \text{NAO}_{t-6} * \text{MNA}_{t-1})p(\sim \text{time})\psi(\sim \text{stratum} * \text{month} * P_{t-5} * T_{t-5} * \text{MNA}_{t-1})$	366	8278.385	0
$S(\sim \text{month} * \text{NINO1.2}_{t-6})p(\sim \text{time})\psi(\sim \text{stratum} * \text{month} * P_{t-5} * T_{t-5} * \text{MNA}_{t-1})$	342	8279.450	0
$S(\sim \text{month} + P_t + T_t)p(\sim \text{month} * P_t * T_t)\psi(\sim \text{stratum} * \text{month})$	86	8280.475	0
$S(\sim \text{month} * P_t)p(\sim \text{month} * P_t)\psi(\sim \text{stratum} * \text{month})$	72	8280.924	0
$S(\sim \text{month} * P_{t-5} + \text{month} * T_{t-5} + \text{MNA}_{t-1})p(\sim \text{time})\psi(\sim \text{stratum} * \text{month} * P_{t-5} * T_{t-5} * \text{MNA}_{t-1})$	355	8281.215	0
$S(\sim \text{month} * P_{t-5} * T_{t-5} * \text{MNA}_{t-1})p(\sim \text{month} * P_{t-5} * T_{t-5} * \text{MNA}_{t-1})\psi(\sim \text{stratum} * \text{month} * P_{t-2} * T_{t-2} * \text{MNA}_{t-1})$	384	8282.009	0
$S(\sim \text{month} * \text{NINO1.2}_{t-6} * \text{MNA}_{t-1})p(\sim \text{time})\psi(\sim \text{stratum} * \text{month} * P_{t-5} * T_{t-5} * \text{MNA}_{t-1})$	366	8282.069	0
$S(\sim \text{month} * P_{t-5} * T_{t-5} * \text{MNA}_{t-1})p(\sim \text{month} * P_t * T_t)\psi(\sim \text{stratum} * \text{month} * P_{t-5} * T_{t-5})$	240	8286.658	0
$S(\sim \text{month} * P_t * T_t)p(\sim \text{month} * P_t * T_t)\psi(\sim \text{stratum} * \text{month} * P_t * T_t)$	192	8291.421	0
$S(\sim \text{month} * T_t)p(\sim \text{month} * P_t)\psi(\sim \text{stratum} * \text{month})$	72	8296.347	0
$S(\sim \text{month} * T_t)p(\sim \text{month} * T_t)\psi(\sim \text{stratum} * \text{month})$	72	8303.592	0
$S(\sim \text{month} * P_t)p(\sim \text{month} * P_t)\psi(\sim \text{stratum} * \text{month} * P_t)$	96	8306.975	0
$S(\sim \text{month} * P_{t-5} * T_{t-5} * \text{MNA}_{t-1} + P_t * T_t)p(\sim \text{time})\psi(\sim \text{stratum} * \text{month} * P_{t-2} * T_{t-2} * \text{MNA}_{t-1})$	417	8307.713	0
$S(\sim \text{month} * P_{t-5} * T_{t-5} * \text{MNA}_{t-1})p(\sim \text{time})\psi(\sim \text{stratum} * \text{month} * P_{t-2} * T_{t-2} * \text{MNA}_{t-1})$	414	8308.173	0
$S(\sim \text{month} * P_{t-2} * T_{t-5} * \text{MNA}_{t-1})p(\sim \text{month} * P_{t-5} * T_{t-5} * \text{MNA}_{t-1})\psi(\sim \text{stratum} * \text{month} * P_{t-2} * T_{t-2} * \text{MNA}_{t-1})$	384	8308.936	0
$S(\sim \text{month} * P_{t-5} * T_{t-5} * \text{MNA}_{t-2})p(\sim \text{time})\psi(\sim \text{stratum} * \text{month} * P_{t-2} * T_{t-2} * \text{MNA}_{t-1})$	414	8309.774	0
$S(\sim \text{month} * P_{t-5} * T_{t-5} * \text{MNA}_{t-1})p(\sim \text{time})\psi(\sim \text{stratum} * \text{month} * P_{t-5} * T_{t-5} * \text{MNA}_{t-1})$	414	8310.452	0
$S(\sim \text{month} * T_t)p(\sim \text{month})\psi(\sim \text{stratum} * \text{month})$	60	8320.258	0

Table A.3. continued.

Model	npar	QAICc	Weight
$S(\sim \text{month} * P_{t-5} * T_{t-5} * \text{MNA}_{t-1})p(\sim \text{month} * P_{t-5} * T_{t-5})\psi(\sim \text{stratum} * \text{month} * P_{t-3} * T_{t-3} * \text{MNA}_{t-1})$	336	8329.188	0
$S(\sim \text{month} * P_{t-5} * T_{t-5} * \text{MNA}_{t-1})p(\sim \text{month} * P_{t-5} * T_{t-5})\psi(\sim \text{stratum} * \text{month} * P_{t-2} * T_{t-2} * \text{MNA})$	336	8331.045	0
$S(\sim \text{month} * P_{t-5} * T_{t-5} * \text{MNA}_{t-1})p(\sim \text{month} * P_{t-5} * T_{t-5} + \text{MNA}_{t-1})\psi(\sim \text{stratum} * \text{month} * P_{t-2} * T_{t-2} * \text{MNA}_{t-1})$	337	8333.277	0
$T_{t-2} * \text{MNA}_{t-1}$			
$S(\sim \text{season} * P_t)p(\sim \text{season} * P_t)\psi(\sim \text{stratum} * \text{month})$	40	8334.293	0
$S(\sim \text{month} * P_{t-5} * T_{t-5} * \text{MNA}_{t-1})p(\sim \text{month} * P_{t-5} * T_{t-5})\psi(\sim \text{stratum} * \text{month} * P_{t-2} * T_{t-2} * \text{MNA}_{t-1})$	336	8338.664	0
$S(\sim \text{month} * P_{t-5} * T_{t-5} * \text{MNA})p(\sim \text{month} * P_{t-5} * T_{t-5})\psi(\sim \text{stratum} * \text{month} * P_{t-5} * T_{t-5} * \text{MNA})$	336	8354.853	0
$S(\sim \text{month})p(\sim \text{month})\psi(\sim \text{stratum} * \text{month})$	48	8363.024	0
$S(\sim \text{season})p(\sim \text{month})\psi(\sim \text{stratum} * \text{month})$	40	8369.953	0
$S(\sim \text{month})p(\sim \text{stratum} * \text{month})\psi(\sim \text{stratum} * \text{month})$	60	8373.090	0
$S(\sim \text{month})p(\sim \text{month})\psi(\sim \text{stratum} * \text{month} * T_t)$	72	8376.956	0
$S(\sim \text{stratum} * \text{month})p(\sim \text{stratum} * \text{month})\psi(\sim \text{stratum} * \text{month})$	72	8383.499	0
$S(\sim \text{stratum} * \text{season})p(\sim \text{stratum} * \text{season})\psi(\sim \text{stratum} * \text{season})$	24	8413.948	0
$S(\sim \text{month})p(\sim \text{month})\psi(\sim \text{stratum})$	26	8461.862	0
$S(\sim \text{month} * P_{t-5} * T_{t-5} * \text{MNA}_{t-1})p(\sim \text{month})\psi(\sim \text{stratum} * \text{month} * P_{t-2} * T_{t-2} * \text{MNA}_{t-1})$	300	8470.449	0
$S(\sim \text{stratum} * P_t)p(\sim \text{stratum} * P_t)\psi(\sim \text{stratum} * \text{month})$	32	8483.175	0
$S(\sim P_t)p(\sim P_t)\psi(\sim \text{stratum} * P_t)$	8	8664.433	0
$S(\sim \text{stratum})p(\sim \text{stratum})\psi(\sim \text{stratum})$	6	8668.996	0
$S(\sim \text{month})p(\sim \text{month})\psi(\sim \text{month})$	36	8781.429	0
$S(\sim 1)p(\sim 1)\psi(\sim 1)$	3	9045.806	0
$S(\sim \text{month})p(\sim \text{month})\psi(\sim \text{month})$	36	57649.136	0
$S(\sim \text{stratum})p(\sim \text{stratum})\psi(\sim \text{stratum})$	5	57879.774	0

(npar is number of parameters, and QAICc is the estimated quasi-Akaike information criterion, using the correction factor,  $\hat{c}=1.28$ , to adjust for lack-of-fit. P is precipitation deviation from monthly mean, T is temperature deviation from monthly mean,  $t$  is the current month and  $t-5$  means 5 months previously, etc. Time indicates the fully time dependent model (a separate value is estimated for each trapping occasion). Stratum means age class (a different estimate for juveniles and adults). MNA is minimum number alive, an index for density. MNA.A is minimum number of adults alive. NINO1.2 and NAO are indices for El Nino Southern Oscillation and Northern Atlantic Oscillation, respectively.)

**Table A.4.** Ranking of Pradel MARK models for recruitment rate (f) with the following models for survival,  $\phi$ , and capture probability,  $p$ :  $\phi(\sim\text{month}*P_{t-5}+\text{month}*T_{t-5}+\text{month}*P_t + \text{month}*P_t)$   $p(\sim\text{time})$ .

Model	npar	QAICc	Weight
$f(\sim\text{month}*P_{t \rightarrow t-4}+\text{month}*T_{t \rightarrow t-4})$	223	15218.68	0.481
$f(\sim\text{month}*P_{t-2}+\text{month}*T_{t-4}+\text{MNA}_t)$	224	15219.53	0.315
$f(\sim\text{month}*P_{t \rightarrow t-4}+\text{month}*T_{t \rightarrow t-4} + \text{MNA}_t)$	224	15220.86	0.162
$f(\sim\text{month}*P_{t \rightarrow t-5}+\text{month}*T_{t \rightarrow t-5}+\text{MNA}_t)$	224	15224.58	0.025
$f(\sim\text{month}*P_{t \rightarrow t-5}+\text{month}*T_{t \rightarrow t-5}+\text{MNA}_{t-1})$	224	15226.60	0.009
$f(\sim\text{month}*P_{t-4}+\text{month}*T_{t-4}+\text{MNA}_{t-1})$	224	15227.04	0.007
$f(\sim\text{month}*P_t+\text{month}*T_t+\text{MNA}_t)$	224	15232.77	0
$f(\sim\text{month}*P_{t-3}+\text{month}*T_{t-3}+\text{MNA}_{t-1})$	224	15236.56	0
$f(\sim\text{month}*P_t+\text{month}*T_t)$	223	15238.57	0
$f(\sim\text{month}*P_{t-4}*T_{t-4})$	235	15241.34	0
$f(\sim\text{month}*P_{t-2}+\text{month}*T_{t-3}+\text{MNA}_t)$	224	15242.60	0
$f(\sim\text{month}*P_{t-2}*T_{t-2})$	235	15244.28	0
$f(\sim\text{month}*T_t)$	211	15246.32	0
$f(\sim\text{month}*P_t*T_t)$	235	15248.38	0
$f(\sim\text{month}*P_t*T_t)$	235	15248.38	0
$f(\sim\text{month}*P_t*T_t+\text{MNA}_t)$	236	15250.34	0
$f(\sim\text{month}*T_{t-5})$	211	15255.89	0
$f(\sim\text{month})$	199	15256.46	0
$f(\sim\text{month}*P_{t-7}+\text{month}*T_{t-7}+\text{MNA}_t)$	224	15257.52	0
$f(\sim\text{year})$	198	15257.61	0
$f(\sim\text{month}*P_{t-1}+\text{month}*T_{t-1}+\text{MNA}_t)$	224	15258.93	0
$f(\sim\text{month}*P_{t-5}+\text{month}*T_{t-5}+\text{MNA}_{t-1})$	224	15259.74	0
$f(\sim\text{month}*P_{t-1}+\text{month}*T_{t-1})$	223	15262.68	0
$f(\sim\text{month}*P_{t-5})$	211	15266.70	0
$f(\sim\text{month}*P_{t-5}*T_{t-5})$	235	15268.98	0
$f(\sim\text{month}*P_{t-5}*T_{t-5}*\text{MNA}_{t-2})$	283	15286.82	0

(npar is number of parameters, and QAICc is the estimated quasi-Akaike information criterion, using the correction factor,  $\hat{c}=1.28$ , to adjust for lack-of-fit.  $P$  is precipitation deviation from monthly mean,  $T$  is temperature deviation from monthly mean,  $t$  indicates the current month and  $t - 5$  means 5 months previously, etc.  $P_{t \rightarrow t-4}$  is the sum of the precipitation deviation over the last 4 months, etc. Time indicates the fully time dependent model (a separate value is estimated for each trapping occasion). MNA is minimum number alive, an index for density.)

Appendix	<b>B</b>
----------	----------

**Supplemental Equations for Chapter 2**  
**Mark-Recapture Models**

Equation for Survival (Eqn B1):

$$\begin{aligned}
 \text{logit}(\text{Survival}_t) = & 31.73 + \begin{bmatrix} 0 \\ -29.47 \\ -31.45 \\ -31.24 \\ -31.25 \\ -31.30 \\ -31.22 \\ -31.12 \\ -31.04 \\ -30.96 \\ -30.85 \\ 1.73 \end{bmatrix} + 7.75 \times P_{t-5} - 7.59 \times T_{t-5} + \begin{bmatrix} 0 \\ -6.36 \\ -6.79 \\ -6.94 \\ -4.47 \\ -7.27 \\ -8.74 \\ -7.71 \\ -7.64 \\ -8.57 \\ -7.94 \\ -22.56 \end{bmatrix} \times P_{t-5} + \begin{bmatrix} 0 \\ 8.23 \\ 7.66 \\ 7.63 \\ 7.72 \\ 7.62 \\ 7.60 \\ 7.59 \\ 7.38 \\ 7.73 \\ 7.89 \\ 4.79 \end{bmatrix} \times T_{t-5} \\
 & + 23.43 \times P_t + 4.03 \times T_t + 4.03 \times T_t + \begin{bmatrix} 0 \\ -34.61 \\ -22.81 \\ -24.37 \\ -23.72 \\ -23.21 \\ -23.25 \\ -23.60 \\ -24.90 \\ -25.05 \\ -23.09 \\ -36.98 \end{bmatrix} \times P_t + \begin{bmatrix} 0 \\ -4.64 \\ -4.01 \\ -4.03 \\ -4.22 \\ -3.70 \\ -3.90 \\ -4.18 \\ -4.11 \\ -4.00 \\ -4.03 \\ -15.05 \end{bmatrix} \times T_t
 \end{aligned}$$

where the vectors represent month of the year, and  $P_{t-5}$  represents precipitation 5 months previously,  $T_t$  represents temperature this month, etc.

Equation for recruitment (Eqn B2):

$$\log(\text{Recruitment}_t) = -0.92 + \begin{bmatrix} 0 \\ -0.78 \\ -0.25 \\ -0.36 \\ 0.13 \\ 0.08 \\ -0.03 \\ 0.04 \\ -0.16 \\ -0.11 \\ -1.45 \\ -8.30 \end{bmatrix} + 0.48 \times P_{t \text{ through } -4} + 0.006 \times T_{t \text{ through } -4}$$

$$+ \begin{bmatrix} 0 \\ -1.18 \\ -0.36 \\ -0.71 \\ -0.73 \\ -0.87 \\ -0.57 \\ -0.54 \\ -0.41 \\ -0.40 \\ 0.28 \\ 11.17 \end{bmatrix} \times P_{t \text{ through } -4} + \begin{bmatrix} 0 \\ -0.06 \\ -0.01 \\ -0.01 \\ -0.02 \\ -0.04 \\ -0.01 \\ -0.05 \\ 0.07 \\ 0.04 \\ 0.05 \\ -0.36 \end{bmatrix} \times T_{t \text{ through } -4}$$

Equation for maturation probability (Eqn B3):

$$\text{logit}(\textit{Maturation}) = -0.6023776 + \begin{bmatrix} 0 \\ 1.2403866 \\ 1.8631116 \\ 2.3671624 \\ 0.4176749 \\ 0.1892686 \\ -0.9130265 \\ 0.3545537 \\ 0.2669607 \\ -0.7781141 \\ -1.0157946 \\ 0.5293170 \end{bmatrix}$$

## Bibliography

- Abbott, K. D., T. G. Ksiazek, and J. N. Mills, 1999. Long-term hantavirus persistence in rodent populations in central arizona. *Emerging Infectious Diseases* **5**:102–12.
- Abramson, G., 2004. The criticality of the hantavirus infected phase at zuni pages (arxiv.org/pdf/q-bio.PE/0407003).
- Abramson, G. and V. M. Kenkre, 2002. Spatiotemporal patterns in the hantavirus infection. *Physical Review E* **66**:011912.
- Abramson, G., V. M. Kenkre, T. L. Yates, and R. R. Parmenter, 2003. Traveling waves of infection in the hantavirus epidemics. *Bulletin of Mathematical Biology* **65**:519–34.
- Adler, F. R., J. M. C. Pearce-Duvet, and M. D. Dearing, 2008. How host population dynamics translate into time-lagged prevalence: an investigation of sin nombre virus in deer mice. *Bulletin of Mathematical Biology* **70**:236:252.
- Aguirre, M. A., G. Abramson, A. R. Bishop, and V. M. Kenkre, 2002. Simulations in the mathematical modeling of the spread of the hantavirus. *Physical Review E* **66**:041908.
- Ahmed, S. A., W. J. Penhale, and N. Talal, 1985. Sex hormones, immune responses, and autoimmune diseases: mechanisms of sex hormone action. *American Journal of Pathology* **121**:531–551.
- Altizer, S., A. P. Dobson, P. Hosseini, P. J. Hudson, M. Pascual, and P. Rohani, 2006. Seasonality and the dynamics of infectious diseases. *Ecology Letters* **9**:467–484.
- Alvarez, F., A. H. Hines, and M. L. Reaka-Kudia, 1995. The effects of parasitism by the barnacle *loxothele panopeae* (gissler) (cirripedia: Rhizocephala) on growth and survival of the host crab *rhithropanopeus harrisi* (gould)(brachyura: Xanthidae). *Journal of Experimental Marine Biology and Ecology* **192**:221–232.

- Anderson, R. M., H. C. Jackson, R. M. May, and A. M. Smith, 1981. Population dynamics of fox rabies in europe. *Nature* **289**:765–771.
- Anderson, R. M. and R. M. May, 1978. Regulation and stability of host-parasite population interactions. 1. regulatory processes. *Journal of Animal Ecology* **47**:219–247.
- Anderson, R. M. and R. M. May, 1981. The population dynamics of microparasites and their invertebrate hosts. *Philosophical Transactions of the Royal Society of London. Series B, Biological Sciences* **291**:451–524.
- Anderson, R. M. and R. M. May, 1991. Infectious diseases of humans. Oxford University Press, Oxford.
- Antia, R., B. R. Levin, and R. M. May, 1994. Within-host population dynamics and the evolution and maintenance of microparasite virulence. *American Naturalist* **144**:457–472.
- Baig, I. A. and J. W. Hopton, 1969. Psychrophilic properties and temperature characteristic of growth of bacteria. *Journal of Bacteriology* **100**:552–&.
- Barnes, B., M. Kretzmann, P. Licht, and I. Zucker, 1986. The influence of hibernation on testis growth and spermatogenesis in the golden-mantled ground squirrel, *spermophilus lateralis*. *Biology of Reproduction* **35**:1289–1297.
- Bartlett, M. S., 1957. Measles periodicity and community size. *Journal of the Royal Statistical Society. Series A* **120**:48–71.
- Begon, M., 2003. Disease: health effects on humans, population effects on rodents. In G. R. Singleton, L. A. Hinds, C. J. Krebs, and D. M. Spratt, editors, *Rats, Mice and People: Rodent Biology and Management*, pages 13–19. Australian Centre for International Agricultural Research, Canberra, Australia.
- Bennett, S. G., J. Webb, J. P., M. B. Madon, J. E. Childs, T. G. Ksiazek, N. Torrez-Martinez, and B. Hjelle, 1999. Hantavirus (bunyaviridae) infections in rodents from orange and san diego counties, california. *American Journal of Tropical Medicine and Hygiene* **60**:75–84. Journal Article United states.
- Bjorkman, C., R. Bommarco, K. Eklund, and S. Hoglund, 2004. Harvesting disrupts biological control of herbivores in a short-rotation coppice system. *Ecological Applications* **14**:1624–1633.
- Bjørnstad, O. N., B. Finkenstädt, and B. T. Grenfell, 2002. Endemic and epidemic dynamics of measles: Estimating epidemiological scaling with a time series sir model. *Ecological Monographs* **72**:169–184.

- Bolker, B. M., 2008. Ecological models and data in R. Princeton Univ Pr.
- Borucki, M. K., J. D. Boone, J. E. Rowe, M. C. Bohlman, E. A. Kuhn, R. De-Baca, and S. C. St Jeor, 2000. Role of maternal antibody in natural infection of *peromyscus maniculatus* with sin nombre virus. *J Virol* **74**:2426–9. [Ai36418/ai/niad](#) [Ai39808/ai/niad](#) [Ca09563/ca/nci](#) Comparative Study Journal Article Research Support, U.S. Gov't, P.H.S. United states.
- Botten, J., K. Mirowsky, D. Kusewitt, M. Bharadwaj, J. Yee, R. Ricci, R. M. Feddersen, and B. Hjelle, 2000. Experimental infection model for sin nombre hantavirus in the deer mouse (*peromyscus maniculatus*). *Proceedings of the National Academy of Sciences, USA* **97**:10578–83.
- Botten, J., K. Mirowsky, D. Kusewitt, C. Ye, K. Gottlieb, J. Prescott, and B. Hjelle, 2003. Persistent sin nombre virus infection in the deer mouse (*peromyscus maniculatus*) model: sites of replication and strand-specific expression. *Journal of Virology* **77**:1540–50.
- Botten, J., K. Mirowsky, C. Ye, K. Gottlieb, M. Saavedra, L. Ponce, and B. Hjelle, 2002. Shedding and intracage transmission of sin nombre hantavirus in the deer mouse (*peromyscus maniculatus*) model. *Journal of Virology* **76**:7587–94.
- Brown, J. H. and E. J. Heske, 1990. Temporal changes in a chihuahuan desert rodent community. *OIKOS* **59**:290–302.
- Buceta, J., C. Escudero, F. J. de la Rubia, and K. Lindenberg, 2004. Outbreaks of hantavirus induced by seasonality. *Physical Review E* **69**:–. Part 1 803UG Times Cited:4 Cited References Count:19.
- Buck, C. and B. Barnes, 2000. Effects of ambient temperature on metabolic rate, respiratory quotient, and torpor in an arctic hibernator. *American Journal of Physiology-Regulatory Integrative and Comparative Physiology* **279**:R255–R262.
- Burns, C., B. J. Goodwin, and R. S. Ostfeld, 2005. A prescription for longer life? bot fly parasitism of the white-footed mouse. *Ecology* **86**:753–761.
- Burton, R. and O. Reichman, 1999. Does immune challenge affect torpor duration? *Functional Ecology* **13**:232–237.
- Calisher, C. H., J. N. Mills, W. P. Sweeney, J. R. Choate, D. E. Sharp, K. M. Canestorp, and B. J. Beaty, 2001. Do unusual site-specific population dynamics of rodent reservoirs provide clues to the natural history of hantaviruses? *Journal of Wildlife Diseases* **37**:280–8.

- Calisher, C. H., J. N. Mills, W. P. Sweeney, J. J. Root, S. A. Reeder, E. S. Jentes, and B. J. Beaty, 2005a. Population dynamics of a diverse rodent assemblage in mixed grass shrub habitat, southeastern colorado, 1995-2000. *Journal of Wildlife Diseases* **41**:12–28.
- Calisher, C. H., J. J. Root, J. N. Mills, J. E. Rowe, S. A. Reeder, E. S. Jentes, K. Wagoner, and B. J. Beaty, 2005b. Epizootiology of sin nombre and el moro canyon hantaviruses, southeastern colorado, 1995-2000. *Journal of Wildlife Diseases* **41**:1–11.
- Calisher, C. H., W. Sweeney, J. N. Mills, and B. J. Beaty, 1999. Natural history of sin nombre virus in western colorado. *Emerging Infectious Diseases* **5**:126–34. U50/ccu809862-03/phs Journal Article Research Support, U.S. Gov't, P.H.S. United states.
- Carey, H., M. Andrews, and S. Martin, 2003. Mammalian hibernation: Cellular and molecular responses to depressed metabolism and low temperature. *Physiological Reviews* **83**:1153–1181.
- Caswell, H. and M. C. Trevisan, 1994. Sensitivity analysis of periodic matrix models. *Ecology* **75**:1299–1303.
- Choquet, R., A. M. Reboulet, J. D. Lebreton, O. Gimenez, and R. Pradel, 2005. U-care 2.2 user's manual. *CEFE, Montpellier, France*. (<http://ftp.cefe.cnrs.fr/biom/Soft-CR/>) .
- Collinge, S. K., W. C. Johnson, C. Ray, R. Matchett, J. Grensten, J. F. Cully, K. L. Gage, J. E. Kosoy, M. Y. adn Loye, and A. P. Martin, 2005. Testing the generality of a trophic-cascade model for plague. *EcoHealth* **2**:102–112.
- Collins, D. and T. Weaver, 1978. Effects of summer weather modification (irrigation) in festuca idahoensis-agropyron spicatum grasslands. *Journal of Range Management* **31**:264–269.
- Daan, S., B. Barnes, and A. M. Strijkstra, 1991. Warming up for sleep- ground-squirrels sleep during arousals fro hibernation. *Neuroscience Letters* **128**:265–268.
- de Magny, G. C., R. Murtugudde, M. R. P. Sapiano, A. Nizam, C. W. Brown, A. J. Busalacchi, M. Yunus, G. B. Nair, A. I. Gil, C. F. Lanata, J. Calkins, B. Manna, K. Rajendran, M. K. Bhattacharya, A. Huq, R. B. Sack, and R. R. Colwell, 2008. Environmental signatures associated with cholera epidemics. *Proceedings of the National Academy of Sciences of the United States of America* **105**:17676–17681.
- Deming, W. J., 2002. Psychrophiles and polar regions. *Current Opinion in Microbiology* **5**.

- Dempster, G., E. I. Grodums, and W. A. Spencer, 1966. Experimental coxsackie b-3 virus infection in *citellus lateralis*. *Journal of Cellular Physiology* **67**:443–454.
- Dietz, K., 1976. The incidence of infectious diseases under the influence of seasonal fluctuations. *Lect. Notes Biomath.* **11**:1–15.
- Dorland, W. A. N., 1994. Dorland's illustrated medical dictionary. W. B. Saunders, London.
- Douglass, R. J., C. H. Calisher, K. D. Wagoner, and J. N. Mills, 2007. Sin nombre virus infection of deer mice in montana: characteristics of newly infected mice, incidence, and temporal pattern of infection. *Journal of Wildlife Diseases* **43**:12–22.
- Douglass, R. J., A. J. Kuenzi, T. Wilson, and R. C. Van Horne, 2000. Effects of bleeding nonanesthetized wild rodents on handling mortality and subsequent recapture. *Journal of Wildlife Diseases* **36**:700–704.
- Douglass, R. J., R. Van Horn, K. W. Coffin, and S. N. Zanto, 1996. Hantavirus in montana deer mouse populations: preliminary results. *Journal of Wildlife Diseases* **32**:527–30.
- Douglass, R. J., T. Wilson, W. J. Semmens, S. N. Zanto, C. W. Bond, R. C. Van Horn, and J. N. Mills, 2001. Longitudinal studies of sin nombre virus in deer mouse-dominated ecosystems of montana. *American Journal of Tropical Medicine and Hygiene* **65**:33–41.
- Easterbrook, J. D., J. B. Kaplan, G. E. Glass, M. V. Pletnikov, and S. L. Klein, 2007. Elevated testosterone and reduced 5-hiaa concentrations are associated with wounding and hantavirus infection in male norway rats. *Hormones and Behavior* **52**:474–481.
- Easterbrook, J. D. and S. L. Klein, 2008. Immunological mechanisms mediating hantavirus persistence in rodent reservoirs. *PLoS Pathogens* **4**:e1000172.
- Elkinton, J., W. M. Healy, J. P. Buonaccorsi, G. H. Boettner, A. M. Hazzard, H. R. Smith, and A. M. Liebhold, 1996. Interactions among gypsy moths, white-footed mice, and acorns. *Ecology* **77**:2332–2342.
- Elkinton, J., A. M. Liebhold, and R. Muzika, 2004. Effects of alternative prey on predation by small mammals on gypsy moth pupae. *Population Ecology* **46**:171–178.

- Engelthaler, D. M., D. G. Mosley, J. E. Cheek, C. E. Levy, K. K. Komatsu, P. Ettestad, T. Davis, D. T. Tanda, L. Miller, J. W. Frampton, R. Porter, and R. T. Bryan, 1999. Climatic and environmental patterns associated with hantavirus pulmonary syndrome, four corners region, united states. *Emerging Infectious Diseases* **5**:87–94.
- Escudero, C., J. Buceta, F. J. de la Rubia, and K. Lindenberg, 2004. Effects of internal fluctuations on the spreading of hantavirus. *Physical Review E* **70**:061907.
- Fairbairn, D. J., 1977. The spring decline in deer mice: Death or dispersal? *Canadian Journal of Zoology* **55**:84–92.
- Feldmann, H., A. Sanchez, S. Morzunov, C. F. Spiropoulou, P. E. Rollin, T. G. Ksiazek, C. J. Peters, and S. T. Nichol, 1993. Utilization of autopsy rna for the synthesis of the nucleocapsid antigen of a newly recognized virus associated with hantavirus pulmonary syndrome. *Virus Research* **30**:351–367.
- Feore, S. M., M. Bennett, J. Chantrey, T. Jones, D. Baxby, and M. Begon, 1997. The effect of cowpox virus infection on fecundity in bank voles and wood mice. *Proceedings of the Royal Society B-Biological Sciences* **264**:1457–1461.
- Fisher, K. C., 1964. On the mechanisms of periodic arousal in the hibernating ground squirrel. *Annales Academiae Scientiarum Fennicae-Biologia* **71**:141–156.
- Fisher, K. C. and J. F. Manery, 1967. Water and electrolyte metabolism in heterotherms. In K. C. Fisher, A. R. Dawe, C. P. Lyman, E. Schonbaum, and F. E. South, editors, *Mammalian Hibernation III*, pages 235–279. Oliver and Boyd, London.
- Frank, S. A., 1996. Models of parasite virulence. *Quarterly Review of Biology* **71**:37–78.
- Furuse, M. and H. Yokota, 1984. Protein and energy-utilization in germ-free and conventional chicks given diets containing different levels of dietary-protein. *British Journal of Nutrition* **51**:255–264.
- Galster, W. A. and P. Morrison, 1970. Cyclic changes in carbohydrate concentrations during hibernation in arctic ground squirrel. *American Journal of Physiology* **218**:1228–&.
- Gao, L. Q. and H. W. Hethcote, 1992. Disease transmission models with density-dependent demographics. *Journal of Mathematical Biology* **30**:717–731.
- Geiser, F. and R. Brigham, 2000. Torpor, thermal biology, and energetics in Australian long-eared bats (*Nyctophilus*). *Journal of Comparative Physiology B-Biochemical Systemic and Environmental Physiology* **170**:153–162.

- Geiser, F., S. Hiebert, and G. J. Kenagy, 1990. Torpor bout duration during the hibernation season of two sciurid rodents: interrelations with temperature and metabolism. *Physiological Zoology* **63**:489–503.
- Geiser, F. and G. J. Kenagy, 1988. Torpor duration in relation to temperature and metabolism in hibernating ground-squirrels. *Physiological Zoology* **61**:442–449.
- Gilbert, B. S. and C. Krebs, 1981. Effects of extra food on peromyscus and clethrionomys populations in the southern yukon. *Oecologia* **51**:326–331.
- Glass, G. E., J. E. Cheek, J. A. Patz, T. M. Shields, T. J. Doyle, D. A. Thoroughman, D. K. Hunt, R. E. Ensore, K. L. Gage, C. Irland, C. J. Peters, and R. Bryan, 2000. Using remotely sensed data to identify areas at risk for hantavirus pulmonary syndrome. *Emerging Infectious Diseases* **6**:238–47.
- Glass, G. E., J. E. Childs, G. W. Korch, and J. W. LeDuc, 1988. Association of intraspecific wounding with hantaviral infection in wild rats (*rattus norvegicus*). *Epidemiology and Infection* **101**:459–472.
- Glass, G. E., T. Shields, B. Cai, T. L. Yates, and R. Parmenter, 2007. Persistently highest risk areas for hantavirus pulmonary syndrome: potential sites for refugia. *Ecological Applications* **17**:129–39.
- Glass, G. E., T. L. Yates, J. B. Fine, T. M. Shields, J. B. Kendall, A. G. Hope, C. A. Parmenter, C. J. Peters, T. G. Ksiazek, C. S. Li, J. A. Patz, and J. N. Mills, 2002. Satellite imagery characterizes local animal reservoir populations of sin nombre virus in the southwestern united states. *Proceedings of the National Academy of Sciences, USA* **99**:16817–22.
- Grant, P. R., 1971. Experimental studies of competitive interaction in a two-species system. iii. microtus and peromyscus species in enclosures. *Journal of Animal Ecology* **40**:323–350.
- Grant, P. R., 1972. Interspecific competition among rodents. *Annual Review of Ecology and Systematics* **3**:79–106.
- Gratton, C. and R. F. Denno, 2003. Inter-year carryover effects of a nutrient pulse on spartina plants, herbivores, and natural enemies. *Ecology* **84**:2692–2707.
- Grear, D. A., S. E. Perkins, and P. J. Hudson, 2009. Does elevated testosterone result in increased exposure and transmission of parasites? *Ecology Letters* **12**:528–37.
- Grenfell, B. T., 2001. Dynamics and epidemiological impact of microparasites. In G. L. Smith, W. L. Irving, and J. W. McCauley, editors, *New challenges to health: the threat of virus infection*, pages 33–52. Cambridge University Press, Cambridge.

- Grenfell, B. T., O. N. Bjørnstad, and B. Finkenstädt, 2002. Endemic and epidemic dynamics of measles: Scaling predictability, noise and determinism with the time series sir model. *Ecological Monographs* **72**:185–202.
- Grobler, D. G., J. P. Raath, L. E. Braack, K. D. F., G. H. Gerdes, B. J. Barnard, N. P. Kriek, J. Jardine, and S. R., 1995. An outbreak of encephalomyocarditis-virus infection in free-ranging african elephants in the kruger national park. *Onderstepoort Journal of Veterinary Research* **62**:97–108.
- Hammel, H. T., 1967. Temperature regulation and hibernation. In K. C. Fisher, A. R. Dawe, C. P. Lyman, E. Schonbaum, and F. E. South, editors, *Mammalian Hibernation III*, pages 86–96. Oliver and Boyd, London.
- Hansen, L. and G. O. Batzli, 1978. The influence of food availability on the white-footed mouse: populations in isolated woodlots. *Canadian Journal of Zoology* **56**:2530–2541.
- Harvell, C. D., C. E. Mitchell, J. R. Ward, S. Altizer, A. P. Dobson, R. S. Ostfeld, and M. D. Samuel, 2002. Climate warming and disease risks for terrestrial and marine biota. *Science* **296**:2158–2162.
- Haydon, D. T., S. Cleaveland, T. L. H., and M. K. Laurenson, 2002. Identifying reservoirs of infection: a conceptual and practical challenge. *Emerging Infectious Diseases* **8**:1468–1473.
- Henning, R., L. Deelman, R. Hut, E. Van der Zee, H. Buikema, S. Nelemans, H. Lip, D. De Zeeuw, S. Daan, and A. Epema, 2002. Normalization of aortic function during arousal episodes in the hibernating ground squirrel. *Life Sciences* **70**:2071–2083.
- Herbold, J. R., W. P. Heuschele, R. L. Berry, and M. A. Parsons, 1983. Reservoir of st-louis encephalitis-virus in ohio bats. *American Journal of Veterinary Research* **44**:1889–1893.
- Higgins, K., A. Hastings, J. N. Sarvela, and L. W. Botsford, 1997. Stochastic dynamics and deterministic skeletons: population behavior of dungeness crab. *Science* **276**:1431–1435.
- Holdo, R. M., A. R. E. Sinclair, A. P. Dobson, K. L. Metzger, B. M. Bolker, M. E. Ritchie, and R. D. Holt, 2009. A disease-mediated trophic cascade in the serengeti and its implication for ecosystem c. *PLOS Biology* **7**:e1000210.
- Hopp, M. J. and J. A. Foley, 2003. Worldwide fluctuations in dengue fever cases related to climate variability. *Climate Research* **25**:85–94.

- Hosseini, P. R., A. A. Dhondt, and A. P. Dobson, 2004. Seasonality and wildlife disease: how seasonal birth, aggregation and variation in immunity affect the dynamics of mycoplasma gallisepticum in house finches. *Proceedings of the Royal Society of London B* **271**:2569–2577.
- Hudson, P. J., A. P. Dobson, and D. Newborn, 1998. Prevention of population cycles by parasite removal. *Science* **282**:2256–2258.
- Hut, R., B. Barnes, and S. Daan, 2002. Body temperature patterns before, during, and after semi-natural hibernation in the European ground squirrel. *Journal of Comparative Physiology B-Biochemical Systemic and Environmental Physiology* **172**:47–58.
- Jackson, A. P. and M. A. Charleston, 2004. A cophylogenetic perspective of rna-virus evolution. *Molecular Biology and Evolution* **21**:45–57.
- Jolly, G. M., 1965. Explicit estimates from capture-recapture data with both death and immigration- stochastic model. *Biometrika* **52**:225–247.
- Jones, C. G., R. S. Ostfeld, M. P. Richard, E. M. Schaubert, and J. O. Wolff, 1998. Chain reactions linking acorns to gypsy moth outbreaks and lyme disease risk. *Science* **279**:1023–1026.
- Kallio, E. R., L. Voutilainen, O. Vapalahti, A. Vaheri, H. Henttonen, E. Koskela, and T. Mappes, 2007. Endemic hantavirus infection impairs the winter survival of its rodent host. *Ecology* **88**:1911–1916.
- Karmanova, I. G., 1995. The physiology and genesis of hibernation. *Journal of Evolutionary Biochemistry and Physiology* **31**:116–122.
- Kaufman, D. W. and G. A. Kaufman, 1989. Population biology. In G. L. J. Kirkland and J. N. Layne, editors, *Advances in the study of Peromyscus (Rodentia)*, pages 233–270. Texas Tech University Press, Lubbock, Texas.
- Kayser, C., 1953. L'hibernation des mammifères. *Annales de Biologie* **29**:109–150.
- Keeling, M., P. Rohani, and B. T. Grenfell, 2001. Seasonally forced disease dynamics explored as switching between attractors. *Physica D* **148**:317–335.
- Kendall, W. L., 1999. Robustness of closed capture-recapture methods to violations of the closure assumption. *Ecology* **80**:2517–2525.
- Kendall, W. L. and K. H. Pollock, 1992. The robust design capture-recapture studies: a review and evaluation by monte carlo simulation. In D. R. McCullough and R. G. Barrett, editors, *Wildlife 2001: Populations*, pages 31–43. Elsevier Applied Science, New York.

- Kenkre, V., 2005. Statistical mechanical considerations in the theory of the spread of the Hantavirus. *Physica A: Statistical Mechanics and its Applications* **356**:121–126.
- Kermack, W. O. and A. G. McKendrick, 1927. A contribution to the mathematical theory of epidemics. *Proceedings of the Royal Society of London. Series A, Containing Paper of a Mathematical or Physical Character* **115**:700–721.
- King, A. A., S. Shrestha, E. T. Harvill, and O. N. Bjørnstad, 2009. Evolution of acute infections and the invasion-persistence trade-off. *The American Naturalist* **173**:446–455.
- Klein, S. L., 2000. The effects of hormones on sex differences in infection: from genes to behavior. *Neuroscience and Biobehavioral Reviews* **24**:627–638.
- Kuenzi, A. J., R. J. Douglass, C. W. Bond, C. H. Calisher, and J. N. Mills, 2005. Long-term dynamics of sin nombre viral rna and antibody in deer mice in montana. *Journal of Wildlife Diseases* **41**:473–81.
- Kuenzi, A. J., M. L. Morrison, D. E. Swann, P. C. Hardy, and G. T. Downard, 1999. A longitudinal study of sin nombre virus prevalence in rodents, southeastern arizona. *Emerging Infectious Diseases* **5**:113–7.
- Laake, J., 2007. Rmark: R code for mark analysis.
- Lafferty, K. D., 2004. Fishing for lobsters indirectly increases epidemics in sea urchins. *Ecological Applications* **14**:1566–1573.
- Lebreton, J.-D., K. P. Burnham, J. Clobert, and D. R. Anderson, 1992. Modeling survival and testing biological hypotheses using marked animals: a unified approach with case studies. *Ecological Monographs* **62**:67–118.
- LeDuc, J. W., 1987. Epidemiology of hantaan and related viruses. *Laboratory Animal Science* **37**:413–418.
- Lewellen, R. H. and S. H. Vessey, 1998a. The effect of density dependence and weather on population size of a polyvoltine species. *Ecological Monographs* **68**:571–594.
- Lewellen, R. H. and S. H. Vessey, 1998b. Modeling biotic and abiotic influences on population size in small mammals. *Oecologia* **113**:210–218.
- Lima, M., N. C. Stenseth, N. G. Yoccoz, and F. M. Jasik, 2001. Demography and population dynamics of the mouse opossum (*thylamys elegans*) in semi-arid chile: seasonality, feedback structure and climate. *Proceedings of the Royal Society of London B* **268**:2053–2064.

- Lochmiller, R. and C. Deerenberg, 2000. Trade-offs in evolutionary immunology: just what is the cost of immunity? *OIKOS* **88**:87–98.
- Lonner, B. N., R. J. Douglass, A. J. Kuenzi, and K. Hughes, 2008. Seroprevalence against sin nombre virus in resident and dispersing deer mice. *Vector Borne and Zoonotic Diseases* **8**:433–441.
- Luis, A. D., R. J. Douglass, J. N. Mills, and O. N. Bjørnstad, 2010. The effect of seasonality, density and climate on the population dynamics of montana deer mice, important reservoir hosts for sin nombre hantavirus. *Journal of Animal Ecology* **79**:462–470.
- Luis, A. D. and P. J. Hudson, 2006. Hibernation patterns in mammals: a role for bacterial growth? *Functional Ecology* **20**:471–477.
- Lyman, C. P., 1958. Metabolic adaptations of hibernators. *Federation Proceedings* **17**:1057–1060.
- Mackey, B. M. and A. L. Kerridge, 1988. The effect of incubation-temperature and inoculum size on growth of salmonellae in minced beef. *International Journal of Food Microbiology* **6**:57–65.
- Madhav, N. K., K. D. Wagoner, R. J. Douglass, and J. N. Mills, 2007. Delayed density-dependent prevalence of sin nombre virus in montana deer mice (*peromyscus maniculatus*) and implications for human disease risk. *Vector Borne and Zoonotic Diseases* **7**:353–364.
- Main, A. J., 1979. Eastern equine encephalomyelitis virus in experimentally infected bats. *Journal of Wildlife Diseases* **15**:467–477.
- Maniero, G., 2000. The influence of temperature and season on mitogen-induced proliferation of ground squirrel lymphocytes. In Heldmaier, G and Klingenspor, M, editor, *Life in the Cold*, pages 493–503.
- Mann, P. B., 2005. Toll Like Receptor 4 mediated host defense during Bordetella infection. Ph.D. thesis, The Pennsylvania State University.
- Marcello, G. J., S. M. Wilder, and D. B. Meikle, 2008. Population dynamics of a generalist rodent in relation to variability in pulsed food resources in a fragmented landscape. *Journal of Animal Ecology* **77**:41–46.
- May, R. M., 1983. Epidemiology and genetics in the coevolution of parasites and hosts. *Proceedings of the Royal Society B-Biological Sciences* **219**:281–313.
- McCallum, H., N. Barlow, and J. Hone, 2001. How should pathogen transmission be modelled? *Trends in Ecology and Evolution* **16**:295–300.

- McCullagh, P. and J. Nelder, 1989. Generalized Linear Models, Second Edition. Chapman and Hall, London.
- McKenna, J. M. and X. J. Musacchi, 1968. Antibody formation in hibernating ground squirrels (*citellus tridecemlineatus*). *Proceedings of the Society for Experimental Biology and Medicine* **129**:720–&.
- Merritt, J. F., M. Lima, and F. Bozinovic, 2001. Seasonal regulation in fluctuating small mammal populations: feedback structure and climate. *OIKOS* **94**:505–514.
- Millar, J. S., 1989. Reproduction and development. In G. L. J. Kirkland and J. N. Layne, editors, *Advances in the study of Peromyscus (Rodentia)*, pages 169–232. Texas Tech University Press.
- Mills, J. N., 2005. Regulation of rodent-borne viruses in the natural host: implications for human disease. *Archives of Virology* **19**:45–57.
- Mills, J. N., T. G. Ksiazek, B. A. Ellis, P. E. Rollin, S. T. Nichol, T. L. Yates, W. L. Gannon, C. E. Levy, D. M. Engelthaler, T. Davis, D. T. Tanda, J. W. Frampton, C. R. Nichols, C. J. Peters, and J. E. Childs, 1997. Patterns of association with host and habitat: antibody reactive with sin nombre virus in small mammals in the major biotic communities of the southwestern united states. *American Journal of Tropical Medicine and Hygiene* **56**:273–84.
- Mills, J. N., T. G. Ksiazek, C. J. Peters, and J. E. Childs, 1999a. Long-term studies of hantavirus reservoir populations in the southwestern united states: A synthesis. *Emerging Infectious Diseases* **5**:135–142.
- Mills, J. N., T. L. Yates, T. G. Ksiazek, C. J. Peters, and J. E. Childs, 1999b. Long-term studies of hantavirus reservoir populations in the southwestern united states: rationale, potential, and methods. *Emerging Infectious Diseases* **5**:95–101.
- Moore, S. L. and K. Wilson, 2002. Parasites as a viability cost of sexual selection in natural populations of mammals. *Science* **297**:2015–2018.
- Myers, P. and L. L. Master, 1983. Reproduction by *peromyscus maniculatus*: size and compromise. *Journal of Mammalogy* **64**:1–18.
- Nagasawa, H. and W. C. Dewey, 1972. Effects of cold treatment on synchronous chinese hamster cells treated in mitosis. *Journal of Cellular Physiology* **80**:89–106.
- Nedergaard, J. and B. Cannon, 1990. Mammalian hibernation. *Philosophical Transactions of the Royal Society of London Series B-Biological Sciences* **326**:669–686.

- Netski, D., B. H. Thran, and S. C. St Jeor, 1999. Sin nombre virus pathogenesis in *peromyscus maniculatus*. *Journal of Virology* **73**:585–91.
- Nichols, J. D., J. R. Sauer, K. H. Pollock, and J. B. Hestbeck, 1992. Estimating transition probabilities for stage-based population projection matrices using capture-recapture data. *Ecology* **73**:306–312.
- Nisbet, R. M. and W. S. C. Gurney, 1982. Modelling fluctuating populations. Wiley, Chichester.
- Noller, G. L., 1968. The relationship of forage production to precipitation, cover, and soils in North Central Wyoming. Ph.D. thesis, University of Wyoming, Laramie, Ph.D. thesis.
- Ostfeld, R. S., C. D. Canham, K. Oggenfuss, R. J. Winchcombe, and F. Keesing, 2006. Climate, deer, rodents, and acorns of determinants of variation in lyme-disease risk. *PLOS Biology* **4**:1058–1068.
- Pace, M. L., J. J. Cole, S. R. Carpenter, and J. F. Kitchell, 1999. Trophic cascades revealed in diverse ecosystems. *Trends in Ecology and Evolution* **14**:483–488.
- Park, K., G. Jones, and R. Ransome, 2000. Torpor, arousal and activity of hibernating Greater Horseshoe Bats (*Rhinolophus ferrumequinum*). *Functional Ecology* **14**:580–588.
- Parmenter, R. R., J. W. Brunt, D. I. Moore, and S. Ernest, 1993. The hantavirus epidemic in the southwest: rodent population dynamics and the implications for transmission of hantavirus-associated adult respiratory distress syndrome (hards) in the four corners region. *Report to the Federal Centers for Disease Control and Prevention, July 1993. Publication No. 31. Sevilleta Long-Term Ecological Research Program (LTER)* **1993**.
- Pascual, M., J. A. Ahumada, L. F. Chaves, X. Rodó, and M. Bouma, 2006. Malaria resurgence in the east african highlands: Temperature trends revisited. *Proceedings of the National Academy of Sciences of the United States of America* **103**:5829–5834.
- Patz, J. A., D. Campbell-Lendrum, T. Holloway, and J. A. Foley, 2005. Impact of regional climate change on human health. *Nature* **438**:310–317.
- Pearson, D. E. and R. M. Callaway, 2006. Biological control agents elevate hantavirus by subsidizing deer mouse populations. *Ecology Letters* **9**:443–50.
- Pedersen, A. B. and T. J. Greives, 2008. The interaction of parasites and resources cause crashes in a wild mouse population. *Journal of Animal Ecology* **77**:370–377.

- Peixoto, I. D. and G. Abramson, 2006. The effect of biodiversity on the hantavirus epizootic. *Ecology* **87**:873–879.
- Pengelley, E. and K. C. Fisher, 1961. Rhythmic arousal from hibernation in golden-mantled ground squirrel, *Citellus lateralis tescorum*. *Canadian Journal of Zoology* **39**:105–&.
- Perry, D. A., 1976. The effects of weather modification on northern great plains grasslands: a preliminary assessment. *Journal of Range Management* **29**:272–278.
- Plyusnin, A. and S. P. Morzunov, editors, 2001. Virus evolution and genetic diversity of hantaviruses and their rodent hosts. Hantaviruses: Current Topics in Microbiology and Immunology. Springer, New York.
- Pollock, K. H., 1982. A capture-recapture design robust to unequal probability of capture. *The Journal of Wildlife Management* **46**:752–757.
- Poulin, R., 1996. Sexual inequalities in helminth infections: a cost of being male? *The American Naturalist* **147**:287–295.
- Pradel, R., 1996. Utilization of capture-mark-recapture for the study of recruitment and population growth rate. *Biometrics* **52**:703–709.
- Pradel, R., C. M. A. Wintrebert, and O. Gimenez, 2003. A proposal for a goodness-of-fit test to the Arnason-Schwarz multisite capture-recapture model. *Biometrics* **59**:43–53.
- Prendergast, B., D. Freeman, I. Zucker, and R. Nelson, 2002. Periodic arousal from hibernation is necessary for initiation of immune responses in ground squirrels. *American Journal of Physiology-Regulatory Integrative and Comparative Physiology* **282**:R1054–R1062.
- R Development Core Team, 2005. R: A language and environment for statistical computing.
- Ramsden, C., F. L. Melo, L. M. Figueiro, E. C. Holmes, P. M. A. Zanotto, and V. Consortium, 2008. High rates of molecular evolution in hantaviruses. *Molecular Biology and Evolution* **25**:1488–1492.
- Ransome, R. D., 1971. Effect of ambient temperature on arousal frequency of hibernating greater horseshoe bat, *Rhinophus ferrumequinum*, in relation to site and hibernation state. *Journal of Zoology* **164**:353–&.
- Ratkowsky, D. A., J. Olley, T. A. McMeekin, and A. Ball, 1982. Relationship between temperature and growth-rate of bacterial cultures. *Journal of Bacteriology* **149**:1–5.

- Roth, L. E., 1967. Electron microscopy of mitosis in amoebae iii. cold and urea treatments: a basis for tests of direct effects of mitotic inhibitors on microtubule formation. *Journal of Cell Biology* **34**:48–59.
- Saitoh, T., O. N. Bjørnstad, and N. C. Stenseth, 1999. Density dependence in voles and mice: a comparative study. *Ecology* **80**:638–650.
- Schwarz, C. J. and A. N. Arnason, 1996. A general methodology for the analysis of open-model capture recapture experiments. *Biometrics* **52**:860–873.
- Seber, G. A. F., 1965. A note on the multiple recapture census. *Biometrika* **52**:249–259.
- Shimada, T. and T. Saitoh, 2006. Re-evaluation of the relationship between rodent populations and acorn masting: a review from the aspect of nutrients and defensive chemicals in acorns. *Population Ecology* **48**:341–352.
- Smith, M. H., 1971. Food as a limiting factor in the population ecology of *Peromyscus polionotus* (wagner). *Ann Zool Fennici* **8**:109–112.
- Smith, M. J., S. Telfer, E. R. Kallio, S. Burthe, A. R. Cook, X. Lambin, and M. Begon, 2009. Host-pathogen time series data in wildlife support a transmission function between density and frequency dependence. *Proceedings of the National Academy of Sciences, USA* **106**:7905–7909.
- Stapp, P. and G. A. Polis, 2003. Influence of pulsed resources and marine subsidies on insular rodent populations. *OIKOS* **102**:111–123.
- Stenseth, N. C., O. N. Bjørnstad, and W. Falck, 1996. Is spacing behaviour coupled with predation causing the microtine density cycle? a synthesis of current process-oriented and pattern-oriented studies. *Proceedings of the Royal Society of London B* **263**:1423–1435.
- Sulkin, S. E., R. Allen, and R. Sims, 1966. Studies of arthropod-borne virus infections in chiroptera. 3. influence of environmental temperature on experimental infection with Japanese B and St Louis encephalitis viruses. *American Journal of Tropical Medicine and Hygiene* **15**:406.
- Sulkin, S. E., R. Allen, R. Sims, P. H. Krutzsch, and C. Kim, 1960. Studies on the pathogenesis of rabies in insectivorous bats. ii. influence of environmental temperature. *Journal of Experimental Medicine* **112**:595–617.
- Sullivan, T. P. and D. S. Sullivan, 2004. Influence of a granivorous diversionary food on population dynamics of montane voles (*Microtus montanus*), deer mice (*Peromyscus maniculatus*), and western harvest mice (*Reithrodontomys megaltis*). *Crop Protection* **23**:191.

- Taitt, M. J., 1981. The effect of extra food on small rodent populations: I. deer mice (*peromyscus maniculatus*). *Journal of Animal Ecology* **50**:111–124.
- Telfer, S., M. Bennett, K. Bown, D. Carslake, R. Cavanagh, S. Hazel, T. Jones, and M. Begon, 2005. Infection with cowpox virus decreases female maturation rates in wild populations of woodland rodents. *OIKOS* **109**:317–322.
- Telfer, S., M. Bennett, K. Bown, R. Cavanagh, L. Crespín, S. Hazel, T. Jones, and M. Begon, 2002. The effects of cowpox virus on survival in natural rodent populations: increases and decreases. *Journal of Animal Ecology* **71**:558–568.
- Terman, C. R., 1968. Population dynamics. In J. A. King, editor, *Biology of Peromyscus (Rodentia)*, pages 412–450. The American Society of Mammalogists, Stillwater, OK.
- Thomas, D. and F. Geiser, 1997. Periodic arousals in hibernating mammals: is evaporative water loss involved? *Functional Ecology* **11**:585–591.
- Vazquez-Torres, A., B. Vallance, M. Bergman, B. Finlay, B. Cookson, J. Jones-Carson, and F. Fang, 2004. Toll-like receptor 4 dependence of innate and adaptive immunity to Salmonella: Importance of the Kupffer cell network. *Journal of Immunology* **172**:6202–6208.
- Wang, L. C. H., 1978. Time patterns and metabolic rates of natural torpor in the richardson's ground squirrel. *Canadian Journal of Zoology* **57**:149–155.
- White, G. C. and K. P. Burnham, 1999. Program mark: survival rate estimation from both live and dead encounters. *Bird Study* **46 (Supplement)**:S120–S139.
- Whitman, W. C. and C. N. Haugse, 1972. Effects of added rainfall on range vegetation production. *North Dakota Agr. Exp. Sta. Interim Report 1971-1972* page ARE Project.
- Wickler, S. J., B. A. Horwitz, and K. S. Kott, 1987. Muscle function in hibernating hamsters—a natural analog to bed rest. *Journal of Thermal Biology* **12**:163–166.
- Willis, J. S., 1982. The mystery of periodic arousal. In C. P. Lyman, J. S. Willis, A. Malan, and L. C. H. Wang, editors, *Hibernation and Torpor in Mammals and Birds*, pages 92–103. Academic, New York.
- Wilmers, C. C., E. Post, R. O. Peterson, and J. A. Vucetich, 2006. Predator disease out-break modulates top-down, bottom-up and climatic effects on herbivore population dynamics. *Ecology Letters* **9**:383–389.
- Wolff, J. O., 1989. Social behavior. In G. L. J. Kirkland and J. N. Layne, editors, *Advances in the Study of Peromyscus*, pages 271–291. Texas Tech University Press, Lubbock, TX.

- Wolff, J. O., 1996. Population fluctuations of mast-eating rodents are correlated with production of acorns. *Journal of Mammalogy* **77**:850–856.
- Xiao, Y., R. G. Bowers, and S. Tang, 2009. The effect of delayed host self-regulation on host-pathogen population cycles in forest insects. *Journal of Theoretical Biology* **258**:240–249.
- Yates, T., J. N. Mills, C. A. Parmenter, and T. G. Ksiazek, 2002. The ecology and evolutionary history of an emergent disease: hantavirus pulmonary syndrome. *Bioscience* **52**:989–998.
- Yunger, J. A., 2002. Response of two low-density populations of *Peromyscus leucopus* to increased food availability. *Journal of Mammalogy* **83**:267–279.
- Zervanos, S. and C. Salsbury, 2003. Seasonal body temperature fluctuations and energetic strategies in free-ranging eastern woodchucks (*Marmota monax*). *Journal of Mammalogy* **84**:299–310.

# Vita

## Angela Dawn Luis

### EDUCATION

August 2004-August 2010 Ph.D. Ecology, Pennsylvania State University, University Park, PA

August 1997-May 2000 B.S. Zoology, Summa cum Laude, University of Oklahoma, Norman, OK

August 1995-May 1997 University of Central Oklahoma, Edmond, OK

### PUBLICATIONS

Luis, A.D., R.J. Douglass, J.N. Mills, O.N. Bjørnstad. 2010. The effect of seasonality, density, and climate on the population dynamics of Montana deer mice, important reservoir hosts for Sin Nombre hantavirus. *Journal of Animal Ecology* **79**:462-470.

Luis, A.D. and P.J. Hudson. Hibernation patterns in mammals: a role for bacterial growth? 2006. *Functional Ecology* **20**: 471-477.

Hickman-Miller, H.D., W. Bardet, A. Gilb, A.D. Luis, K.W. Jackson, D.I. Watkins, W.H. Hildebrand. 2005. Rhesus macaque MHC class I molecules present HLA-B-like peptides. *Journal of Immunology* **175**: 367-75.

Hickman H.D., A.D. Luis, R. Buchli, S.R. Few, M. Sathiamurthy, R.S. VanGundy, C.F. Giberson, W.H. Hildebrand. 2004. Toward a definition of self: proteomic evaluation of the class I peptide repertoire. *Journal of Immunology* **172**: 2944-52.

Hickman, H.D., A.D. Luis, W. Bardet, R. Buchli, C.L. Battson, M.H. Shearer. K.W. Jackson, R.C. Kennedy, W.H. Hildebrand. 2003. Cutting Edge: Class I presentation of host peptides following HIV infection. *Journal of Immunology* **171**: 22-26.

### FELLOWSHIPS AND AWARDS

Penn State University Academic Computing Fellowship 2007-2010

Braddock Award, Dept of Biology 2008

Brian Horton Memorial Award, for service to the Ecology Program Spring 2007

College of Agricultural Sciences Competitive Grant, Penn State Spring 2007

NASA Pennsylvania Space Grant Consortium Fellowship 2006-2008

National Science Foundation Fellowship, Honorable Mention 2005

University Graduate Fellowship, Penn State University 2004-2005

### TEACHING EXPERIENCE

Co-instructor, ENT 420 Introduction to Population Dynamics, Fall 2007

Co-instructor, ECLGY 597E Concepts in Ecology, Fall 2008 and Fall 2009

Teaching Assistant, BIO 419/519 Ecological and Environmental Problem Solving, Spring 2006 and Spring 2008